Acta Mech
https://doi.org/10.1007/s00707-024-04028-4

ORIGINAL PAPER

Mohamed Shaat · Xin-Lin Gao · Amandine Battentier ·
Nicolas Massué

New analytical model for multi-layered composite plates with imperfect interfaces under thermomechanical loading

Received: 8 May 2024 / Revised: 6 June 2024 / Accepted: 27 June 2024

Abstract A new analytical model for thermoelastic responses of a multi-layered composite plate with imperfect interfaces is developed. The composite plate contains an arbitrary number of layers of dissimilar materials and is subjected to general mechanical loads (both distributed internally and applied on edges for each layer) and temperature changes, which can vary from layer to layer and along two in-plane directions. Each layer is regarded as a Kirchhoff plate, and each imperfect interface is described using a spring-layer interface model, which can capture discontinuities in the displacement and stress fields across the interface. Unlike existing models, the governing equations and boundary conditions are simultaneously derived for each layer by using a variational procedure based on the first and second laws of thermodynamics, which are then combined to obtain the global equilibrium equations and boundary conditions for the multi-layered composite plate. A general analytical solution is developed for a symmetrically loaded composite square plate with an arbitrary number of layers and imperfect interfaces by using a new approach that first determines the interfacial normal and shear stress components on one interface. Closed-form solutions for two- and three-layer composite square plates are obtained as examples by directly applying the general analytical solution. Numerical results for two-, three- and five-layer composite plates under different loading and boundary conditions predicted by the current model are provided, which compare well with those obtained from finite element simulations using COMSOL, thereby validating the newly developed analytical model.

1 Introduction

Multi-layered plates have been widely used in various industries, including aerospace, automotive, electronics and defense. They can be engineered to provide tailored electrical and thermal properties, offering efficient heat dissipation and electrical signal transmission within electronic components (e.g., [36, 57, 72, 77, 78]). In addition, multi-layered plates can be customized to achieve high flexibility and biocompatibility, enabling advanced wearable electronics and ergonomic portable devices (e.g., [15, 16, 37, 39, 54, 76]). Furthermore, multi-layered plates with exceptional thermomechanical stabilities and electrochemical capabilities can be designed to foster innovations in energy storage systems, including Li-metal batteries (e.g., [34, 38, 43, 44]).

A significant challenge in using multi-layered plates is the thermomechanical stability of interfaces, which is crucial for maintaining structural integrity and mitigating incompatibility arising from the mismatch in thermoelastic properties of adjacent layers (e.g., [36, 64, 75]). In a multi-layered plate, each layer can undergo

M. Shaat · X.-L. Gao (✉)
Department of Mechanical Engineering, Southern Methodist University, Dallas, TX 75275, USA
e-mail: xlgao@smu.edu

A. Battentier
Modeling and Virtualization Center, Schlumberger Technology Corp, Sugar Land, TX 77478, USA

N. Massué
Research and Development Hydrogen Stack, GENVIA, 38000 Grenoble, France

Published online: 17 September 2024

stretching and bending due to thermal and mechanical loading. Because of the differences in material properties of dissimilar layers, the deformation in one layer can differ significantly from those in the adjacent layers, ultimately leading to excessive bending of the multi-layered plate and crack initiation and propagation on interfaces between layers. Therefore, models capable of describing plate responses to various thermal and mechanical loads and predicting deformation and stress states in layers and at interfaces are needed in optimally designing multi-layered plates.

Various thermomechanical models have been developed for multi-layered plates using three-dimensional (3D) elasticity (e.g., [3, 13, 42, 55, 56, 59, 66, 67]) and various plate theories, including equivalent single-layer plate theories (e.g., [1, 11, 26, 48, 60, 65, 79]) and layer-wise plate theories (e.g., [2, 5, 6, 14, 35, 40, 51]). In these models, perfect bonding at interfaces between layers is assumed, which ensures that the traction and displacement are continuous across each interface. Although the existing models for multi-layered plates with perfectly bonded interfaces offer the advantage of enabling simple analytical solutions, they lack the capability to accurately represent imperfections at interfaces of multi-layered plates.

The existence of imperfect interfaces in a multi-layered plate can lead to complex deformation patterns and stress states in the plate. A number of thermomechanical models have been proposed to address imperfect interfaces in multi-layered beams and plates (e.g., [7–10, 17, 32, 33, 45–47, 52, 57, 63, 69, 72, 80–82]). In these models, continuity conditions are imposed for the traction at each interface, while the displacement field is allowed to be discontinuous across the same interface. The boundary value problem for a multi-layered plate with such imperfect interfaces has to satisfy local equilibrium equations for each layer, global equilibrium equations of the entire plate, and compatibility conditions at each interface (e.g., [64]). As a result, the number of coupled differential equations that need to be solved for a multi-layered plate increases with the number of layers, which makes it very challenging to obtain closed-form solutions for plates with a large number of layers. Solutions of boundary value problems for multi-layered plates with imperfect interfaces have been limited to plates with a small number of layers (e.g., [7, 18, 19, 41, 50, 73]) even if asymptotic methods are used. Hence, it is very desirable to provide models that can deal with composite plates with a large number of layers that are imperfectly bonded. This motivated the current work.

In the present study, a new analytical model is developed for thermomechanical responses of a multi-layered plate with an arbitrary number of imperfectly bonded layers by using the Kirchhoff plate theory and a spring-layer imperfect interface model. The rest of the paper is organized as follows. In Sect. 2, the new model is formulated using a variational procedure based on the first and second laws of thermodynamics, which is done for the first time. In Sect. 3, a general solution is analytically derived for a symmetrically loaded multi-layered composite square plate. In Sect. 4, closed-form solutions for two- and three-layer composite square plates are obtained as examples by directly applying the general solution. In Sect. 5, numerical results for two-, three- and five-layer composite square plates predicted by the current new model and closed-form solutions are presented, which compare well with those from finite element simulations using COMSOL, thereby validating the newly developed analytical model. The paper concludes in Sect. 6 with a summary.

2 New model for a multi-layered composite plate with imperfect interfaces

2.1 Plate configuration

Consider a composite plate consisting of N_l isotropic linear elastic thin layers of dissimilar materials, as shown in Fig. 1. Each layer is thin and has a thickness t_m such that the total thickness of the composite plate t is much smaller than its in-plane dimensions, i.e.,

$$t = \sum_{m=1}^{N_l} t_m \ll a \text{ or } b, \tag{1}$$

where the subscript m denotes the mth layer of the plate (with $m \in \{1,2, \ldots, N_l\}$), and a and b are the length and width of the plate, respectively.

In the current study, all layers are taken to have the same length and width. Additionally, each interface between two adjacent layers in the plate is assumed to be imperfect, which allows the displacement to be discontinuous across the interface. A global coordinate system $\{x, y, z\}$ with its origin located at the center of the mid-plane of the first layer is introduced. In addition, a local coordinate system $\{x, y, z_m\}$ with its origin placed at the center of the mid-plane of the layer is chosen for each layer, with $m \in \{1,2, \ldots, N_l\}$. The

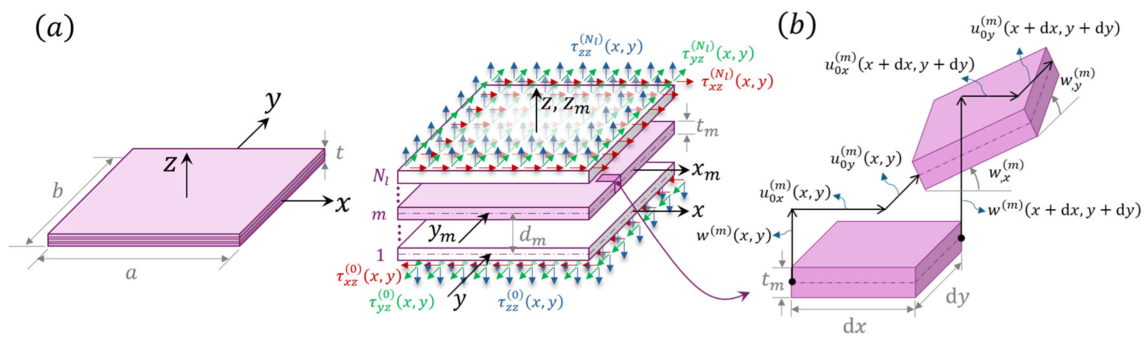

Fig. 1 Composite plate consisting of N_l thin layers and containing $N_l - 1$ imperfect interfaces

vertical distance between the mid-plane of the mth layer and the mid-plane of the first layer is denoted by d_m, as illustrated in Fig. 1.

2.2 Kinematic relations

Each layer in the composite plate is regarded as a Kirchhoff plate satisfying the following kinematic relations (see Fig. 1b) (e.g. [25, 61],):

$$u_\alpha^{(m)}(x, y, z_m) = u_{0\alpha}^{(m)}(x, y) - z_m w_{,\alpha}^{(m)}(x, y),\ u_z^{(m)}(x, y) = w^{(m)}(x, y), \tag{2a,b}$$

where $u_\alpha^{(m)}$ (with $\alpha \in \{x,\ y\}$) and $u_z^{(m)}$ are, respectively, the x-, y- and z-components of the displacement vector $\mathbf{u}^{(m)}$ of a point $(x,\ y,\ z_m)$ in the mth layer, $u_{0\alpha}^{(m)}$ and $w^{(m)}$ are, respectively, the in-plane displacements and deflection in the transverse direction of a point $(x,\ y,\ 0)$ on the midplane of the mth layer, the superscript or subscript m denotes the mth layer (with $m \in \{1,2,\ \ldots,\ N_l\}$), and $\square_{,\alpha} = \partial\square/\partial\alpha$ (with $\alpha \in \{x,\ y\}$). Note that the stretching in each of the two in-plane directions is included in the kinematic relations for the Kirchhoff plate adopted in the current study, which is represented by the first term $u_{0\alpha}^{(m)}(x,\ y)$ in Eq. (2a).

From Eqs. (2a, b), the non-zero components of the strain tensor $\boldsymbol{\epsilon}^{(m)}$ for the mth layer (with $m \in \{1,2,\ \ldots,\ N_l\}$) can be determined as

$$\epsilon_{\alpha\beta}^{(m)}(x, y, z_m) = \epsilon_{0\alpha\beta}^{(m)}(x, y) - z_m \kappa_{\alpha\beta}^{(m)}(x, y), \tag{3a}$$

where

$$\epsilon_{0\alpha\beta}^{(m)}(x, y) = \frac{1}{2}\left[u_{0\alpha,\beta}^{(m)}(x, y) + u_{0\beta,\alpha}^{(m)}(x, y)\right],\ \kappa_{\alpha\beta}^{(m)}(x, y) = w_{,\alpha\beta}^{(m)}(x, y), \tag{3b,c}$$

with $\alpha, \beta \in \{x, y\}$.

2.3 Interface model

As the layers of the composite plate are made from dissimilar materials, each layer can deform differently, resulting in stresses at the interfaces due to the thermomechanical mismatch. To describe these interfacial stresses, each interface is modeled as a fictitious thin film (adhesive) with an infinitesimal thickness $\tilde{t}_k$, in which two shear strain components $\tilde{\epsilon}_{xz}^{(k)}$ and $\tilde{\epsilon}_{yz}^{(k)}$ and one normal strain component $\tilde{\epsilon}_{zz}^{(k)}$ are non-vanishing, where the subscript or superscript k (with $k \in \{1,\ 2,\ \ldots,\ N_l - 1\}$) denotes the kth interface between the kth and $(k+1)$th layers of the composite plate.

The traction continuity requires that at the kth interface,

$$\hat{t}_\alpha^{(k)}(x, y) = -\hat{t}_\alpha^{(k+1)}(x, y),\ \hat{t}_z^{(k)}(x, y) = -\hat{t}_z^{(k+1)}(x, y), \tag{4}$$

where $\hat{t}_{\alpha}^{(k)}$ (with $\alpha \in \{x, y\}$) and $\hat{t}_{z}^{(k)}$ are the components of the traction vector at the top surface of the kth layer, and $\hat{t}_{\alpha}^{(k+1)}$ (with $\alpha \in \{x, y\}$) and $\hat{t}_{z}^{(k+1)}$ are the components of the traction vector at the bottom surface of the $(k+1)$th layer. Note that $\hat{t}_{\alpha}^{(k)}$ and $\hat{t}_{z}^{(k)}$ are related to the stress components through

$$\hat{t}_{\alpha}^{(k)} = \tau_{\alpha z}^{(k)} n_z, \; \hat{t}_{z}^{(k)} = \tau_{zz}^{(k)} n_z, \tag{5a}$$

where $\tau_{\alpha z}^{(k)}$ (with $\alpha \in \{x, y\}$) are the interfacial shear stress components, $\tau_{zz}^{(k)}$ is the interfacial normal (or peel) stress component, and n_z is the z-component of the unit outward normal on the kth interface (with $n_x = n_y = 0$). Substituting Eq. (5a) into Eq. (4) yields

$$\hat{t}_{\alpha}^{(k+1)} = -\tau_{\alpha z}^{(k)} n_z, \; \hat{t}_{z}^{(k+1)} = -\tau_{zz}^{(k)} n_z. \tag{5b}$$

On the other hand, the displacement vector can be discontinuous at the same interface, i.e.,

$$\mathbf{u}^{(k+1)}\,|_{z_{k+1}=-t_{k+1}/2} \neq \mathbf{u}^{(k)}\,|_{z_k=t_k/2}, \tag{6}$$

where $\mathbf{u}$ is the displacement vector.

The interfacial stress components $\tau_{\alpha z}^{(k)}$ and $\tau_{zz}^{(k)}$ can be related to the non-vanishing interfacial strain components through Hooke's law as follows:

$$\tau_{\alpha z}^{(k)} = 2\tilde{\mu}_k \tilde{\epsilon}_{\alpha z}^{(k)}, \tag{7a}$$

$$\tau_{zz}^{(k)} = \left(\tilde{\lambda}_k + 2\tilde{\mu}_k\right)\tilde{\epsilon}_{zz}^{(k)}, \tag{7b}$$

where $\tilde{\epsilon}_{\alpha z}^{(k)}$ (with $\alpha \in \{x, y\}$) and $\tilde{\epsilon}_{zz}^{(k)}$ are the non-vanishing interfacial strain components at the kth interface, and $\tilde{\lambda}_k$ and $\tilde{\mu}_k$ are the Lamé constants for the kth interface (modeled as a thin film).

From Eqs. (4), (5a), (5b), (7a) and (7b), it is seen that the traction continuity at the kth interface is satisfied if each of the interfacial strain components in the thin film is constant along the z-direction such that

$$\tilde{\epsilon}_{\alpha z,z}^{(k)} = 0, \; \tilde{\epsilon}_{zz,z}^{(k)} = 0, \tag{8a,b}$$

where $\alpha \in \{x, y\}$. Based on Eqs. (6) and (8a,b), the interfacial strain components $\tilde{\epsilon}_{\alpha z}^{(k)}$ and $\tilde{\epsilon}_{zz}^{(k)}$, which are taken to be uniform along the thickness of the thin film, can be identified as

$$\tilde{\epsilon}_{\alpha z}^{(k)} = \frac{1}{\tilde{t}_k}\left(u_{\alpha}^{(k+1)}\,|_{z_{k+1}=-t_{k+1}/2} - u_{\alpha}^{(k)}\,|_{z_k=t_k/2}\right), \tag{9a}$$

$$\tilde{\epsilon}_{zz}^{(k)} = \frac{1}{\tilde{t}_k}\left(u_{z}^{(k+1)}\,|_{z_{k+1}=-t_{k+1}/2} - u_{z}^{(k)}\,|_{z_k=t_k/2}\right), \tag{9b}$$

where z_k and z_{k+1} denote, respectively, the local z-coordinates of the kth and $(k+1)$th layers, t_k and t_{k+1} are, respectively, the thicknesses of the kth and $(k+1)$th layers, and $\tilde{t}_k$ is the thickness of the kth interface.

From Eqs. (2a,b), (9a) and (9b), the non-vanishing interfacial strain components at the kth interface can be obtained as

$$\tilde{\epsilon}_{\alpha z}^{(k)}(x, y) = \frac{1}{\tilde{t}_k}\left[u_{0\alpha}^{(k+1)} - u_{0\alpha}^{(k)} + \frac{1}{2}\left(t_{k+1} w_{,\alpha}^{(k+1)} + t_k w_{,\alpha}^{(k)}\right)\right], \tag{10a}$$

$$\tilde{\epsilon}_{zz}^{(k)}(x, y) = \frac{1}{\tilde{t}_k}\left(w^{(k+1)} - w^{(k)}\right). \tag{10b}$$

Note that the expressions of $\tilde{\epsilon}_{\alpha z}^{(k)}$ (with $\alpha \in \{x, y\}$) and $\tilde{\epsilon}_{zz}^{(k)}$ in Eqs. (10a) and (10b) are the same as those in the adhesive layer of a three-layer electronic assembly [36] or of an adhesively bonded composite joint [69]. These adhesive joint models evolved from the pioneering studies of Volkersen [71] and Goland and Reissner [28].

Substituting Eqs. (10a) and (10b) into Eqs. (7a) and (7b) gives the interfacial stress components as

$$\tau_{\alpha z}^{(k)}(x, y) = K_s^{(k)}\left[u_{0\alpha}^{(k+1)} - u_{0\alpha}^{(k)} + \frac{1}{2}\left(t_{k+1} w_{,\alpha}^{(k+1)} + t_k w_{,\alpha}^{(k)}\right)\right], \tag{11a}$$

$$\tau_{zz}^{(k)}(x, y) = K_n^{(k)}\left(w^{(k+1)} - w^{(k)}\right), \tag{11b}$$

where $\alpha \in \{x,\ y\}$ and

$$K_s^{(k)} = \frac{2\tilde{\mu}_k}{\tilde{t}_k},\ K_n^{(k)} = \frac{\tilde{\lambda}_k + 2\tilde{\mu}_k}{\tilde{t}_k} \tag{11c}$$

are the stiffness constants of the kth interface (with a unit of Pa/m), which are directly related to the interface thickness $\tilde{t}_k$ and interface modulus (through the Lamé constants $\tilde{\lambda}_k$ and $\tilde{\mu}_k$). It should be noted that $K_s^{(k)} \to \infty$ and $K_n^{(k)} \to \infty$ when the kth and $(k+1)$th layers are perfectly bonded and $K_s^{(k)} = K_n^{(k)} = 0$ when the two layers are completely separated. For the case with a slip interface (e.g., [64]), $w^{(k+1)} = w^{(k)}$, $u_{0\alpha}^{(k+1)} \neq u_{0\alpha}^{(k)}$, $K_n^{(k)} \to \infty$ and $0 < K_s^{(k)} < \infty$.

The interfacial constitutive model described by Eqs. (11a) and (11b) is of the spring-layer type, in which the interfacial traction vector is related to the jump in the displacement vector through the elastic stiffness of the interface (treated as a spring layer) (e.g., [7, 10, 74]). Such spring-layer interface models differ from the general imperfect interface model (e.g., [4, 30]).

The interfacial constitutive relations given in Eqs. (11a) and (11b) are similar to those used in the shear-lag model for bonded layers (joints) proposed in Chen and Nelson [9], which was expounded by Murray and Noyan [52]. Shear-lag models have also been developed to study load transfer mechanisms in fiber-reinforced composites by using cylindrical configurations (e.g., [24, 53, 74]).

2.4 Equilibrium analysis

2.4.1 Equilibrium for each layer

The energy balance for a continuum during a thermoelastic deformation, which is reversible, is governed by the first and second laws of thermodynamics and can be expressed as (e.g., [31])

$$T\,\mathrm{d}S = \mathrm{d}U - \delta W, \tag{12}$$

where T is the absolute temperature, S is the entropy, U is the internal energy, W is the mechanical work, and "d" and "δ" denote, respectively, the differentials of a state variable and a non-state variable. By using the relation $\mathrm{d}(TS) = T\,\mathrm{d}S + S\,\mathrm{d}T$ in Eq. (12), the energy balance for the mth layer of the composite plate (see Fig. 1) can be written as

$$-\mathrm{d}\Psi^{(m)} + \delta W^{(m)} - S^{(m)}\mathrm{d}T^{(m)} = 0, \tag{13}$$

where $\Psi^{(m)} = U^{(m)} - T^{(m)}S^{(m)}$ is the Helmholtz free energy of the mth layer (with $m \in \{1,2,\ \ldots,\ N_l\}$). Note that the temperature change is taken to be different in each layer of the composite plate such that $\Delta T^{(m+1)} \neq \Delta T^{(m)}$ (with $m \in \{1,2,\ \ldots,\ N_l\}$).

In a thermoelastic deformation, the Helmholtz free energy $\Psi^{(m)}$ is a function of the strain tensor $\boldsymbol{\epsilon}$ and the absolute temperature T (e.g., [29, 49]). It then follows that the change in the free energy $\mathrm{d}\Psi^{(m)}$ of the mth layer in the plate during a thermoelastic deformation can be expressed as

$$\mathrm{d}\Psi^{(m)} = \int_{V_m} \left(\sigma_{\alpha\beta}^{(m)}\delta\epsilon_{\alpha\beta}^{(m)} - s^{(m)}\mathrm{d}T^{(m)}\right)\mathrm{d}V, \tag{14}$$

where $\sigma_{\alpha\beta}^{(m)}$ (with $\alpha, \beta \in \{x, y\}$) are the stress components, $s^{(m)}$ is the entropy per unit volume, V_m is the volume occupied by the layer, and the superscript or subscript m denotes the mth layer (with $m \in \{1,2,\ \ldots,\ N_l\}$).

For isotropic linear elastic layers in the plate, the Helmholtz free energy density function $\psi^{(m)}$ in the mth layer (with $m \in \{1,2,\ \ldots,\ N_l\}$) is given by (e.g., [29, 49])

$$\begin{aligned}\psi^{(m)} = &\frac{1}{2}\lambda_m\epsilon_{\alpha\alpha}^{(m)}\epsilon_{\beta\beta}^{(m)} + \mu_m\epsilon_{\alpha\beta}^{(m)}\epsilon_{\alpha\beta}^{(m)} - 2\alpha_m(\lambda_m + \mu_m)\epsilon_{\alpha\beta}^{(m)}\delta_{\alpha\beta}\left(T^{(m)} - T_0\right)\\ &- \frac{c_0^{(m)}}{2T_0}\left(T^{(m)} - T_0\right)^2 - s_0^{(m)}T^{(m)},\end{aligned} \tag{15}$$

where λ_m and μ_m are the Lamé constants, α_m is the coefficient of thermal expansion, $c_0^{(m)}$ is the specific heat at constant strain, $s_0^{(m)}$ is the specific entropy, T_0 is the reference temperature, and $\delta_{\alpha\beta}$ is the Kronecker delta (with $\alpha,\ \beta \in \{x,\ y\}$). In reaching Eq. (15), the plane stress state has been assumed for each plate layer, with

$$\lambda_m = \frac{E_m \nu_m}{1-\nu_m^2},\ \mu_m = \frac{E_m}{2(1+\nu_m)}, \tag{16}$$

where E_m and ν_m are, respectively, Young's modulus and Poisson's ratio of the material for the mth layer (with $m \in \{1,2,\ \ldots,\ N_l\}$).

From Eq. (15), the stress components $\sigma_{\alpha\beta}^{(m)}$ and entropy per unit volume $s^{(m)}$ in the mth layer can be determined as

$$\sigma_{\alpha\beta}^{(m)}(x,y,z_m) = \frac{\partial \psi^{(m)}}{\partial \epsilon_{\alpha\beta}^{(m)}} = \lambda_m \epsilon_{\gamma\gamma}^{(m)} \delta_{\alpha\beta} + 2\mu_m \epsilon_{\alpha\beta}^{(m)} - 2\alpha_m(\lambda_m+\mu_m)\Delta T^{(m)}\delta_{\alpha\beta}, \tag{17a}$$

$$s^{(m)}(x,y,z_m) = -\frac{\partial \psi^{(m)}}{\partial T^{(m)}} = 2\alpha_m(\lambda_m+\mu_m)\epsilon_{\gamma\gamma}^{(m)} + \frac{c_0^{(m)}}{T_0}\Delta T^{(m)} + s_0^{(m)}, \tag{17b}$$

where $\Delta T^{(m)}(x,\ y) = T^{(m)}(x,\ y) - T_0$ is the temperature change in the mth layer (with $m \in \{1,2,\ \ldots,\ N_l\}$), which is taken to be varying along the x- and y-directions (but not changing with z_m).

Substituting Eq. (3a) into Eqs. (17a) and (17b) gives

$$\begin{aligned}\sigma_{\alpha\beta}^{(m)}(x,y,z_m) = {} & \lambda_m \epsilon_{0\gamma\gamma}^{(m)} \delta_{\alpha\beta} + 2\mu_m \epsilon_{0\alpha\beta}^{(m)} - z_m\left(\lambda_m \kappa_{\gamma\gamma}^{(m)}\delta_{\alpha\beta} + 2\mu_m \kappa_{\alpha\beta}^{(m)}\right) \\ & - 2\alpha_m(\lambda_m+\mu_m)\Delta T^{(m)}\delta_{\alpha\beta},\end{aligned} \tag{18a}$$

$$s^{(m)}(x,y,z_m) = 2\alpha_m(\lambda_m+\mu_m)\left(\epsilon_{0\gamma\gamma}^{(m)} - z_m\kappa_{\gamma\gamma}^{(m)}\right) + \frac{c_0^{(m)}}{T_0}\Delta T^{(m)} + s_0^{(m)}. \tag{18b}$$

The first variation of the mechanical work $W^{(m)}$ in the mth layer of the plate can be written in terms of the traction components $t_i^{(m)}$ (with $i \in \{x,\ y,\ z\}$) acting on the layer boundaries (edges), the interfacial shear stress components $\tau_{\alpha z}^{(m)}$ and $\tau_{\alpha z}^{(m-1)}$ (with $\alpha \in \{x,\ y\}$) and interfacial normal stress components $\tau_{zz}^{(m)}$ and $\tau_{zz}^{(m-1)}$ acting on the top and bottom surfaces of the layer, and the body forces $f_i^{(m)}$ acting in the layer as

$$\begin{aligned}\delta W^{(m)} = {} & \int_{V_m}\left(f_\alpha^{(m)}\delta u_\alpha^{(m)} + f_z^{(m)}\delta u_z^{(m)}\right)\mathrm{d}V + \oint_{\partial A}\int_{-t_m/2}^{t_m/2}\left(t_\alpha^{(m)}\delta u_\alpha^{(m)} + t_z^{(m)}\delta u_z^{(m)}\right)\mathrm{d}z_m\mathrm{d}l \\ & + \int_A\left[\left(\tau_{\alpha z}^{(m)}\delta u_\alpha^{(m)}\right)\Big|_{z_m=t_m/2} + \left(\tau_{zz}^{(m)}\delta u_z^{(m)}\right)\Big|_{z_m=t_m/2}\right]\mathrm{d}A \\ & - \int_A\left[\left(\tau_{\alpha z}^{(m-1)}\delta u_\alpha^{(m)}\right)\Big|_{z_m=-t_m/2} + \left(\tau_{zz}^{(m-1)}\delta u_z^{(m)}\right)\Big|_{z_m=-t_{m/2}}\right]\mathrm{d}A,\end{aligned} \tag{19}$$

where $\mathrm{d}V$, $\mathrm{d}A$ and $\mathrm{d}l$ are, respectively, the volume, area and line elements, A is the in-plane area of the layer (or plate), which is the same for all layers, and ∂A is the bounding contour of the mid-plane of the mth layer (with the area A). Note that the summation on $\alpha(\in \{x,\ y\})$ is implied in Eq. (19).

Substituting Eqs. (2a,b) and (3a)–(3c) into Eqs. (14) and (19) yields, with the help of Eqs. (11a) and (11b),

$$\begin{aligned}\mathrm{d}\Psi^{(m)} = {} & \int_A\left(-N_{\alpha\beta,\beta}^{(m)}\delta u_{0\alpha}^{(m)} + M_{\alpha\beta,\alpha\beta}^{(m)}\delta w^{(m)}\right)\mathrm{d}A + \oint_{\partial A}\left(N_{\alpha\beta}^{(m)}\delta u_{0\alpha}^{(m)}n_\beta + M_{\alpha\beta}^{(m)}\delta w_{,\alpha}^{(m)}n_\beta\right. \\ & \left. - M_{\alpha\beta,\alpha}^{(m)}\delta w^{(m)}n_\beta\right)\mathrm{d}l + \int_{V_m}\left(-s^{(m)}\mathrm{d}T^{(m)}\right)\mathrm{d}V,\end{aligned} \tag{20a}$$

$$\delta W^{(m)} = \int_A \left(q_\alpha^{(m)}\delta u_{0\alpha}^{(m)} + m_{\alpha,\alpha}^{(m)}\delta w^{(m)} + q_z^{(m)}\delta w^{(m)}\right)dA - \oint_{\partial A} m_\alpha^{(m)}\delta w^{(m)} n_\alpha dl$$
$$+ \oint_{\partial A}\left(\overline{N}_\alpha^{(m)}\delta u_{0\alpha}^{(m)} + \overline{M}_\alpha^{(m)}\delta w_{,\alpha}^{(m)} - \overline{V}_z^{(m)}\delta w^{(m)}\right)dl$$
$$+ \int_A \left[\left(\tau_{\alpha z}^{(m)} - \tau_{\alpha z}^{(m-1)}\right)\delta u_{0\alpha}^{(m)} + \frac{t_m}{2}\left(\tau_{\alpha z}^{(m)} + \tau_{\alpha z}^{(m-1)}\right)\delta w_{,\alpha}^{(m)} + \left(\tau_{zz}^{(m)} - \tau_{zz}^{(m-1)}\right)\delta w^{(m)}\right]dA$$
$$- \frac{t_m}{2}\oint_{\partial A}\left(\tau_{\alpha z}^{(m)} + \tau_{\alpha z}^{(m-1)}\right)\delta w^{(m)} n_\alpha dl, \tag{20b}$$

where the resultants are defined as

$$N_{\alpha\beta}^{(m)}(x,y) = \int_{-\frac{t_m}{2}}^{\frac{t_m}{2}} \sigma_{\alpha\beta}^{(m)}\mathrm{d}z_m,\ M_{\alpha\beta}^{(m)} = -\int_{-\frac{t_m}{2}}^{\frac{t_m}{2}} z_m\sigma_{\alpha\beta}^{(m)}\mathrm{d}z_m, \tag{21a,b}$$

$$\left(q_\alpha^{(m)}, q_z^{(m)}, m_\alpha^{(m)}\right) = \int_{-\frac{t_m}{2}}^{\frac{t_m}{2}} \left(f_\alpha^{(m)}, f_z^{(m)}, z_m f_\alpha^{(m)}\right)\mathrm{d}z_m, \tag{22a-c}$$

$$\left(\overline{N}_\alpha^{(m)}, \overline{V}_z^{(m)}, \overline{M}_\alpha^{(m)}\right) = \int_{-\frac{t_m}{2}}^{\frac{t_m}{2}} \left(t_\alpha^{(m)},\ -t_z^{(m)},\ -z_m t_\alpha^{(m)}\right)\mathrm{d}z_m. \tag{23a-c}$$

Note that the stretching energy is explicitly incorporated in the current model through the $u_{0\alpha}^{(m)}(x,\ y)$ terms, as clearly shown in Eqs. (20a) and (20b).

As Eq. (13) holds for thermoelastic deformations with arbitrary displacement and temperature fields in the mth layer (with $m \in \{1,2,\ \ldots,\ N_l\}$), the following equilibrium equations are obtained after substituting Eqs. (20a) and (20b) into Eq. (13) and applying the fundamental lemma of the calculus of variations (e.g., [68]):

$$N_{\alpha\beta,\beta}^{(m)} + \tau_{\alpha z}^{(m)} - \tau_{\alpha z}^{(m-1)} + q_\alpha^{(m)} = 0, \tag{24a}$$

$$M_{\alpha\beta,\alpha\beta}^{(m)} - \frac{t_m}{2}\left(\tau_{\alpha z,\alpha}^{(m)} + \tau_{\alpha z,\alpha}^{(m-1)}\right) - \tau_{zz}^{(m)} + \tau_{zz}^{(m-1)} - q_z^{(m)} - m_{\alpha,\alpha}^{(m)} = 0, \tag{24b}$$

along with the boundary conditions:

$$N_{\alpha\beta}^{(m)} n_\beta = \overline{N}_\alpha^{(m)} \text{ or } u_{0\alpha}^{(m)} = \overline{u}_\alpha^{(m)} \text{ on } \Gamma_m^\beta, \tag{25a}$$

$$M_{\alpha\beta,\alpha}^{(m)} n_\beta - \frac{t_m}{2}\left(\tau_{\beta z}^{(m)} + \tau_{\beta z}^{(m-1)}\right)n_\beta - m_\beta^{(m)} n_\beta = \overline{V}_z^{(m)} \text{ or } w^{(m)} = \overline{w}^{(m)} \text{ on } \Gamma_m^\beta, \tag{25b}$$

$$M_{\alpha\beta}^{(m)} n_\beta = \overline{M}_\alpha^{(m)} \text{ or } w_{,\alpha}^{(m)} = \overline{w}_{,\alpha}^{(m)} \text{ on } \Gamma_m^\beta, \tag{25c}$$

where the overhead bar indicates a prescribed value on an edge (boundary) of the mth layer, and Γ_m^β denotes an edge with the normal n_β. Note that the standard index notation with the summation convention is used in Eqs. (20a), (20b), (24a), (24b) and (25a)–(25c).

By substituting Eq. (18a) into Eqs. (21a,b), the stress resultants $N_{\alpha\beta}^{(m)}$ and $M_{\alpha\beta}^{(m)}$ in the mth layer (with $m = \{1,\ 2,\ \ldots,\ N_l\}$) can be determined in terms of $\epsilon_{0\alpha\beta}^{(m)}$ and $\kappa_{\alpha\beta}^{(m)}$ (with $\alpha,\ \beta \in \{x,\ y\}$) as

$$N_{\alpha\beta}^{(m)}(x,y) = \left(\lambda_m\epsilon_{0\gamma\gamma}^{(m)}\delta_{\alpha\beta} + 2\mu_m\epsilon_{0\alpha\beta}^{(m)}\right)t_m - 2\alpha_m(\lambda_m + \mu_m)t_m\Delta T^{(m)}\delta_{\alpha\beta}, \tag{26a}$$

$$M_{\alpha\beta}^{(m)}(x,y) = \frac{t_m^3}{12}\left(\lambda_m\kappa_{\gamma\gamma}^{(m)}\delta_{\alpha\beta} + 2\mu_m\kappa_{\alpha\beta}^{(m)}\right). \tag{26b}$$

2.4.2 Global equilibrium of the multi-layered composite plate

The summation of the local equilibrium equations in Eqs. (24a) and (24b) over all N_l layers of the plate gives

$$\sum_{m=1}^{N_l} N_{\alpha\beta,\beta}^{(m)} + \sum_{m=1}^{N_l} \tau_{\alpha z}^{(m)} - \sum_{m=1}^{N_l} \tau_{\alpha z}^{(m-1)} + \sum_{m=1}^{N_l} q_{\alpha}^{(m)} = 0, \tag{27a}$$

$$\sum_{m=1}^{N_l} M_{\alpha\beta,\alpha\beta}^{(m)} - \sum_{m=1}^{N_l} \left[\frac{t_m}{2} \left(\tau_{\alpha z,\alpha}^{(m)} + \tau_{\alpha z,\alpha}^{(m-1)} \right) \right] - \sum_{m=1}^{N_l} \tau_{zz}^{(m)} + \sum_{m=1}^{N_l} \tau_{zz}^{(m-1)} - \sum_{m=1}^{N_l} q_{z}^{(m)} - \sum_{m=1}^{N_l} m_{\alpha,\alpha}^{(m)} = 0, \tag{27b}$$

which can be rewritten as

$$\sum_{m=1}^{N_l} N_{\alpha\beta,\beta}^{(m)} + \tau_{\alpha z}^{(N_l)} - \tau_{\alpha z}^{(0)} + \sum_{m=1}^{N_l} q_{\alpha}^{(m)} = 0, \tag{28}$$

$$\sum_{m=1}^{N_l} M_{\alpha\beta,\alpha\beta}^{(m)} - \sum_{m=1}^{N_l-1} (d_{m+1} - d_m) \tau_{\alpha z,\alpha}^{(m)} - \frac{t_{N_l}}{2} \tau_{\alpha z,\alpha}^{(N_l)} - \frac{t_1}{2} \tau_{\alpha z,\alpha}^{(0)} - \tau_{zz}^{(N_l)} + \tau_{zz}^{(0)} - \sum_{m=1}^{N_l} q_{z}^{(m)} - \sum_{m=1}^{N_l} m_{\alpha,\alpha}^{(m)} = 0. \tag{29}$$

Multiplying Eq. (24a) by d_m and then summing the resulting equation from 1 to N_l will lead to

$$\sum_{m=1}^{N_l} d_m N_{\alpha\beta,\beta}^{(m)} + \sum_{m=1}^{N_l-1} (d_m - d_{m+1}) \tau_{\alpha z}^{(m)} + d_{N_l} \tau_{\alpha z}^{(N_l)} + \sum_{m=1}^{N_l} d_m q_{\alpha}^{(m)} = 0, \tag{30}$$

where use has been made of the relations $\sum_{m=1}^{N_l} d_m \tau_{\alpha z}^{(m)} - \sum_{m=1}^{N_l} d_m \tau_{\alpha z}^{(m-1)} = \sum_{m=1}^{N_l-1} (d_m - d_{m+1}) \tau_{\alpha z}^{(m)} + d_{N_l} \tau_{\alpha z}^{(N_l)} - d_1 \tau_{\alpha z}^{(0)}$ and $d_1 = 0$. Differentiating Eq. (30) with respect to x_α gives

$$\sum_{m=1}^{N_l-1} (d_{m+1} - d_m) \tau_{\alpha z,\alpha}^{(m)} = \sum_{m=1}^{N_l} d_m N_{\alpha\beta,\beta\alpha}^{(m)} + d_{N_l} \tau_{\alpha z,\alpha}^{(N_l)} + \sum_{m=1}^{N_l} d_m q_{\alpha,\alpha}^{(m)}. \tag{31}$$

Substituting Eq. (31) into Eq. (29) yields

$$\sum_{m=1}^{N_l} M_{\alpha\beta,\alpha\beta}^{(m)} - \sum_{m=1}^{N_l} d_m N_{\alpha\beta,\alpha\beta}^{(m)} - \left(\frac{t_{N_l}}{2} + d_{N_l} \right) \tau_{\alpha z,\alpha}^{(N_l)} - \frac{t_1}{2} \tau_{\alpha z,\alpha}^{(0)} - \tau_{zz}^{(N_l)} + \tau_{zz}^{(0)} - \sum_{m=1}^{N_l} d_m q_{\alpha,\alpha}^{(m)} - \sum_{m=1}^{N_l} q_{z}^{(m)} - \sum_{m=1}^{N_l} m_{\alpha,\alpha}^{(m)} = 0. \tag{32}$$

The global equilibrium equations in Eqs. (28) and (32) for the multi-layered composite plate can be written in the form:

$$\hat{N}_{\alpha\beta,\beta} + \tau_{\alpha z}^{(N_l)} - \tau_{\alpha z}^{(0)} + \hat{q}_\alpha = 0, \tag{33a}$$

$$\hat{M}_{\alpha\beta,\alpha\beta} - \left(\frac{t_{N_l}}{2} + d_{N_l} \right) \tau_{\alpha z,\alpha}^{(N_l)} - \frac{t_1}{2} \tau_{\alpha z,\alpha}^{(0)} - \tau_{zz}^{(N_l)} + \tau_{zz}^{(0)} - \sum_{m=1}^{N_l} d_m q_{\alpha,\alpha}^{(m)} - \hat{q}_z - \hat{m}_{\alpha,\alpha} = 0, \tag{33b}$$

where

$$\hat{N}_{\alpha\beta} = \sum_{m=1}^{N_l} N_{\alpha\beta}^{(m)}, \ \hat{q}_\alpha = \sum_{m=1}^{N_l} q_{\alpha}^{(m)}, \ \hat{M}_{\alpha\beta} = \sum_{m=1}^{N_l} \left(M_{\alpha\beta}^{(m)} - d_m N_{\alpha\beta}^{(m)} \right),$$

$$\hat{q}_z = \sum_{m=1}^{N_l} q_z^{(m)},\ \hat{m}_\alpha = \sum_{m=1}^{N_l} m_\alpha^{(m)}. \tag{34a-e}$$

Similarly, the global boundary conditions for the multi-layered composite plate can be obtained as

$$\hat{N}_{\alpha\beta} n_\beta = \overline{\hat{N}}_\alpha \text{ or } u_{0\alpha}^{(1)} = \overline{u}_\alpha^{(1)} \text{ on } \Gamma^\beta, \tag{35a}$$

$$\left[\hat{M}_{\alpha\beta,\alpha} - \sum_{m=1}^{N_l}\left(d_m q_\beta^{(m)}\right) - \left(\frac{t_{N_l}}{2} + d_{N_l}\right)\tau_{\beta z}^{(N_l)} - \frac{t_1}{2}\tau_{\beta z}^{(0)} - \hat{m}_\beta\right] n_\beta = \overline{\hat{V}}_z^{(m)} \text{ or } w^{(1)} = \overline{w}^{(1)} \text{ on } \Gamma^\beta, \tag{35b}$$

$$\hat{M}_{\alpha\beta} n_\beta = \overline{\hat{M}}_\alpha \text{ or } w_{,\alpha}^{(1)} = \overline{w}_{,\alpha}^{(1)} \text{ on } \Gamma^\beta, \tag{35c}$$

where

$$\overline{\hat{N}}_\alpha = \sum_{m=1}^{N_l} \overline{N}_\alpha^{(m)},\ \overline{\hat{V}}_z = \sum_{m=1}^{N_l} \overline{V}_z^{(m)},\ \overline{\hat{M}}_\alpha = \sum_{m=1}^{N_l}\left(\overline{M}_\alpha^{(m)} - d_m \overline{N}_\alpha^{(m)}\right). \tag{36}$$

3 Analytical solution

The boundary-value problem (BVP) of a multi-layered composite plate with N_l layers is defined by the $3N_l$ equilibrium equations listed in Eqs. (24a) and (24b), the $5N_l$ boundary conditions given in Eqs. (25a)–(25c), the $6N_l$ constitutive relations provided in Eqs. (26a) and (26b), and the $3(N_l - 1)$ compatibility conditions at interfaces presented in Eqs. (11a) and (11b). The solution of this BVP for a multi-layered plate subjected to arbitrary thermomechanical loading would require solving a system of coupled partial differential equations (PDEs), which can hardly be done analytically. However, symmetrically loaded square plates exhibit equal normal strains along the x- and y-directions and zero shear strain (e.g. [27, 58],), namely,

$$\epsilon_{xx}^{(m)} = \epsilon_{yy}^{(m)} = \epsilon_0^{(m)} - z_m \kappa^{(m)},\ \epsilon_{xy}^{(m)} = 0, \tag{37a,b}$$

where $\epsilon_0^{(m)}$ and $\kappa^{(m)}$ are the in-plane strain and curvature for the mth layer in the plate (with $m \in \{1, 2, \dots, N_l\}$). Note that use has been made of $\epsilon_0^{(m)} = \epsilon_{0xx}^{(m)} = \epsilon_{0yy}^{(m)}, \epsilon_{0xy}^{(m)} = 0, \kappa_{xy}^{(m)} = 0$ and $\kappa_{xx}^{(m)} = \kappa_{yy}^{(m)} = \kappa^{(m)}$ in reaching Eqs. (37a,b) from Eq. (3a). For this simplified case, the BVP for the multi-layered composite plate is governed by a system of coupled ordinary differential equations (ODEs) (rather than PDEs), for which a general analytical solution can be obtained, as shown below.

3.1 BVP for a symmetrically loaded composite square plate

For a symmetrically loaded square plate (i.e., $a = b = L$), the stress resultants $N_{\alpha\beta}^{(m)}$ and $M_{\alpha\beta}^{(m)}$ can be determined in terms of $\epsilon_0^{(m)}$ and $\kappa^{(m)}$ as, after substituting Eqs. (37a,b) into Eqs. (26a) and (26b),

$$N_{xx}^{(m)} = N_{yy}^{(m)} = N^{(m)} = 2(\lambda_m + \mu_m)\epsilon_0^{(m)} t_m - 2\alpha_m(\lambda_m + \mu_m) t_m \Delta T^{(m)},\ N_{xy}^{(m)} = 0, \tag{38a,b}$$

$$M_{xx}^{(m)} = M_{yy}^{(m)} = M^{(m)} = \frac{t_m^3}{6}(\lambda_m + \mu_m)\kappa^{(m)},\ M_{xy}^{(m)} = 0. \tag{38c,d}$$

Similarly, the interfacial shear stress components in Eq. (11a) can be expressed in terms of $\epsilon_0^{(m)}$ and $\kappa^{(m)}$. Differentiating Eq. (11a) once with respect to β (with $\beta \in \{x, y\}$) gives

$$\tau_{\alpha z,\beta}^{(m)} = K_s^{(m)}\left[u_{0\alpha,\beta}^{(m+1)} - u_{0\alpha,\beta}^{(m)} + \frac{1}{2}\left(t_{m+1} w_{,\alpha\beta}^{(m+1)} + t_m w_{,\alpha\beta}^{(m)}\right)\right], \tag{39}$$

where $\alpha \in \{x, y\}$. Using Eqs. (3b,c) and (37a,b) in Eq. (39) then leads to

$$\tau_{yz,y}^{(m)} = \tau_{xz,x}^{(m)} = \tau_{\hat{x}z,\hat{x}}^{(m)} = K_s^{(m)}\left[\epsilon_0^{(m+1)} - \epsilon_0^{(m)} + \frac{1}{2}\left(t_{m+1}\kappa^{(m+1)} + t_m \kappa^{(m)}\right)\right], \tag{40}$$

where $\hat{x}$ is either x or y.

For the current case, the equations of equilibrium in Eqs. (24a) and (24b) can be explicitly written as

$$N^{(m)}_{xx,xx} + N^{(m)}_{xy,xy} + \tau^{(m)}_{xz,x} - \tau^{(m-1)}_{xz,x} + q^{(m)}_{x,x} = 0, \tag{41a}$$

$$N^{(m)}_{yy,yy} + N^{(m)}_{yx,yx} + \tau^{(m)}_{yz,y} - \tau^{(m-1)}_{yz,y} + q^{(m)}_{y,y} = 0, \tag{41b}$$

$$M^{(m)}_{xx,xx} + 2M^{(m)}_{xy,xy} + M^{(m)}_{yy,yy} - \frac{t_m}{2}\left(\tau^{(m)}_{xz,x} + \tau^{(m)}_{yz,y} + \tau^{(m-1)}_{xz,x} + \tau^{(m-1)}_{yz,y}\right) - \tau^{(m)}_{zz} + \tau^{(m-1)}_{zz} - q^{(m)}_{z} - m^{(m)}_{x,x} - m^{(m)}_{y,y} = 0. \tag{41c}$$

Note that Eq. (41a) and Eq. (41b) are, respectively, obtained by differentiating Eq. (24a) with respect to x and y. It is clear from Eqs. (41a)–(41c) that the three equilibrium equations of the mth layer of the composite plate, which include the interfacial stresses on both the top and bottom surfaces of the layer, are coupled.

For the square plate under symmetric loading, $q^{(m)}_{x,x} = q^{(m)}_{y,y} = q^{(m)}_{\hat{x},\hat{x}}$, $m^{(m)}_{x,x} = m^{(m)}_{y,y} = m^{(m)}_{\hat{x},\hat{x}}$, $N^{(m)}_{xx} = N^{(m)}_{yy} = N^{(m)}$, $M^{(m)}_{xx} = M^{(m)}_{yy} = M^{(m)}$, $\tau^{(m)}_{xz,x} = \tau^{(m)}_{yz,y} = \tau^{(m)}_{\hat{x}z,\hat{x}}$ and $N^{(m)}_{xy} = M^{(m)}_{xy} = 0$, where the last five relations are directly obtained from Eqs. (38a)–(38d) and (40). Then, the equilibrium equations in Eqs. (41a)–(41c) reduce to

$$N^{(m)}_{,\hat{x}\hat{x}} + \tau^{(m)}_{\hat{x}z,\hat{x}} - \tau^{(m-1)}_{\hat{x}z,\hat{x}} + q^{(m)}_{\hat{x},\hat{x}} = 0, \tag{42a}$$

$$2M^{(m)}_{,\hat{x}\hat{x}} - t_m\left(\tau^{(m)}_{\hat{x}z,\hat{x}} + \tau^{(m-1)}_{\hat{x}z,\hat{x}}\right) - \tau^{(m)}_{zz} + \tau^{(m-1)}_{zz} - q^{(m)}_{z} - 2m^{(m)}_{\hat{x},\hat{x}} = 0, \tag{42b}$$

and the boundary conditions in Eqs. (25a)–(25c) become

$$N^{(m)} = \overline{N}^{(m)} \text{ or } u^{(m)}_{0\hat{x}} = \overline{u}^{(m)}_{\hat{x}} \text{ at } \hat{x} = \pm\frac{L}{2}, \tag{43a}$$

$$M^{(m)}_{,\hat{x}} - \frac{t_m}{2}\left(\tau^{(m)}_{\hat{x}z} + \tau^{(m-1)}_{\hat{x}z}\right) - m^{(m)}_{\hat{x}} = \overline{V}^{(m)}_{z} \text{ or } w^{(m)} = \overline{w}^{(m)} \text{ at } \hat{x} = \pm\frac{L}{2}, \tag{43b}$$

$$M^{(m)} = \overline{M}^{(m)} \text{ or } w^{(m)}_{,\hat{x}} = \overline{w}^{(m)}_{,\hat{x}} \text{ at } \hat{x} = \pm\frac{L}{2}, \tag{43c}$$

where $\hat{x}$ is either x or y.

Equation (42a) represents two ODEs (with $\hat{x} = x$ and $\hat{x} = y$, respectively). These ODEs are uncoupled with each other, but each of them is coupled with Eq. (42b) through $\tau^{(m)}_{\hat{x}z,\hat{x}}$ and $\tau^{(m-1)}_{\hat{x}z,\hat{x}}$. Therefore, only one of the two ODEs in Eq. (42a) needs to be solved along with Eq. (42b) as two independent equations to obtain the interfacial stress components $\tau^{(m)}_{\hat{x}z}$ and $\tau^{(m)}_{zz}$.

3.2 Analytical solution for the BVP

3.2.1 General solution

From Eqs. (38a) and (38c), it follows that

$$\epsilon^{(m)}_{0} = \frac{N^{(m)}}{c^{(m)}_{11} t_m} + \frac{d^{(m)}_{11}}{c^{(m)}_{11}}\Delta T^{(m)},\ \ \kappa^{(m)} = \frac{12M^{(m)}}{c^{(m)}_{11} t^3_m}, \tag{44a,b}$$

where

$$c^{(m)}_{11} = 2(\lambda_m + \mu_m),\ \ d^{(m)}_{11} = 2(\lambda_m + \mu_m)\alpha_m. \tag{45a,b}$$

Substituting Eqs. (44a,b) into Eq. (40) gives

$$\tau^{(m)}_{\hat{x}z,\hat{x}} = K^{(m)}_{s}\left[\frac{N^{(m+1)}}{c^{(m+1)}_{11} t_{m+1}} - \frac{N^{(m)}}{c^{(m)}_{11} t_m} + \frac{d^{(m+1)}_{11}}{c^{(m+1)}_{11}}\Delta T^{(m+1)} - \frac{d^{(m)}_{11}}{c^{(m)}_{11}}\Delta T^{(m)} + 6\left(\frac{M^{(m+1)}}{c^{(m+1)}_{11} t^2_{m+1}} + \frac{M^{(m)}}{c^{(m)}_{11} t^2_m}\right)\right]. \tag{46}$$

Differentiating Eq. (46) twice with respect to $\hat{x}$ leads to

$$\tau^{(m)}_{\hat{x}z,\hat{x}\hat{x}\hat{x}} = K_s^{(m)}\left[\frac{N^{(m+1)}_{,\hat{x}\hat{x}}}{c^{(m+1)}_{11}t_{m+1}} - \frac{N^{(m)}_{,\hat{x}\hat{x}}}{c^{(m)}_{11}t_m} + \frac{d^{(m+1)}_{11}}{c^{(m+1)}_{11}}\Delta T^{(m+1)}_{,\hat{x}\hat{x}} - \frac{d^{(m)}_{11}}{c^{(m)}_{11}}\Delta T^{(m)}_{,\hat{x}\hat{x}} + 6\left(\frac{M^{(m+1)}_{,\hat{x}\hat{x}}}{c^{(m+1)}_{11}t^2_{m+1}} + \frac{M^{(m)}_{,\hat{x}\hat{x}}}{c^{(m)}_{11}t^2_m}\right)\right]. \tag{47}$$

From the equilibrium equations in Eqs. (42a) and (42b),

$$N^{(m)}_{,\hat{x}\hat{x}} = -\tau^{(m)}_{\hat{x}z,\hat{x}} + \tau^{(m-1)}_{\hat{x}z,\hat{x}} - q^{(m)}_{\hat{x},\hat{x}}, \tag{48a}$$

$$M^{(m)}_{,\hat{x}\hat{x}} = \frac{t_m}{2}\left(\tau^{(m)}_{\hat{x}z,\hat{x}} + \tau^{(m-1)}_{\hat{x}z,\hat{x}}\right) + \frac{1}{2}\tau^{(m)}_{zz} - \frac{1}{2}\tau^{(m-1)}_{zz} + \frac{1}{2}q^{(m)}_z + m^{(m)}_{\hat{x},\hat{x}}. \tag{48b}$$

Using Eqs. (48a) and (48b) in Eq. (47) yields

$$\begin{aligned}\tau^{(m)}_{\hat{x}z,\hat{x}\hat{x}\hat{x}} = K_s^{(m)}\Bigg\{&\frac{2\tau^{(m+1)}_{\hat{x}z,\hat{x}}}{c^{(m+1)}_{11}t_{m+1}} + \frac{4\tau^{(m)}_{\hat{x}z,\hat{x}}}{c^{(m+1)}_{11}t_{m+1}} + \frac{4\tau^{(m)}_{\hat{x}z,\hat{x}}}{c^{(m)}_{11}t_m} + \frac{2\tau^{(m-1)}_{\hat{x}z,\hat{x}}}{c^{(m)}_{11}t_m} + \frac{3\tau^{(m+1)}_{zz}}{c^{(m+1)}_{11}t^2_{m+1}} - \frac{3\tau^{(m)}_{zz}}{c^{(m+1)}_{11}t^2_{m+1}}\\ &+ \frac{3\tau^{(m)}_{zz}}{c^{(m)}_{11}t^2_m} - \frac{3\tau^{(m-1)}_{zz}}{c^{(m)}_{11}t^2_m} + \frac{q^{(m)}_{\hat{x},\hat{x}}}{c^{(m)}_{11}t_m} - \frac{q^{(m+1)}_{\hat{x},\hat{x}}}{c^{(m+1)}_{11}t_{m+1}} + \frac{d^{(m+1)}_{11}}{c^{(m+1)}_{11}}\Delta T^{(m+1)}_{,\hat{x}\hat{x}}\\ &-\frac{d^{(m)}_{11}}{c^{(m)}_{11}}\Delta T^{(m)}_{,\hat{x}\hat{x}} + \frac{3q^{(m+1)}_z + 6m^{(m+1)}_{\hat{x},\hat{x}}}{c^{(m+1)}_{11}t^2_{m+1}} + \frac{3q^{(m)}_z + 6m^{(m)}_{\hat{x},\hat{x}}}{c^{(m)}_{11}t^2_m}\Bigg\}.\end{aligned} \tag{49}$$

Equation (49) can be rewritten in the form:

$$\tau^{(m)}_{\hat{x}z,\hat{x}\hat{x}\hat{x}} = \beta^{(m)}_1\tau^{(m+1)}_{\hat{x}z,\hat{x}} + \beta^{(m)}_0\tau^{(m)}_{\hat{x}z,\hat{x}} + \beta^{(m)}_{-1}\tau^{(m-1)}_{\hat{x}z,\hat{x}} + \alpha^{(m)}_1\tau^{(m+1)}_{zz} + \alpha^{(m)}_0\tau^{(m)}_{zz} + \alpha^{(m)}_{-1}\tau^{(m-1)}_{zz} + \eta^{(m)}_{\hat{x}} + \eta^{(m)}_z, \tag{50}$$

where

$$\begin{aligned}\beta^{(m)}_{-1} &= \frac{2K^{(m)}_s}{c^{(m)}_{11}t_m},\quad \beta^{(m)}_0 = \frac{4K^{(m)}_s}{c^{(m+1)}_{11}t_{m+1}} + \frac{4K^{(m)}_s}{c^{(m)}_{11}t_m},\quad \beta^{(m)}_1 = \frac{2K^{(m)}_s}{c^{(m+1)}_{11}t_{m+1}},\\ \alpha^{(m)}_{-1} &= -\frac{3K^{(m)}_s}{c^{(m)}_{11}t^2_m},\quad \alpha^{(m)}_0 = \frac{3K^{(m)}_s}{c^{(m)}_{11}t^2_m} - \frac{3K^{(m)}_s}{c^{(m+1)}_{11}t^2_{m+1}},\quad \alpha^{(m)}_1 = \frac{3K^{(m)}_s}{c^{(m+1)}_{11}t^2_{m+1}},\\ \eta^{(m)}_{\hat{x}} &= \frac{K^{(m)}_s}{c^{(m)}_{11}}\left(\frac{q^{(m)}_{\hat{x},\hat{x}}}{t_m} - d^{(m)}_{11}\Delta T^{(m)}_{,\hat{x}\hat{x}}\right) - \frac{K^{(m)}_s}{c^{(m+1)}_{11}}\left(\frac{q^{(m+1)}_{\hat{x},\hat{x}}}{t_{m+1}} - d^{(m+1)}_{11}\Delta T^{(m+1)}_{,\hat{x}\hat{x}}\right),\\ \eta^{(m)}_z &= \frac{3K^{(m)}_s}{c^{(m+1)}_{11}t^2_{m+1}}\left(q^{(m+1)}_z + 2m^{(m+1)}_{\hat{x},\hat{x}}\right) + \frac{3K^{(m)}_s}{c^{(m)}_{11}t^2_m}\left(q^{(m)}_z + 2m^{(m)}_{\hat{x},\hat{x}}\right).\end{aligned} \tag{51}$$

The unknowns in Eq. (50) are the interfacial shear stresses $\tau^{(m+1)}_{\hat{x}z}$, $\tau^{(m)}_{\hat{x}z}$ and $\tau^{(m-1)}_{\hat{x}z}$ and interfacial normal stresses $\tau^{(m+1)}_{zz}$, $\tau^{(m)}_{zz}$ and $\tau^{(m-1)}_{zz}$. To find these quantities, an additional differential equation is required for each layer, which can be obtained by considering the constitutive relation for the interfacial normal stress in Eq. (11b). In particular, differentiating Eq. (11b) four times with respect to $\hat{x}$ yields

$$\tau^{(m)}_{zz,\hat{x}\hat{x}\hat{x}\hat{x}} = K^{(m)}_n\left(\kappa^{(m+1)}_{,\hat{x}\hat{x}} - \kappa^{(m)}_{,\hat{x}\hat{x}}\right), \tag{52}$$

where use has been made of Eq. (3c). Using Eq. (44b) in Eq. (52) gives

$$\tau^{(m)}_{zz,\hat{x}\hat{x}\hat{x}\hat{x}} = 12K^{(m)}_n\left(\frac{M^{(m+1)}_{,\hat{x}\hat{x}}}{c^{(m+1)}_{11}t^3_{m+1}} - \frac{M^{(m)}_{,\hat{x}\hat{x}}}{c^{(m)}_{11}t^3_m}\right). \tag{53}$$

Substituting Eq. (48b) into Eq. (53) leads to

$$\tau^{(m)}_{zz,\hat{x}\hat{x}\hat{x}\hat{x}} = 6K^{(m)}_n\left(\frac{\tau^{(m+1)}_{\hat{x}z,\hat{x}}}{c^{(m+1)}_{11}t^2_{m+1}} + \frac{\tau^{(m)}_{\hat{x}z,\hat{x}}}{c^{(m+1)}_{11}t^2_{m+1}} + \frac{\tau^{(m+1)}_{zz}}{c^{(m+1)}_{11}t^3_{m+1}} - \frac{\tau^{(m)}_{zz}}{c^{(m+1)}_{11}t^3_{m+1}} + \frac{q^{(m+1)}_z + 2m^{(m+1)}_{\hat{x},\hat{x}}}{c^{(m+1)}_{11}t^3_{m+1}}\right.$$
$$\left. - \frac{\tau^{(m)}_{\hat{x}z,\hat{x}}}{c^{(m)}_{11}t^2_{m}} - \frac{\tau^{(m-1)}_{\hat{x}z,\hat{x}}}{c^{(m)}_{11}t^2_{m}} - \frac{\tau^{(m)}_{zz}}{c^{(m)}_{11}t^3_{m}} + \frac{\tau^{(m-1)}_{zz}}{c^{(m)}_{11}t^3_{m}} - \frac{q^{(m)}_z + 2m^{(m)}_{\hat{x},\hat{x}}}{c^{(m)}_{11}t^3_{m}}\right). \tag{54}$$

Equation (54) can be rewritten in the following form:

$$\tau^{(m)}_{zz,\hat{x}\hat{x}\hat{x}\hat{x}} = \gamma^{(m)}_1\tau^{(m+1)}_{\hat{x}z,\hat{x}} + \gamma^{(m)}_0\tau^{(m)}_{\hat{x}z,\hat{x}} + \gamma^{(m)}_{-1}\tau^{(m-1)}_{\hat{x}z,\hat{x}} + \xi^{(m)}_1\tau^{(m+1)}_{zz} + \xi^{(m)}_0\tau^{(m)}_{zz} + \xi^{(m)}_{-1}\tau^{(m-1)}_{zz} + \chi^{(m)}_z, \tag{55}$$

where

$$\gamma^{(m)}_{-1} = -\frac{6K^{(m)}_n}{c^{(m)}_{11}t^2_m},\ \gamma^{(m)}_0 = \frac{6K^{(m)}_n}{c^{(m+1)}_{11}t^2_{m+1}} - \frac{6K^{(m)}_n}{c^{(m)}_{11}t^2_m},\ \gamma^{(m)}_1 = \frac{6K^{(m)}_n}{c^{(m+1)}_{11}t^2_{m+1}},$$
$$\xi^{(m)}_{-1} = \frac{6K^{(m)}_n}{c^{(m)}_{11}t^3_m},\ \xi^{(m)}_0 = -\frac{6K^{(m)}_n}{c^{(m+1)}_{11}t^3_{m+1}} - \frac{6K^{(m)}_n}{c^{(m)}_{11}t^3_m},\ \xi^{(m)}_1 = \frac{6K^{(m)}_n}{c^{(m+1)}_{11}t^3_{m+1}}, \tag{56}$$
$$\chi^{(m)}_z = \frac{6K^{(m)}_n}{c^{(m+1)}_{11}t^3_{m+1}}\left(q^{(m+1)}_z + 2m^{(m+1)}_{\hat{x},\hat{x}}\right) - \frac{6K^{(m)}_n}{c^{(m)}_{11}t^3_m}\left(q^{(m)}_z + 2m^{(m)}_{\hat{x},\hat{x}}\right).$$

Equations (50) and (55) form a system of $2(N_l-1)$ equations, which can be explicitly expressed as

$$\begin{aligned}
\tau^{(1)}_{\hat{x}z,\hat{x}\hat{x}\hat{x}} &= \beta^{(1)}_1\tau^{(2)}_{\hat{x}z,\hat{x}} + \beta^{(1)}_0\tau^{(1)}_{\hat{x}z,\hat{x}} + \beta^{(1)}_{-1}\tau^{(0)}_{\hat{x}z,\hat{x}} + \alpha^{(1)}_1\tau^{(2)}_{zz} + \alpha^{(1)}_0\tau^{(1)}_{zz} + \alpha^{(1)}_{-1}\tau^{(0)}_{zz} + \eta^{(1)}_{\hat{x}} + \eta^{(1)}_z,\\
\tau^{(2)}_{\hat{x}z,\hat{x}\hat{x}\hat{x}} &= \beta^{(2)}_1\tau^{(3)}_{\hat{x}z,\hat{x}} + \beta^{(2)}_0\tau^{(2)}_{\hat{x}z,\hat{x}} + \beta^{(2)}_{-1}\tau^{(1)}_{\hat{x}z,\hat{x}} + \alpha^{(2)}_1\tau^{(3)}_{zz} + \alpha^{(2)}_0\tau^{(2)}_{zz} + \alpha^{(2)}_{-1}\tau^{(1)}_{zz} + \eta^{(2)}_{\hat{x}} + \eta^{(2)}_z,\\
&\ \ \vdots\\
\tau^{(N_l-2)}_{\hat{x}z,\hat{x}\hat{x}\hat{x}} &= \beta^{(N_l-2)}_1\tau^{(N_l-1)}_{\hat{x}z,\hat{x}} + \beta^{(N_l-2)}_0\tau^{(N_l-2)}_{\hat{x}z,\hat{x}} + \beta^{(N_l-2)}_{-1}\tau^{(N_l-3)}_{\hat{x}z,\hat{x}} + \alpha^{(N_l-2)}_1\tau^{(N_l-1)}_{zz}\\
&\quad + \alpha^{(N_l-2)}_0\tau^{(N_l-2)}_{zz} + \alpha^{(N_l-2)}_{-1}\tau^{(N_l-3)}_{zz} + \eta^{(N_l-2)}_{\hat{x}} + \eta^{(N_l-2)}_z,\\
\tau^{(N_l-1)}_{\hat{x}z,\hat{x}\hat{x}\hat{x}} &= \beta^{(N_l-1)}_1\tau^{(N_l)}_{\hat{x}z,\hat{x}} + \beta^{(N_l-1)}_0\tau^{(N_l-1)}_{\hat{x}z,\hat{x}} + \beta^{(N_l-1)}_{-1}\tau^{(N_l-2)}_{\hat{x}z,\hat{x}} + \alpha^{(N_l-1)}_1\tau^{(N_l)}_{zz}\\
&\quad + \alpha^{(N_l-1)}_0\tau^{(N_l-1)}_{zz} + \alpha^{(N_l-1)}_{-1}\tau^{(N_l-2)}_{zz} + \eta^{(N_l-1)}_{\hat{x}} + \eta^{(N_l-1)}_z,
\end{aligned} \tag{57a}$$

$$\begin{aligned}
\tau^{(1)}_{zz,\hat{x}\hat{x}\hat{x}\hat{x}} &= \gamma^{(1)}_1\tau^{(2)}_{\hat{x}z,\hat{x}} + \gamma^{(1)}_0\tau^{(1)}_{\hat{x}z,\hat{x}} + \gamma^{(1)}_{-1}\tau^{(0)}_{\hat{x}z,\hat{x}} + \xi^{(1)}_1\tau^{(2)}_{zz} + \xi^{(1)}_0\tau^{(1)}_{zz} + \xi^{(1)}_{-1}\tau^{(0)}_{zz} + \chi^{(1)}_z,\\
\tau^{(2)}_{zz,\hat{x}\hat{x}\hat{x}\hat{x}} &= \gamma^{(2)}_1\tau^{(3)}_{\hat{x}z,\hat{x}} + \gamma^{(2)}_0\tau^{(2)}_{\hat{x}z,\hat{x}} + \gamma^{(2)}_{-1}\tau^{(1)}_{\hat{x}z,\hat{x}} + \xi^{(2)}_1\tau^{(3)}_{zz} + \xi^{(2)}_0\tau^{(2)}_{zz} + \xi^{(2)}_{-1}\tau^{(1)}_{zz} + \chi^{(2)}_z,\\
&\ \ \vdots\\
\tau^{(N_l-2)}_{zz,\hat{x}\hat{x}\hat{x}\hat{x}} &= \gamma^{(N_l-2)}_1\tau^{(N_l-1)}_{\hat{x}z,\hat{x}} + \gamma^{(N_l-2)}_0\tau^{(N_l-2)}_{\hat{x}z,\hat{x}} + \gamma^{(N_l-2)}_{-1}\tau^{(N_l-3)}_{\hat{x}z,\hat{x}} + \xi^{(N_l-2)}_1\tau^{(N_l-1)}_{zz}\\
&\quad + \xi^{(N_l-2)}_0\tau^{(N_l-2)}_{zz} + \xi^{(N_l-2)}_{-1}\tau^{(N_l-3)}_{zz} + \chi^{(N_l-2)}_z,\\
\tau^{(N_l-1)}_{zz,\hat{x}\hat{x}\hat{x}\hat{x}} &= \gamma^{(N_l-1)}_1\tau^{(N_l)}_{\hat{x}z,\hat{x}} + \gamma^{(N_l-1)}_0\tau^{(N_l-1)}_{\hat{x}z,\hat{x}} + \gamma^{(N_l-1)}_{-1}\tau^{(N_l-2)}_{\hat{x}z,\hat{x}} + \xi^{(N_l-1)}_1\tau^{(N_l)}_{zz}\\
&\quad + \xi^{(N_l-1)}_0\tau^{(N_l-1)}_{zz} + \xi^{(N_l-1)}_{-1}\tau^{(N_l-2)}_{zz} + \chi^{(N_l-1)}_z.
\end{aligned} \tag{57b}$$

From Eqs. (57a) and (57b), $\tau^{(2)}_{\hat{x}z,\hat{x}}$, $\tau^{(3)}_{\hat{x}z,\hat{x}}$, …, $\tau^{(N_l-1)}_{\hat{x}z,\hat{x}}$ and $\tau^{(2)}_{zz}$, $\tau^{(3)}_{zz}$, …, $\tau^{(N_l-1)}_{zz}$ can be sequentially obtained in terms of $\tau^{(1)}_{\hat{x}z,\hat{x}}$ and $\tau^{(1)}_{zz}$ as, by using the first to the (N_l-2)th (the second last) equations in Eqs. (57a) and (57b), respectively,

$$\tau^{(2)}_{\hat{x}z,\hat{x}} = \frac{1}{\beta^{(1)}_1}\left\{\tau^{(1)}_{\hat{x}z,\hat{x}\hat{x}\hat{x}} - \beta^{(1)}_0\tau^{(1)}_{\hat{x}z,\hat{x}} - \beta^{(1)}_{-1}\tau^{(0)}_{\hat{x}z,\hat{x}} - \alpha^{(1)}_1\tau^{(2)}_{zz} - \alpha^{(1)}_0\tau^{(1)}_{zz} - \alpha^{(1)}_{-1}\tau^{(0)}_{zz} - \eta^{(1)}_{\hat{x}} - \eta^{(1)}_z\right\},$$

$$\tau_{\hat{x}z,\hat{x}}^{(3)} = \frac{1}{\beta_1^{(2)}}\left\{\tau_{\hat{x}z,\hat{x}\hat{x}\hat{x}}^{(2)} - \beta_0^{(2)}\tau_{\hat{x}z,\hat{x}}^{(2)} - \beta_{-1}^{(2)}\tau_{\hat{x}z,\hat{x}}^{(1)} - \alpha_1^{(2)}\tau_{zz}^{(3)} - \alpha_0^{(2)}\tau_{zz}^{(2)} - \alpha_{-1}^{(2)}\tau_{zz}^{(1)} - \eta_{\hat{x}}^{(2)} - \eta_z^{(2)}\right\},$$

$$\vdots$$

$$\tau_{\hat{x}z,\hat{x}}^{(N_l-1)} = \frac{1}{\beta_1^{(N_l-2)}}\left\{\tau_{\hat{x}z,\hat{x}\hat{x}\hat{x}}^{(N_l-2)} - \beta_0^{(N_l-2)}\tau_{\hat{x}z,\hat{x}}^{(N_l-2)} - \beta_{-1}^{(N_l-2)}\tau_{\hat{x}z,\hat{x}}^{(N_l-3)} - \alpha_1^{(N_l-2)}\tau_{zz}^{(N_l-1)}\right.$$
$$\left. -\alpha_0^{(N_l-2)}\tau_{zz}^{(N_l-2)} - \alpha_{-1}^{(N_l-2)}\tau_{zz}^{(N_l-3)} - \eta_{\hat{x}}^{(N_l-2)} - \eta_z^{(N_l-2)}\right\}, \tag{58a}$$

$$\tau_{zz}^{(2)} = \frac{1}{\xi_1^{(1)}}\left\{\tau_{zz,\hat{x}\hat{x}\hat{x}\hat{x}}^{(1)} - \gamma_1^{(1)}\tau_{\hat{x}z,\hat{x}}^{(2)} - \gamma_0^{(1)}\tau_{\hat{x}z,\hat{x}}^{(1)} - \gamma_{-1}^{(1)}\tau_{\hat{x}z,\hat{x}}^{(0)} - \xi_0^{(1)}\tau_{zz}^{(1)} - \xi_{-1}^{(1)}\tau_{zz}^{(0)} - \chi_z^{(1)}\right\},$$

$$\tau_{zz}^{(3)} = \frac{1}{\xi_1^{(2)}}\left\{\tau_{zz,\hat{x}\hat{x}\hat{x}\hat{x}}^{(2)} - \gamma_1^{(2)}\tau_{\hat{x}z,\hat{x}}^{(3)} - \gamma_0^{(2)}\tau_{\hat{x}z,\hat{x}}^{(2)} - \gamma_{-1}^{(2)}\tau_{\hat{x}z,\hat{x}}^{(1)} - \xi_0^{(2)}\tau_{zz}^{(2)} - \xi_{-1}^{(2)}\tau_{zz}^{(1)} - \chi_z^{(2)}\right\},$$

$$\vdots$$

$$\tau_{zz}^{(N_l-1)} = \frac{1}{\xi_1^{(N_l-2)}}\left\{\tau_{zz,\hat{x}\hat{x}\hat{x}\hat{x}}^{(N_l-2)} - \gamma_1^{(N_l-2)}\tau_{\hat{x}z,\hat{x}}^{(N_l-1)} - \gamma_0^{(N_l-2)}\tau_{\hat{x}z,\hat{x}}^{(N_l-2)} - \gamma_{-1}^{(N_l-2)}\tau_{\hat{x}z,\hat{x}}^{(N_l-3)}\right.$$
$$\left. -\xi_0^{(N_l-2)}\tau_{zz}^{(N_l-2)} - \xi_{-1}^{(N_l-2)}\tau_{zz}^{(N_l-3)} - \chi_z^{(N_l-2)}\right\}. \tag{58b}$$

Substituting Eqs. (58a) and (58b) into the $(N_l - 1)$th (the last) equation in Eqs. (57a) and (57b), respectively, leads to two coupled ODEs in terms of $\tau_{\hat{x}z,\hat{x}}^{(1)}$ and $\tau_{zz}^{(1)}$, which can be written in the following general form:

$$A_{2(2N_l-4)}\frac{\mathrm{d}^{2(2N_l-4)}\tau_{\hat{x}z,\hat{x}}^{(1)}}{\mathrm{d}\hat{x}^{2(2N_l-4)}} + A_{2(2N_l-5)}\frac{\mathrm{d}^{2(2N_l-5)}\tau_{\hat{x}z,\hat{x}}^{(1)}}{\mathrm{d}\hat{x}^{2(2N_l-5)}} + A_{2(2N_l-6)}\frac{\mathrm{d}^{2(2N_l-6)}\tau_{\hat{x}z,\hat{x}}^{(1)}}{\mathrm{d}\hat{x}^{2(2N_l-6)}} + \cdots + A_2\frac{\mathrm{d}^2\tau_{\hat{x}z,\hat{x}}^{(1)}}{\mathrm{d}\hat{x}^2}$$
$$+ A_0\tau_{\hat{x}z,\hat{x}}^{(1)} + B_{2(2N_l-3)}\frac{\mathrm{d}^{2(2N_l-3)}\tau_{zz}^{(1)}}{\mathrm{d}\hat{x}^{2(2N_l-3)}} + B_{2(2N_l-4)}\frac{\mathrm{d}^{2(2N_l-4)}\tau_{zz}^{(1)}}{\mathrm{d}\hat{x}^{2(2N_l-4)}}$$
$$+ B_{2(2N_l-5)}\frac{\mathrm{d}^{2(2N_l-5)}\tau_{zz}^{(1)}}{\mathrm{d}\hat{x}^{2(2N_l-5)}} + \cdots + B_2\frac{\mathrm{d}^2\tau_{zz}^{(1)}}{\mathrm{d}\hat{x}^2} + B_0\tau_{zz}^{(1)} = P_1, \tag{59}$$

$$C_{2(2N_l-3)}\frac{\mathrm{d}^{2(2N_l-3)}\tau_{\hat{x}z,\hat{x}}^{(1)}}{\mathrm{d}\hat{x}^{2(2N_l-3)}} + C_{2(2N_l-4)}\frac{\mathrm{d}^{2(2N_l-4)}\tau_{\hat{x}z,\hat{x}}^{(1)}}{\mathrm{d}\hat{x}^{2(2N_l-4)}} + C_{2(2N_l-5)}\frac{\mathrm{d}^{2(2N_l-5)}\tau_{\hat{x}z,\hat{x}}^{(1)}}{\mathrm{d}\hat{x}^{2(2N_l-5)}} + \cdots + C_2\frac{\mathrm{d}^2\tau_{\hat{x}z,\hat{x}}^{(1)}}{\mathrm{d}\hat{x}^2}$$
$$+ C_0\tau_{\hat{x}z,\hat{x}}^{(1)} + D_{2(2N_l-2)}\frac{\mathrm{d}^{2(2N_l-2)}\tau_{zz}^{(1)}}{\mathrm{d}\hat{x}^{2(2N_l-2)}} + D_{2(2N_l-3)}\frac{\mathrm{d}^{2(2N_l-3)}\tau_{zz}^{(1)}}{\mathrm{d}\hat{x}^{2(2N_l-3)}}$$
$$+ D_{2(2N_l-4)}\frac{\mathrm{d}^{2(2N_l-4)}\tau_{zz}^{(1)}}{\mathrm{d}\hat{x}^{2(2N_l-4)}} + \cdots + D_2\frac{\mathrm{d}^2\tau_{zz}^{(1)}}{\mathrm{d}\hat{x}^2} + D_0\tau_{zz}^{(1)} = P_2, \tag{60}$$

where $A_{2(2N_l-4)}$, $A_{2(2N_l-5)}$, …, A_2, A_0, $B_{2(2N_l-3)}$, $B_{2(2N_l-4)}$, …, B_2, B_0, $C_{2(2N_l-3)}$, $C_{2(2N_l-4)}$, …, C_2, C_0, $D_{2(2N_l-2)}$, $D_{2(2N_l-3)}$, …, D_2 and D_0 are constant coefficients that depend on the material properties and geometrical parameters of the layers in the composite plate, and P_1 and P_2 are inhomogeneous terms that depend on the applied mechanical and thermal loads as well as the geometrical and material constants of each layer. The expressions of these coefficients and inhomogeneous terms are case-specific. For the two-layer and three-layer composite plates, these expressions are explicitly provided in Sect. 4.

The two ODEs in Eqs. (59) and (60) can be analytically solved for $\tau_{\hat{x}z,\hat{x}}^{(1)}$ and $\tau_{zz}^{(1)}$ by using the superposition principle. For the case with P_1 and P_2 being constants, the general solution of these two ODEs can be obtained in the form:

$$\tau_{\hat{x}z,\hat{x}}^{(1)} = \sum_{n=1}^{4(2N_l-3)} \overline{C}_n\Lambda_n\exp\left(\lambda_n\hat{x}\right) - \frac{B_0P_2 - D_0P_1}{A_0D_0 - B_0C_0}, \tag{61a}$$

$$\tau_{zz}^{(1)} = \sum_{n=1}^{4(2N_l-3)} \overline{C}_n\exp\left(\lambda_n\hat{x}\right) + \frac{A_0P_2 - C_0P_1}{A_0D_0 - B_0C_0}, \tag{61b}$$

where the summation in each expression represents the general solution of the homogeneous part of the final, decoupled ODE for $\tau^{(1)}_{\hat{x}z,\hat{x}}$ or $\tau^{(1)}_{zz}$, $\hat{x}$ denotes x or y, $\overline{C}_n$ (with $n \in \{1,2,\ldots,4(2N_l-3)\}$) are constants to be determined from the boundary conditions, λ_n is the nth root of the $4(2N_l-3)$th–degree polynomial equation:

$$\sum_{q=0}^{2(2N_l-3)}\left[\sum_{m=0}^{(2N_l-3)}\left(A_{2m}D_{2(q-m)}-B_{2m}C_{2(q-m)}\right)\right]\lambda^{2q}=0, \tag{62}$$

and Λ_n (with $n \in \{1,2,\ldots,4(2N_l-3)\}$) are constants related to λ_n through

$$\Lambda_n=-\frac{\sum_{q=0}^{2(2N_l-3)-1}Q_{2q}\lambda_n^{2q}}{Q_d}, \tag{63}$$

where Q_{2q} (with $q \in \{0,1,2,\ldots,2(2N_l-3)-1\}$) and Q_d are constants that depend on the coefficients $A_{2(2N_l-4)}, A_{2(2N_l-5)},\ldots,A_2,A_0,B_{2(2N_l-3)},B_{2(2N_l-4)},\ldots,B_2,B_0,C_{2(2N_l-3)},C_{2(2N_l-4)},\ldots,C_2,C_0,D_{2(2N_l-2)}$, $D_{2(2N_l-3)},\ldots,D_2$ and D_0.

From Eqs. (61b) and (58b), the interfacial normal stress $\tau^{(m)}_{zz}$ (with $m \in \{1,2,\ldots,N_l-1\}$) can be determined, and from Eqs. (61a) and (58a) the interfacial shear stress $\tau^{(m)}_{\hat{x}z}$ (with $m \in \{1,2,\ldots,N_l-1\}$ and $\hat{x}=x$ or y) can be obtained by directly integrating $\tau^{(m)}_{\hat{x}z,\hat{x}}$, which gives

$$\tau^{(m)}_{\hat{x}z}=\int\tau^{(m)}_{\hat{x}z,\hat{x}}\mathrm{d}\hat{x}+F^{(m)}, \tag{64}$$

where $F^{(m)}$ ($m \in \{1,2,\ldots,N_l-1\}$) are integration constants.

After $\tau^{(m)}_{\hat{x}z}$ and $\tau^{(m)}_{zz}$ ($m \in \{1,2,\ldots,N_l-1\}$) become known, the axial force $N^{(m)}$ and bending moment $M^{(m)}$ can be found from the equilibrium equations in Eqs. (42a) and (42b) as

$$N^{(m)}=\int\tau^{(m-1)}_{\hat{x}z}\mathrm{d}\hat{x}-\int\tau^{(m)}_{\hat{x}z}\mathrm{d}\hat{x}-\int q^{(m)}_{\hat{x}}\mathrm{d}\hat{x}+G^{(m)}, \tag{65a}$$

$$\begin{aligned}M^{(m)}=&\frac{t_m}{2}\left(\int\tau^{(m)}_{\hat{x}z}\mathrm{d}\hat{x}+\int\tau^{(m-1)}_{\hat{x}z}\mathrm{d}\hat{x}\right)+\frac{1}{2}\int\left[\int\left(\tau^{(m)}_{zz}-\tau^{(m-1)}_{zz}+q^{(m)}_z+2m^{(m)}_{\hat{x},\hat{x}}\right)\mathrm{d}\hat{x}\right]\mathrm{d}\hat{x}\\&+J^{(m)}_1\hat{x}+J^{(m)}_2,\end{aligned} \tag{65b}$$

where $G^{(m)}$, $J^{(m)}_1$ and $J^{(m)}_2$ ($m \in \{1,2,\ldots,N_l\}$) are integration constants to be determined from the boundary conditions in Eqs. (43a)–(43c).

With the axial force $N^{(m)}$ and bending moment $M^{(m)}$ obtained in Eqs. (65a) and (65b), the axial strain $\epsilon^{(m)}_0$ and curvature $\kappa^{(m)}$ (with $m \in \{1,2,\ldots,N_l\}$) can be readily determined from Eqs. (44a,b).

3.2.2 Determination of $\overline{C}_n$

To obtain the constants $\overline{C}_n$ in Eqs. (61a) and (61b), the following $4(N_l-1)$ boundary conditions for $\tau^{(m)}_{\hat{x}z,\hat{x}}$ and $\tau^{(m)}_{zz}$ (with $m \in \{1,2,\ldots,N_l-1\}$) can be employed:

$$\begin{aligned}\tau^{(m)}_{\hat{x}z,\hat{x}}|_{\hat{x}=\pm L/2}=&K^{(m)}_s\left[\frac{\overline{N}^{(m+1)}}{c^{(m+1)}_{11}t_{m+1}}-\frac{\overline{N}^{(m)}}{c^{(m)}_{11}t_m}+\frac{d^{(m+1)}_{11}}{c^{(m+1)}_{11}}\Delta T^{(m+1)}-\frac{d^{(m)}_{11}}{c^{(m)}_{11}}\Delta T^{(m)}+6\left(\frac{\overline{M}^{(m+1)}}{c^{(m+1)}_{11}t^2_{m+1}}+\frac{\overline{M}^{(m)}}{c^{(m)}_{11}t^2_m}\right)\right]\Bigg|_{\hat{x}=\pm\frac{L}{2}}\\ \text{or }&\left(\int\tau^{(m)}_{\hat{x}z,\hat{x}}\mathrm{d}\hat{x}\right)\Bigg|_{\hat{x}=\pm L/2}=K^{(m)}_s\left[\overline{u}^{(m+1)}_{\hat{x}}-\overline{u}^{(m)}_{\hat{x}}+\frac{1}{2}\left(t_{m+1}\overline{w}^{(m+1)}_{,\hat{x}}+t_m\overline{w}^{(m)}_{,\hat{x}}\right)\right]\Bigg|_{\hat{x}=\pm\frac{L}{2}},\end{aligned} \tag{66a}$$

$$\tau^{(m)}_{zz,\hat{x}\hat{x}}\Big|_{\hat{x}=\pm L/2}=12K^{(m)}_n\left(\frac{\overline{M}^{(m+1)}}{c^{(m+1)}_{11}t^3_{m+1}}-\frac{\overline{M}^{(m)}}{c^{(m)}_{11}t^3_m}\right)\Bigg|_{\hat{x}=\pm\frac{L}{2}}\text{ or }\tau^{(m)}_{zz,\hat{x}}|_{\hat{x}=\pm L/2}=K^{(m)}_n\left(\overline{w}^{(m+1)}_{,\hat{x}}-\overline{w}^{(m)}_{,\hat{x}}\right)\Big|_{\hat{x}=\pm\frac{L}{2}}, \tag{66b}$$

where Eq. (66a) is directly obtained from Eqs. (46), (11a), (43a) and (43c), while Eq. (66b) follows from Eqs. (53), (11b) and (43c), with $\overline{N}^{(m)}$ and $\overline{M}^{(m)}$ being the force and moment acting at the edges of the mth layer,

$\overline{u}_{\hat{x}}^{(m)}$ (with $\hat{x} = x$ or y) and $\overline{w}^{(m)}$ being the in-plane displacement and deflection prescribed at the edges of the mth layer, and $\Delta T^{(m)}|_{\hat{x}=\pm L/2}$ being the amount of the temperature change at the edges of the mth layer ($m \in \{1,2, \ldots, N_l\}$). Each of Eqs. (66a) and (66b) provides $2(N_l - 1)$ boundary conditions, which form a system of $4(N_l - 1)$ algebraic equations that can be solved for the constants $\overline{C}_n$.

The expressions of $\tau_{\hat{x}z,\hat{x}}^{(1)}$ and $\tau_{zz}^{(1)}$ depend on λ_n, which are the roots of the polynomial equation in Eq. (62). This polynomial equation can be rewritten in terms of $Z = \lambda^2$ as

$$\sum_{q=0}^{2(2N_l-3)} \left[\sum_{m=0}^{(2N_l-3)} \left(A_{2m} D_{2(q-m)} - B_{2m} C_{2(q-m)} \right) \right] Z^q = 0, \tag{67}$$

which can be solved to obtain its $2(2N_l - 3)$ roots Z_k (with $k \in \{1,2, \ldots, 2(2N_l - 3)\}$).

The roots of Eq. (67) can be real or complex. Based on Descartes's rule of signs, the $2(2N_l - 3)$ roots of Eq. (67) can be obtained all real, denoted by Z_p. In this case, the roots are associated with $4(2N_l - 3)$ constants $\overline{C}_n$ involved in the interfacial stress components $\tau_{\hat{x}z}^{(1)}$ and $\tau_{zz}^{(1)}$ listed in Eqs. (61a) and (61b). This requires $4(2N_l - 3)$ independent equations to determine $\overline{C}_n$ (with $n \in \{1,2, \ldots, 4(2N_l - 3)\}$). However, the total number of independent boundary conditions for $\tau_{\hat{x}z}^{(1)}$ and $\tau_{zz}^{(1)}$ given in Eqs. (66a) and (66b) is only 4 $(N_l - 1)$. This mismatch leads to an ill-posed BVP for the case where all the roots are real. For a well-posed BVP, Eq. (67) must have some conjugated complex roots. Each pair of the conjugated complex roots Z_{2n-1} and Z_{2n} of Eq. (67) can provide two additional relations among the constants $\overline{C}_n$ (see Eqs. (A7a,b) in Appendix A), thereby resulting in a set of supplemental equations to be used along with the $4(N_l - 1)$ boundary conditions in determining $\overline{C}_n$.

The number of distinct positive real roots of Eq. (67) can be obtained using Sturm's theorem (e.g., [70]). Each positive real root $Z_p = \varpi_p^2$ of Eq. (67) is associated with two roots λ_{2p-1} and λ_{2p} of Eq. (62) such that λ_{2p-1}, $\lambda_{2p} = \pm\sqrt{Z_p} = \pm\varpi_p$, where ϖ_p is a real number. Additionally, each pair of the conjugated complex roots Z_{2n-1}, $Z_{2n} = \omega_n^2 - \omega_n^{*2} \pm \mathrm{i}2\omega_n\omega_n^*$ of Eq. (67) is associated with four complex roots $\lambda_{4n-3}, \lambda_{4n-2}, \lambda_{4n-1}, \lambda_{4n} = \pm\omega_n \pm \mathrm{i}\omega_n^*$ of Eq. (62), where ω_n and ω_n^* are two real numbers. By introducing R_r and R_{cc} as, respectively, the number of real roots and the number of pairs of conjugated complex roots of Eq. (67), the interfacial stress components $\tau_{\hat{x}z}^{(1)}$ and $\tau_{zz}^{(1)}$ in Eqs. (61a) and (61b) can be expressed as (see Appendix A)

$$\tau_{\hat{x}z,\hat{x}}^{(1)} = \sum_{p=1}^{R_r} \mathcal{S}_p \Omega_p \cosh(\varpi_p \hat{x}) + \sum_{n=1}^{R_{cc}} \left[\overline{S}_n \overline{\Lambda}_n \cosh(\omega_n \hat{x}) \cos(\omega_n^* \hat{x}) - \overline{S}_n \overline{\Lambda}_n^* \sinh(\omega_n \hat{x}) \sin(\omega_n^* \hat{x}) \right] - \frac{B_0 P_2 - D_0 P_1}{A_0 D_0 - B_0 C_0}, \tag{68a}$$

$$\tau_{zz}^{(1)}(\hat{x}) = \sum_{p=1}^{R_r} \mathcal{S}_p \cosh(\varpi_p \hat{x}) + \sum_{n=1}^{R_{cc}} \overline{S}_n \cosh(\omega_n \hat{x}) \cos(\omega_n^* \hat{x}) + \frac{A_0 P_2 - C_0 P_1}{A_0 D_0 - B_0 C_0}, \tag{68b}$$

where use has been made of the symmetric loading conditions (see Appendix A), $R_r + R_{cc} = 2(N_l - 1)$, $\mathcal{S}_p$ (with $p \in \{1,2, \ldots, R_r\}$) and $\overline{S}_n$ (with $n \in \{1,2, \ldots, R_{cc}\}$) are constants to be determined using the 2 $(N_l - 1)$ boundary conditions in Eqs. (66a) and (66b), and Ω_p (with $p \in \{1,2, \ldots, R_r\}$), $\overline{\Lambda}_n$ and $\overline{\Lambda}_n^*$ (with $n \in \{1,2, \ldots, R_{cc}\}$) can be obtained from Eq. (63) as

$$\Omega_p = -\frac{\sum_{q=0}^{2(2N_l-3)-1} Q_{2q} \varpi_p^{2q}}{Q_d}, \tag{69a}$$

$$\overline{\Lambda}_n = \mathrm{Re}\left(-\frac{\sum_{q=0}^{2(2N_l-3)-1} \left[Q_{2q} \left(\omega_n^2 - \omega_n^{*2} \pm \mathrm{i}2\omega_n\omega_n^* \right)^q \right]}{Q_d} \right), \tag{69b}$$

$$\overline{\Lambda}_n^* = \left| \mathrm{Im}\left(-\frac{\sum_{q=0}^{2(2N_l-3)-1} \left[Q_{2q} \left(\omega_n^2 - \omega_n^{*2} \pm \mathrm{i}2\omega_n\omega_n^* \right)^q \right]}{Q_d} \right) \right|, \tag{69c}$$

where $\mathrm{Re}(\cdot)$ and $\mathrm{Im}(\cdot)$ denote, respectively, the real and imaginary parts.

4 Examples: closed-form solutions for two- and three-layer composite plates

The analytical solution for a multi-layered composite plate with a specific number of layers can be readily determined from the general analytical solution obtained in Sect. 3.2. The closed-form solutions for two-layer and three-layer plates are derived herein as examples by directly applying the general solution. The solution for the two-layer case forms the basis for designing coating-substrate material systems such as sensors, flexible electronics and thermostats, while the solution for the three-layer case provides the foundation for analyzing sandwich composite structures and all-solid-state batteries containing stacks of anode-electrolyte-cathode units.

4.1 Two-layer composite plate

Consider a two-layer composite square plate subjected to the temperature changes $\Delta T^{(1)}(x,\ y)$ and $\Delta T^{(2)}(x,\ y)$, respectively, in the first (bottom) and second (top) layers, and the mechanical loads $\tau_{\hat{x}z}^{(2)}(x,\ y)$ and $\tau_{zz}^{(2)}(x,\ y)$ on the top surface and $\tau_{\hat{x}z}^{(0)}$ and $\tau_{zz}^{(0)}$ on the bottom surface (with $\hat{x}=x$ or y). This two-layer case is the simplest among all multi-layered composite plates and can be analytically solved by hands, as shown below.

In this case, the number of layers $N_l=2$, and only one interface is present. Then, it follows from Eqs. (50) and (55) that the interfacial stress components $\tau_{\hat{x}z}^{(1)}$ and $\tau_{zz}^{(1)}$ satisfy

$$\tau_{\hat{x}z,\hat{x}\hat{x}\hat{x}}^{(1)}=\beta_{1}^{(1)}\tau_{\hat{x}z,\hat{x}}^{(2)}+\beta_{0}^{(1)}\tau_{\hat{x}z,\hat{x}}^{(1)}+\beta_{-1}^{(1)}\tau_{\hat{x}z,\hat{x}}^{(0)}+\alpha_{1}^{(1)}\tau_{zz}^{(2)}+\alpha_{0}^{(1)}\tau_{zz}^{(1)}+\alpha_{-1}^{(1)}\tau_{zz}^{(0)}+\eta_{\hat{x}}^{(1)}+\eta_{z}^{(1)}, \tag{70a}$$

$$\tau_{zz,\hat{x}\hat{x}\hat{x}\hat{x}}^{(1)}=\gamma_{1}^{(1)}\tau_{\hat{x}z,\hat{x}}^{(2)}+\gamma_{0}^{(1)}\tau_{\hat{x}z,\hat{x}}^{(1)}+\gamma_{-1}^{(1)}\tau_{\hat{x}z,\hat{x}}^{(0)}+\xi_{1}^{(1)}\tau_{zz}^{(2)}+\xi_{0}^{(1)}\tau_{zz}^{(1)}+\xi_{-1}^{(1)}\tau_{zz}^{(0)}+\chi_{z}^{(1)}, \tag{70b}$$

where the coefficients can be readily obtained from Eqs. (51) and (56) as

$$\begin{aligned}
&\beta_{-1}^{(1)}=\frac{2K_s^{(1)}}{c_{11}^{(1)}t_1},\ \beta_{0}^{(1)}=\frac{4K_s^{(1)}}{c_{11}^{(2)}t_2}+\frac{4K_s^{(1)}}{c_{11}^{(1)}t_1},\ \beta_{1}^{(1)}=\frac{2K_s^{(1)}}{c_{11}^{(2)}t_2},\ \alpha_{-1}^{(1)}=-\frac{3K_s^{(1)}}{c_{11}^{(1)}t_1^2},\ \alpha_{0}^{(1)}=\frac{3K_s^{(1)}}{c_{11}^{(1)}t_1^2}-\frac{3K_s^{(1)}}{c_{11}^{(2)}t_2^2},\\
&\alpha_{1}^{(1)}=\frac{3K_s^{(1)}}{c_{11}^{(2)}t_2^2},\ \eta_{\hat{x}}^{(1)}=\frac{K_s^{(1)}}{c_{11}^{(1)}}\left(\frac{q_{\hat{x},\hat{x}}^{(1)}}{t_1}-d_{11}^{(1)}\Delta T_{,\hat{x}\hat{x}}^{(1)}\right)-\frac{K_s^{(1)}}{c_{11}^{(2)}}\left(\frac{q_{\hat{x},\hat{x}}^{(2)}}{t_2}-d_{11}^{(2)}\Delta T_{,\hat{x}\hat{x}}^{(2)}\right),\\
&\eta_{z}^{(1)}=\frac{3K_s^{(1)}}{c_{11}^{(2)}t_2^2}\left(q_z^{(2)}+2m_{\hat{x},\hat{x}}^{(2)}\right)+\frac{3K_s^{(1)}}{c_{11}^{(1)}t_1^2}\left(q_z^{(1)}+2m_{\hat{x},\hat{x}}^{(1)}\right),\ \gamma_{-1}^{(1)}=-\frac{6K_n^{(1)}}{c_{11}^{(1)}t_1^2}\\
&\gamma_{0}^{(1)}=\frac{6K_n^{(1)}}{c_{11}^{(2)}t_2^2}-\frac{6K_n^{(1)}}{c_{11}^{(1)}t_1^2},\ \gamma_{1}^{(1)}=\frac{6K_n^{(1)}}{c_{11}^{(2)}t_2^2},\ \xi_{-1}^{(1)}=\frac{6K_n^{(1)}}{c_{11}^{(1)}t_1^3},\ \xi_{0}^{(1)}=-\frac{6K_n^{(1)}}{c_{11}^{(2)}t_2^3}-\frac{6K_n^{(1)}}{c_{11}^{(1)}t_1^3},\\
&\xi_{1}^{(1)}=\frac{6K_n^{(1)}}{c_{11}^{(2)}t_2^3},\ \chi_{z}^{(1)}=\frac{6K_n^{(1)}}{c_{11}^{(2)}t_2^3}\left(q_z^{(2)}+2m_{\hat{x},\hat{x}}^{(2)}\right)-\frac{6K_n^{(1)}}{c_{11}^{(1)}t_1^3}\left(q_z^{(1)}+2m_{\hat{x},\hat{x}}^{(1)}\right),
\end{aligned} \tag{71}$$

where $q_{\hat{x}}^{(1)}$, $q_z^{(1)}$, $m_{\hat{x}}^{(1)}$ and $q_{\hat{x}}^{(2)}$, $q_z^{(2)}$, $m_{\hat{x}}^{(2)}$ are, respectively, the resultant forces and moment for the first and second layers, which are directly linked to the body force components $f_{\hat{x}}^{(1)}$, $f_z^{(1)}$ and $f_{\hat{x}}^{(2)}$, $f_z^{(2)}$ acting on the two layers (see Eq. (22a-c)).

From Eq. (70a),

$$\tau_{zz}^{(1)}=\frac{1}{\alpha_0^{(1)}}\left[\tau_{\hat{x}z,\hat{x}\hat{x}\hat{x}}^{(1)}-\beta_{1}^{(1)}\tau_{\hat{x}z,\hat{x}}^{(2)}-\beta_{0}^{(1)}\tau_{\hat{x}z,\hat{x}}^{(1)}-\beta_{-1}^{(1)}\tau_{\hat{x}z,\hat{x}}^{(0)}-\alpha_{1}^{(1)}\tau_{zz}^{(2)}-\alpha_{-1}^{(1)}\tau_{zz}^{(0)}-\eta_{\hat{x}}^{(1)}-\eta_{z}^{(1)}\right]. \tag{72}$$

Using Eq. (72) in Eq. (70b) leads to

$$\tau_{\hat{x}z,\hat{x}\hat{x}\hat{x}\hat{x}\hat{x}\hat{x}\hat{x}}^{(1)}-\beta_{0}^{(1)}\tau_{\hat{x}z,\hat{x}\hat{x}\hat{x}\hat{x}\hat{x}}^{(1)}-\xi_{0}^{(1)}\tau_{\hat{x}z,\hat{x}\hat{x}\hat{x}}^{(1)}+\left(\xi_{0}^{(1)}\beta_{0}^{(1)}-\alpha_{0}^{(1)}\gamma_{0}^{(1)}\right)\tau_{\hat{x}z,\hat{x}}^{(1)}=P_1, \tag{73}$$

where

$$P_1=\beta_{1}^{(1)}\tau_{\hat{x}z,\hat{x}\hat{x}\hat{x}\hat{x}\hat{x}}^{(2)}+\beta_{-1}^{(1)}\tau_{\hat{x}z,\hat{x}\hat{x}\hat{x}\hat{x}\hat{x}}^{(0)}+\left(\alpha_{0}^{(1)}\gamma_{1}^{(1)}-\xi_{0}^{(1)}\beta_{1}^{(1)}\right)\tau_{\hat{x}z,\hat{x}}^{(2)}+\left(\alpha_{0}^{(1)}\gamma_{-1}^{(1)}-\xi_{0}^{(1)}\beta_{-1}^{(1)}\right)\tau_{\hat{x}z,\hat{x}}^{(0)}$$

$$+\alpha_1^{(1)}\tau_{zz,\hat{x}\hat{x}\hat{x}\hat{x}}^{(2)}+\alpha_{-1}^{(1)}\tau_{zz,\hat{x}\hat{x}\hat{x}\hat{x}}^{(0)}+\left(\xi_1^{(1)}\alpha_0^{(1)}-\xi_0^{(1)}\alpha_1^{(1)}\right)\tau_{zz}^{(2)}+\left(\alpha_0^{(1)}\xi_{-1}^{(1)}-\xi_0^{(1)}\alpha_{-1}^{(1)}\right)\tau_{zz}^{(0)}$$
$$+\eta_{\hat{x},\hat{x}\hat{x}\hat{x}\hat{x}}^{(1)}+\eta_{z,\hat{x}\hat{x}\hat{x}\hat{x}}^{(1)}-\xi_0^{(1)}\left(\eta_{\hat{x}}^{(1)}+\eta_z^{(1)}\right)+\alpha_0^{(1)}\chi_z^{(1)}. \tag{74}$$

Note that $\tau_{\hat{x}z}^{(2)}$,$\tau_{zz}^{(2)}$, $\tau_{\hat{x}z}^{(0)}$ and $\tau_{zz}^{(0)}$ are prescribed on the top and bottom surfaces of the composite plate, $q_{\hat{x}}^{(1)}$, $q_{\hat{x}}^{(2)}$, $q_z^{(1)}$, $q_z^{(2)}$, $m_{\hat{x}}^{(1)}$ and $m_{\hat{x}}^{(2)}$ are readily obtainable from the body forces specified in the two layers, and $\Delta T^{(1)}$ and $\Delta T^{(2)}$ are given for each layer.

Equation (73) is a sixth-order ODE with constant coefficients for $\tau_{\hat{x}z,\hat{x}}^{(1)}$, which is inhomogeneous. When P_1 is a constant, a particular solution of Eq. (73) can be readily obtained, thereby leading to a closed-form solution of Eq. (73).

The characteristic equation of the homogeneous part of Eq. (73) is given by

$$\lambda^6-\beta_0^{(1)}\lambda^4-\xi_0^{(1)}\lambda^2+\left(\xi_0^{(1)}\beta_0^{(1)}-\alpha_0^{(1)}\gamma_0^{(1)}\right)=0. \tag{75}$$

This is a cubic equation in λ^2, which can be analytically solved to get its three roots, resulting in the determination of λ_j ($j\in\{1, 2, 3, 4, 5, 6\}$) [20–23].

From Eq. (71), it can be shown that

$$\beta_0^{(1)}>0, \xi_0^{(1)}<0, \left(\xi_0^{(1)}\beta_0^{(1)}-\alpha_0^{(1)}\gamma_0^{(1)}\right)<0. \tag{76}$$

It then follows from the Descartes rule of signs that Eq. (75) cannot have any negative real root λ^2. In fact, Eq. (75) has only one positive real root and two conjugated complex roots according to the Sturm theorem (e.g., [9, 52]). As a result, the six roots λ_j ($j\in\{1, 2, 3, 4, 5, 6\}$) of Eq. (75) have the following forms [52]:

$$\lambda_1=\left(\phi_0-\frac{\phi_1}{\phi_2}+\phi_2\right)^{\frac{1}{2}}, \lambda_2=-\left(\phi_0-\frac{\phi_1}{\phi_2}+\phi_2\right)^{\frac{1}{2}}=-\lambda_1,$$
$$\lambda_3=\beta_h+\mathrm{i}\beta_v, \lambda_4=-(\beta_h+\mathrm{i}\beta_v)=-\lambda_3,$$
$$\lambda_5=\beta_h-\mathrm{i}\beta_v, \lambda_6=-(\beta_h-\mathrm{i}\beta_v)=-\lambda_6, \tag{77}$$

where "i" is the imaginary unit (with $\mathrm{i}^2=-1$),

$$\phi_0=\frac{\beta_0^{(1)}}{3}, \phi_1=-\frac{3\xi_0^{(1)}+\left(\beta_0^{(1)}\right)^2}{9},$$
$$\phi_2=\frac{1}{3\sqrt[3]{2}}\left\{2\left(\beta_0^{(1)}\right)^3+9\beta_0^{(1)}\xi_0^{(1)}-27\left(\xi_0^{(1)}\beta_0^{(1)}-\alpha_0^{(1)}\gamma_0^{(1)}\right)\right.$$
$$\left.+\left[-4\left\langle 3\,\xi_0^{(1)}+\left(\beta_0^{(1)}\right)^2\right\rangle^3+\left\langle 2\left(\beta_0^{(1)}\right)^3+9\beta_0^{(1)}\xi_0^{(1)}-27\left(\xi_0^{(1)}\beta_0^{(1)}-\alpha_0^{(1)}\gamma_0^{(1)}\right)\right\rangle^2\right]^{1/2}\right\}^{1/3},$$
$$\beta_h=\left[\frac{\left(y_h^2+y_v^2\right)^{1/2}}{1+\tan^2\left(\frac{1}{2}\tan^{-1}\frac{y_v}{y_h}\right)}\right]^{1/2}, \beta_v=\beta_h\tan\left(\frac{1}{2}\tan^{-1}\frac{y_v}{y_h}\right),$$
$$y_h=\phi_0+\frac{1}{2}\left(\frac{\phi_1}{\phi_2}-\phi_2\right), y_v=\frac{\sqrt{3}}{2}\left(\frac{\phi_1}{\phi_2}+\phi_2\right). \tag{78}$$

The solution of Eq. (73) can then be written as, with the help of Eq. (77),

$$\tau_{\hat{x}z,\hat{x}}^{(1)}=\sum_{j=1}^{6}\tilde{C}_j e^{\lambda_j\hat{x}}+\left(\tau_{\hat{x}z,\hat{x}}^{(1)}\right)_p=C_1\cosh\left(\lambda_1\hat{x}\right)+C_2\sinh\left(\lambda_1\hat{x}\right)+C_3\cosh\left(\beta_h\hat{x}\right)\cos\left(\beta_v\hat{x}\right)$$
$$+C_4\sinh\left(\beta_h\hat{x}\right)\cos\left(\beta_v\hat{x}\right)+\left(\tau_{\hat{x}z,\hat{x}}^{(1)}\right)_p, \tag{79}$$

where $\hat{x} = x$ or y, $\tilde{C}_j$ are six constants ($j \in \{1, 2, 3, 4, 5, 6\}$), C_j ($j \in \{1, 2, 3, 4\}$) are four real-valued constants to be determined from the BCs, and $\left(\tau^{(1)}_{\hat{x}z,\hat{x}}\right)_p$ is a particular solution of Eq. (73). Note that in obtaining the second equality in Eq. (79) use has been made of $\tilde{C}_3 = \tilde{C}_5$ and $\tilde{C}_4 = \tilde{C}_6$ to ensure that $\tau^{(1)}_{\hat{x}z,\hat{x}}$ is real-valued. This is discussed in Appendix A for the general case.

Using Eq. (79) in Eq. (72) yields the normal (peel) stress at the interface of the two layers as

$$\begin{aligned}\tau^{(1)}_{zz} = \frac{1}{\alpha^{(1)}_0}\Big\{ & C_1\left(\lambda_1^2 - \beta^{(1)}_0\right)\cosh(\lambda_1\hat{x}) + C_2\left(\lambda_1^2 - \beta^{(1)}_0\right)\sinh(\lambda_1\hat{x}) \\ & + C_3\Big[\left(\beta_h^2 - \beta_v^2 - \beta^{(1)}_0\right)\cosh(\beta_h\hat{x})\cos(\beta_v\hat{x}) - 2\beta_h\beta_v\sinh(\beta_h\hat{x})\sin(\beta_v\hat{x})\Big] \\ & + C_4\Big[\left(\beta_h^2 - \beta_v^2 - \beta^{(1)}_0\right)\sinh(\beta_h\hat{x})\cos(\beta_v\hat{x}) - 2\beta_h\beta_v\cosh(\beta_h\hat{x})\sin(\beta_v\hat{x})\Big] \\ & - \beta^{(1)}_0\left(\tau^{(1)}_{\hat{x}z,\hat{x}}\right)_p - \beta^{(1)}_1\tau^{(2)}_{\hat{x}z,\hat{x}} - \beta^{(1)}_{-1}\tau^{(0)}_{\hat{x}z,\hat{x}} - \alpha^{(1)}_1\tau^{(2)}_{zz} - \alpha^{(1)}_{-1}\tau^{(0)}_{zz} - \eta^{(1)}_{\hat{x}} - \eta^{(1)}_z\Big\}. \end{aligned} \tag{80}$$

When $\tau^{(2)}_{\hat{x}z,\hat{x}}$, $\tau^{(2)}_{zz}$, $\tau^{(0)}_{\hat{x}z,\hat{x}}$, $\tau^{(0)}_{zz}$, $\eta^{(1)}_{\hat{x}}$, $\eta^{(1)}_z$ and $\chi^{(1)}_z$ are constants, Eq. (74) gives

$$\begin{aligned}P_1 = & \left(\alpha^{(1)}_0\gamma^{(1)}_1 - \beta^{(1)}_1\xi^{(1)}_0\right)\tau^{(2)}_{\hat{x}z,\hat{x}} + \left(\alpha^{(1)}_0\gamma^{(1)}_{-1} - \beta^{(1)}_{-1}\xi^{(1)}_0\right)\tau^{(0)}_{\hat{x}z,\hat{x}} + \left(\alpha^{(1)}_0\xi^{(1)}_1 - \alpha^{(1)}_1\xi^{(1)}_0\right)\tau^{(2)}_{zz} \\ & + \left(\alpha^{(1)}_0\xi^{(1)}_{-1} - \alpha^{(1)}_{-1}\xi^{(1)}_0\right)\tau^{(0)}_{zz} - \xi^{(1)}_0\left(\eta^{(1)}_{\hat{x}} + \eta^{(1)}_z\right) + \alpha^{(1)}_0\chi^{(1)}_z, \end{aligned} \tag{81}$$

which is a constant. A particular solution of Eq. (73) in this case can then be readily obtained from Eqs. (73) and (81) as

$$\left(\tau^{(1)}_{\hat{x}z,\hat{x}}\right)_p = \frac{P_1}{\beta^{(1)}_0\xi^{(1)}_0 - \alpha^{(1)}_0\gamma^{(1)}_0}. \tag{82}$$

The four constants C_j ($j \in \{1, 2, 3, 4\}$) in Eqs. (79) and (80) can be determined from the following four BCs:

$$\tau^{(1)}_{\hat{x}z,\hat{x}}\Big|_{\hat{x}=\pm L/2} = K^{(1)}_s\left[\frac{\overline{N}^{(2)}}{c^{(2)}_{11}t_2} - \frac{\overline{N}^{(1)}}{c^{(1)}_{11}t_1} + \frac{d^{(2)}_{11}}{c^{(2)}_{11}}\Delta T^{(2)} - \frac{d^{(1)}_{11}}{c^{(1)}_{11}}\Delta T^{(1)} + 6\left(\frac{\overline{M}^{(2)}}{c^{(2)}_{11}t_2^2} + \frac{\overline{M}^{(1)}}{c^{(1)}_{11}t_1^2}\right)\right]\Bigg|_{\hat{x}=\pm\frac{L}{2}}, \tag{83a}$$

$$\tau^{(1)}_{zz,\hat{x}\hat{x}}\Big|_{\hat{x}=\pm L/2} = 12K^{(1)}_n\left(\frac{\overline{M}^{(2)}}{c^{(2)}_{11}t_2^3} - \frac{\overline{M}^{(1)}}{c^{(1)}_{11}t_1^3}\right)\Bigg|_{\hat{x}=\pm\frac{L}{2}}, \tag{83b}$$

which are directly obtained from Eqs. (66a) and (66b) with $m = 1$.

Using Eq. (79) in Eq. (83a) gives

$$\begin{aligned} & C_1\cosh\left(\frac{\lambda_1 L}{2}\right) + C_2\sinh\left(\frac{\lambda_1 L}{2}\right) + C_3\cosh\left(\frac{\beta_h L}{2}\right)\cos\left(\frac{\beta_v L}{2}\right) + C_4\sinh\left(\frac{\beta_h L}{2}\right)\cos\left(\frac{\beta_v L}{2}\right) \\ & = -\left(\tau^{(1)}_{\hat{x}z,\hat{x}}\right)_p + K^{(1)}_s\left[\frac{\overline{N}^{(2)}}{c^{(2)}_{11}t_2} - \frac{\overline{N}^{(1)}}{c^{(1)}_{11}t_1} + \frac{d^{(2)}_{11}}{c^{(2)}_{11}}\Delta T^{(2)} - \frac{d^{(1)}_{11}}{c^{(1)}_{11}}\Delta T^{(1)} + 6\left(\frac{\overline{M}^{(2)}}{c^{(2)}_{11}t_2^2} + \frac{\overline{M}^{(1)}}{c^{(1)}_{11}t_1^2}\right)\right]\Bigg|_{\hat{x}=\frac{L}{2}}, \end{aligned} \tag{84a}$$

$$\begin{aligned} & C_1\cosh\left(\frac{\lambda_1 L}{2}\right) - C_2\sinh\left(\frac{\lambda_1 L}{2}\right) + C_3\cosh\left(\frac{\beta_h L}{2}\right)\cos\left(\frac{\beta_v L}{2}\right) - C_4\sinh\left(\frac{\beta_h L}{2}\right)\cos\left(\frac{\beta_v L}{2}\right) \\ & = -\left(\tau^{(1)}_{\hat{x}z,\hat{x}}\right)_p + K^{(1)}_s\left[\frac{\overline{N}^{(2)}}{c^{(2)}_{11}t_2} - \frac{\overline{N}^{(1)}}{c^{(1)}_{11}t_1} + \frac{d^{(2)}_{11}}{c^{(2)}_{11}}\Delta T^{(2)} - \frac{d^{(1)}_{11}}{c^{(1)}_{11}}\Delta T^{(1)} + 6\left(\frac{\overline{M}^{(2)}}{c^{(2)}_{11}t_2^2} + \frac{\overline{M}^{(1)}}{c^{(1)}_{11}t_1^2}\right)\right]\Bigg|_{\hat{x}=-\frac{L}{2}}. \end{aligned} \tag{84b}$$

Substituting Eq. (80) into Eq. (83b) yields

$$C_1\lambda_1^2\left(\lambda_1^2 - \beta^{(1)}_0\right)\cosh\left(\frac{\lambda_1 L}{2}\right) + C_2\lambda_1^2\left(\lambda_1^2 - \beta^{(1)}_0\right)\sinh\left(\frac{\lambda_1 L}{2}\right)$$

$$
\begin{aligned}
&+C_3\left\{\left[\beta_h^4-6\beta_h^2\beta_v^2+\beta_v^4-\beta_0^{(1)}\left(\beta_h^2-\beta_v^2\right)\right]\cosh\left(\frac{\beta_h L}{2}\right)\cos\left(\frac{\beta_v L}{2}\right)\right.\\
&\left.-2\beta_h\beta_v\left(2\beta_h^2-2\beta_v^2-\beta_0^{(1)}\right)\sinh\left(\frac{\beta_h L}{2}\right)\sin\left(\frac{\beta_v L}{2}\right)\right\}\\
&+C_4\left\{\left[\beta_h^4-6\beta_h^2\beta_v^2+\beta_v^4-\beta_0^{(1)}\left(\beta_h^2-\beta_v^2\right)\right]\sinh\left(\frac{\beta_h L}{2}\right)\cos\left(\frac{\beta_v L}{2}\right)\right.\\
&\left.-2\beta_h\beta_v\left(2\beta_h^2-2\beta_v^2-\beta_0^{(1)}\right)\cosh\left(\frac{\beta_h L}{2}\right)\sin\left(\frac{\beta_v L}{2}\right)\right\}\\
&=12K_n^{(1)}\alpha_0^{(1)}\left(\frac{\overline{M}^{(2)}}{c_{11}^{(2)}t_2^3}-\frac{\overline{M}^{(1)}}{c_{11}^{(1)}t_1^3}\right)\Bigg|_{\hat{x}=\frac{L}{2}},
\end{aligned}
\tag{85a}
$$

$$
\begin{aligned}
&C_1\lambda_1^2\left(\lambda_1^2-\beta_0^{(1)}\right)\cosh\left(\frac{\lambda_1 L}{2}\right)-C_2\lambda_1^2\left(\lambda_1^2-\beta_0^{(1)}\right)\sinh\left(\frac{\lambda_1 L}{2}\right)\\
&+C_3\left\{\left[\beta_h^4-6\beta_h^2\beta_v^2+\beta_v^4-\beta_0^{(1)}\left(\beta_h^2-\beta_v^2\right)\right]\cosh\left(\frac{\beta_h L}{2}\right)\cos\left(\frac{\beta_v L}{2}\right)\right.\\
&\left.-2\beta_h\beta_v\left(2\beta_h^2-2\beta_v^2-\beta_0^{(1)}\right)\sinh\left(\frac{\beta_h L}{2}\right)\sin\left(\frac{\beta_v L}{2}\right)\right\}\\
&-C_4\left\{\left[\beta_h^4-6\beta_h^2\beta_v^2+\beta_v^4-\beta_0^{(1)}\left(\beta_h^2-\beta_v^2\right)\right]\sinh\left(\frac{\beta_h L}{2}\right)\cos\left(\frac{\beta_v L}{2}\right)\right.\\
&\left.-2\beta_h\beta_v\left(2\beta_h^2-2\beta_v^2-\beta_0^{(1)}\right)\cosh\left(\frac{\beta_h L}{2}\right)\sin\left(\frac{\beta_v L}{2}\right)\right\}\\
&=12K_n^{(1)}\alpha_0^{(1)}\left(\frac{\overline{M}^{(2)}}{c_{11}^{(2)}t_2^3}-\frac{\overline{M}^{(1)}}{c_{11}^{(1)}t_1^3}\right)\Bigg|_{\hat{x}=-\frac{L}{2}}.
\end{aligned}
\tag{85b}
$$

Solving Eqs. (84a,b) and (85a,b) will lead to the determination of C_1–C_4.

When the loading and geometry are both symmetric about $\hat{x}=0$, $\tau_{\hat{x}z,\hat{x}}^{(1)}(\hat{x})=\tau_{\hat{x}z,\hat{x}}^{(1)}(-\hat{x})$ according to Eq. (46). It then follows from Eq. (79) that $C_2=C_4=0$. With these relations, Eqs. (84a), (84b), (85a) and (85b) reduce to

$$
\begin{aligned}
&C_1\cosh\left(\frac{\lambda_1 L}{2}\right)+C_3\cosh\left(\frac{\beta_h L}{2}\right)\cos\left(\frac{\beta_v L}{2}\right)\\
&=K_s^{(1)}\left[\frac{\overline{N}^{(2)}}{c_{11}^{(2)}t_2}-\frac{\overline{N}^{(1)}}{c_{11}^{(1)}t_1}+\frac{d_{11}^{(2)}}{c_{11}^{(2)}}\Delta T^{(2)}-\frac{d_{11}^{(1)}}{c_{11}^{(1)}}\Delta T^{(1)}+6\left(\frac{\overline{M}^{(2)}}{c_{11}^{(2)}t_2^2}+\frac{\overline{M}^{(1)}}{c_{11}^{(1)}t_1^2}\right)\right]\Bigg|_{\hat{x}=\frac{L}{2}}-\left(\tau_{\hat{x}z,\hat{x}}^{(1)}\right)_p,
\end{aligned}
\tag{86a}
$$

$$
\begin{aligned}
&C_1\lambda_1^2\left(\lambda_1^2-\beta_0^{(1)}\right)\cosh\left(\frac{\lambda_1 L}{2}\right)+C_3\left\{\left[\beta_h^4-6\beta_h^2\beta_v^2+\beta_v^4-\beta_0^{(1)}\left(\beta_h^2-\beta_v^2\right)\right]\cosh\left(\frac{\beta_h L}{2}\right)\cos\left(\frac{\beta_v L}{2}\right)\right.\\
&\left.-2\beta_h\beta_v\left(2\beta_h^2-2\beta_v^2-\beta_0^{(1)}\right)\sinh\left(\frac{\beta_h L}{2}\right)\sin\left(\frac{\beta_v L}{2}\right)\right\}=12K_n^{(1)}\alpha_0^{(1)}\left(\frac{\overline{M}^{(2)}}{c_{11}^{(2)}t_2^3}-\frac{\overline{M}^{(1)}}{c_{11}^{(1)}t_1^3}\right)\Bigg|_{\hat{x}=\frac{L}{2}}.
\end{aligned}
\tag{86b}
$$

By using the Cramer rule, Eqs. (86a) and (86b) can be solved to obtain the two constants C_1 and C_3 as

$$
\begin{aligned}
C_1=\frac{1}{D}\Bigg\langle&\left\{K_s^{(1)}\left[\frac{\overline{N}^{(2)}}{c_{11}^{(2)}t_2}-\frac{\overline{N}^{(1)}}{c_{11}^{(1)}t_1}+\frac{d_{11}^{(2)}}{c_{11}^{(2)}}\Delta T^{(2)}-\frac{d_{11}^{(1)}}{c_{11}^{(1)}}\Delta T^{(1)}+6\left(\frac{\overline{M}^{(2)}}{c_{11}^{(2)}t_2^2}+\frac{\overline{M}^{(1)}}{c_{11}^{(1)}t_1^2}\right)\right]\Bigg|_{\hat{x}=\frac{L}{2}}\right.\\
&\left.-\left(\tau_{\hat{x}z,\hat{x}}^{(1)}\right)_p\right\}\left\{\left[\beta_h^4-6\beta_h^2\beta_v^2+\beta_v^4-\beta_0^{(1)}\left(\beta_h^2-\beta_v^2\right)\right]\cosh\left(\frac{\beta_h L}{2}\right)\cos\left(\frac{\beta_v L}{2}\right)\right.\\
&\left.-2\beta_h\beta_v\left(2\beta_h^2-2\beta_v^2-\beta_0^{(1)}\right)\sinh\left(\frac{\beta_h L}{2}\right)\sin\left(\frac{\beta_v L}{2}\right)\right\}
\end{aligned}
$$

$$-12K_n^{(1)}\alpha_0^{(1)}\left(\frac{\overline{M}^{(2)}}{c_{11}^{(2)}t_2^3}-\frac{\overline{M}^{(1)}}{c_{11}^{(1)}t_1^3}\right)\Bigg|_{\hat{x}=\frac{L}{2}}\cosh\left(\frac{\beta_h L}{2}\right)\cos\left(\frac{\beta_v L}{2}\right)\Bigg\rangle, \tag{87a}$$

$$C_3=\frac{1}{D}\Bigg\langle 12K_n^{(1)}\alpha_0^{(1)}\left(\frac{\overline{M}^{(2)}}{c_{11}^{(2)}t_2^3}-\frac{\overline{M}^{(1)}}{c_{11}^{(1)}t_1^3}\right)\Bigg|_{\hat{x}=\frac{L}{2}}\cosh\left(\frac{\lambda_1 L}{2}\right)-\lambda_1^2\left(\lambda_1^2-\beta_0^{(1)}\right)\cosh\left(\frac{\lambda_1 L}{2}\right)\Bigg\{K_s^{(1)}\Bigg[\frac{\overline{N}^{(2)}}{c_{11}^{(2)}t_2}-\frac{\overline{N}^{(1)}}{c_{11}^{(1)}t_1}+\frac{d_{11}^{(2)}}{c_{11}^{(2)}}\Delta T^{(2)}$$
$$-\frac{d_{11}^{(1)}}{c_{11}^{(1)}}\Delta T^{(1)}+6\left(\frac{\overline{M}^{(2)}}{c_{11}^{(2)}t_2^2}+\frac{\overline{M}^{(1)}}{c_{11}^{(1)}t_1^2}\right)\Bigg]\Bigg|_{\hat{x}=\frac{L}{2}}-\left(\tau_{\hat{x}z,\hat{x}}^{(1)}\right)_p\Bigg\}\Bigg\rangle, \tag{87b}$$

where

$$D=\cosh\left(\frac{\lambda_1 L}{2}\right)\left\{\left[\beta_h^4-6\beta_h^2\beta_v^2+\beta_v^4-\beta_0^{(1)}\left(\beta_h^2-\beta_v^2\right)\right]\cosh\left(\frac{\beta_h L}{2}\right)\cos\left(\frac{\beta_v L}{2}\right)\right.$$
$$\left.-2\beta_h\beta_v\left(2\beta_h^2-2\beta_v^2-\beta_0^{(1)}\right)\sinh\left(\frac{\beta_h L}{2}\right)\sin\left(\frac{\beta_v L}{2}\right)\right\}-\lambda_1^2\left(\lambda_1^2-\beta_0^{(1)}\right)\cosh\left(\frac{\lambda_1 L}{2}\right)\cosh\left(\frac{\beta_h L}{2}\right)\cos\left(\frac{\beta_v L}{2}\right). \tag{87c}$$

Substituting C_1 and C_3 listed in Eqs. (87a) and (87b) and $C_2=C_4=0$ into Eqs. (79) and (80) will yield the final expressions of $\tau_{\hat{x}z,\hat{x}}^{(1)}$ and $\tau_{zz}^{(1)}$, which are valid for the general case.

For the special case of a simply supported square plate subjected to the temperature changes $\Delta T^{(1)}$ and $\Delta T^{(2)}$ in the bottom and top layers respectively and with $\overline{N}^{(1)}=\overline{N}^{(2)}=\overline{M}^{(1)}=\overline{M}^{(2)}=0$, $\tau_{zz}^{(0)}=\tau_{zz}^{(2)}=\tau_{\hat{x}z}^{(0)}=\tau_{\hat{x}z}^{(2)}=0$, $q_{\hat{x}}^{(1)}=q_{\hat{x}}^{(2)}=q_z^{(1)}=q_z^{(2)}=0$, $m_{\hat{x}}^{(1)}=m_{\hat{x}}^{(2)}=0$, and $\Delta T_{,\hat{x}\hat{x}}^{(1)}=\Delta T_{,\hat{x}\hat{x}}^{(2)}=0$, Eqs. (87a) and (87b) are simplified to

$$C_1=\frac{1}{D}K_s^{(1)}\left[\frac{d_{11}^{(2)}}{c_{11}^{(2)}}\Delta T^{(2)}|_{\hat{x}=\frac{L}{2}}-\frac{d_{11}^{(1)}}{c_{11}^{(1)}}\Delta T^{(1)}|_{\hat{x}=\frac{L}{2}}\right]\left\{\left[\beta_h^4-6\beta_h^2\beta_v^2+\beta_v^4-\beta_0^{(1)}\left(\beta_h^2-\beta_v^2\right)\right]\cosh\left(\frac{\beta_h L}{2}\right)\cos\left(\frac{\beta_v L}{2}\right)\right.$$
$$\left.-2\beta_h\beta_v\left(2\beta_h^2-2\beta_v^2-\beta_0^{(1)}\right)\sinh\left(\frac{\beta_h L}{2}\right)\sin\left(\frac{\beta_v L}{2}\right)\right\},$$
$$C_3=-\frac{1}{D}K_s^{(1)}\left[\frac{d_{11}^{(2)}}{c_{11}^{(2)}}\Delta T^{(2)}|_{\hat{x}=\frac{L}{2}}-\frac{d_{11}^{(1)}}{c_{11}^{(1)}}\Delta T^{(1)}|_{\hat{x}=\frac{L}{2}}\right]\lambda_1^2\left(\lambda_1^2-\beta_0^{(1)}\right)\cosh\left(\frac{\lambda_1 L}{2}\right), \tag{88a,b}$$

where use has been made of Eqs. (71), (81) and (82), which gives $P_1=0$ and $\left(\tau_{\hat{x}z,\hat{x}}^{(1)}\right)_p=0$.

Inserting C_1 and C_3 listed in Eqs. (88a,b) and $C_2=C_4=0$ into Eqs. (79) and (80) then leads to $\tau_{\hat{x}z,\hat{x}}^{(1)}$ and $\tau_{zz}^{(1)}$ on the interface between the two layers for the special case as

$$\tau_{\hat{x}z,\hat{x}}^{(1)}=\frac{1}{D}K_s^{(1)}\left[\frac{d_{11}^{(2)}}{c_{11}^{(2)}}\Delta T^{(2)}\Bigg|_{\hat{x}=\frac{L}{2}}-\frac{d_{11}^{(1)}}{c_{11}^{(1)}}\Delta T^{(1)}\Bigg|_{\hat{x}=\frac{L}{2}}\right]\left\{\left[\beta_h^4-6\beta_h^2\beta_v^2+\beta_v^4-\beta_0^{(1)}\left(\beta_h^2-\beta_v^2\right)\right]\cosh\left(\frac{\beta_h L}{2}\right)\cos\left(\frac{\beta_v L}{2}\right)\right.$$
$$\left.-2\beta_h\beta_v\left(2\beta_h^2-2\beta_v^2-\beta_0^{(1)}\right)\sinh\left(\frac{\beta_h L}{2}\right)\sin\left(\frac{\beta_v L}{2}\right)\right\}\cosh(\lambda_1\hat{x})$$
$$-\frac{1}{D}\lambda_1^2\left(\lambda_1^2-\beta_0^{(1)}\right)K_s^{(1)}\left[\frac{d_{11}^{(2)}}{c_{11}^{(2)}}\Delta T^{(2)}\Bigg|_{\hat{x}=\frac{L}{2}}-\frac{d_{11}^{(1)}}{c_{11}^{(1)}}\Delta T^{(1)}\Bigg|_{\hat{x}=\frac{L}{2}}\right]\cosh\left(\frac{\lambda_1 L}{2}\right)\cosh(\beta_h\hat{x})\cos(\beta_v\hat{x}), \tag{89a}$$

$$\tau_{zz}^{(1)}=\frac{1}{\alpha_0^{(1)}D}\left(\lambda_1^2-\beta_0^{(1)}\right)K_s^{(1)}\left[\frac{d_{11}^{(2)}}{c_{11}^{(2)}}\Delta T^{(2)}\Bigg|_{\hat{x}=\frac{L}{2}}-\frac{d_{11}^{(1)}}{c_{11}^{(1)}}\Delta T^{(1)}\Bigg|_{\hat{x}=\frac{L}{2}}\right]\{[\beta_h^4-6\beta_h^2\beta_v^2+\beta_v^4$$
$$-\beta_0^{(1)}(\beta_h^2-\beta_v^2)]\cosh\left(\frac{\beta_h L}{2}\right)\cos\left(\frac{\beta_v L}{2}\right)-2\beta_h\beta_v(2\beta_h^2-2\beta_v^2$$
$$-\beta_0^{(1)})\sinh\left(\frac{\beta_h L}{2}\right)\sin\left(\frac{\beta_v L}{2}\right)\Bigg\}\cosh(\lambda_1\hat{x})-\frac{1}{D}\lambda_1^2\left(\lambda_1^2-\beta_0^{(1)}\right)K_s^{(1)}\left[\frac{d_{11}^{(2)}}{c_{11}^{(2)}}\Delta T^{(2)}\Bigg|_{\hat{x}=\frac{L}{2}}\right.$$

$$-\frac{d_{11}^{(1)}}{c_{11}^{(1)}}\Delta T^{(1)}\Bigg|_{\hat{x}=\frac{L}{2}}\Bigg]\cosh\left(\frac{\lambda_1 L}{2}\right)\Big[\left(\beta_h^2-\beta_v^2-\beta_0^{(1)}\right)\cosh\left(\beta_h\hat{x}\right)\cos\left(\beta_v\hat{x}\right)$$
$$-2\beta_h\beta_v\sinh\left(\beta_h\hat{x}\right)\sin\left(\beta_v\hat{x}\right)\Big]. \tag{89b}$$

With $\tau_{\hat{x}z,\hat{x}}^{(1)}$ and $\tau_{zz}^{(1)}$ determined, the axial force $N^{(m)}$ and bending moment $M^{(m)}$ can be readily obtained from Eqs. (65a,b), and the axial strain $\epsilon_0^{(m)}$ and curvature $\kappa^{(m)}$ (with $m \in \{1,2\}$) can be computed using Eqs. (44a,b) for the two-layer plate.

4.2 Three-layer composite plate

For a composite plate with three layers, Eqs. (59) and (60) become, after setting $N_l = 3$,

$$A_4\frac{\mathrm{d}^4\tau_{\hat{x}z,\hat{x}}^{(1)}}{\mathrm{d}\hat{x}^4}+A_2\frac{\mathrm{d}^2\tau_{\hat{x}z,\hat{x}}^{(1)}}{\mathrm{d}\hat{x}^2}+A_0\tau_{\hat{x}z,\hat{x}}^{(1)}+B_6\frac{\mathrm{d}^6\tau_{zz}^{(1)}}{\mathrm{d}\hat{x}^6}+B_4\frac{\mathrm{d}^4\tau_{zz}^{(1)}}{\mathrm{d}\hat{x}^4}+B_2\frac{\mathrm{d}^2\tau_{zz}^{(1)}}{\mathrm{d}\hat{x}^2}+B_0\tau_{zz}^{(1)}=P_1, \tag{90a}$$

$$C_6\frac{\mathrm{d}^6\tau_{\hat{x}z,\hat{x}}^{(1)}}{\mathrm{d}\hat{x}^6}+C_4\frac{\mathrm{d}^4\tau_{\hat{x}z,\hat{x}}^{(1)}}{\mathrm{d}\hat{x}^4}+C_2\frac{\mathrm{d}^2\tau_{\hat{x}z,\hat{x}}^{(1)}}{\mathrm{d}\hat{x}^2}+C_0\tau_{\hat{x}z,\hat{x}}^{(1)}+D_8\frac{\mathrm{d}^8\tau_{zz}^{(1)}}{\mathrm{d}\hat{x}^8}+D_6\frac{\mathrm{d}^6\tau_{zz}^{(1)}}{\mathrm{d}\hat{x}^6}+D_4\frac{\mathrm{d}^4\tau_{zz}^{(1)}}{\mathrm{d}\hat{x}^4}+D_2\frac{\mathrm{d}^2\tau_{zz}^{(1)}}{\mathrm{d}\hat{x}^2}+D_0\tau_{zz}^{(1)}=P_2, \tag{90b}$$

where the coefficients A_4, A_2, A_0, B_6, B_4, B_2, B_0, C_6, C_4, C_2, C_0, D_8, D_6, D_4, D_2 and D_0 and the inhomogeneous terms P_1 and P_2 are given by (see Appendix B for more details)

$$A_4=-\frac{\xi_1^{(1)}}{\beta_1^{(1)}\xi_1^{(1)}-\alpha_1^{(1)}\gamma_1^{(1)}},\ A_2=\frac{\left(\beta_0^{(1)}+\beta_0^{(2)}\right)\xi_1^{(1)}-\alpha_0^{(2)}\gamma_1^{(1)}-\alpha_1^{(1)}\gamma_0^{(1)}}{\beta_1^{(1)}\xi_1^{(1)}-\alpha_1^{(1)}\gamma_1^{(1)}},$$
$$A_0=\frac{\xi_1^{(1)}\left(-\beta_0^{(1)}\beta_0^{(2)}+\beta_{-1}^{(2)}\beta_1^{(1)}\right)+\alpha_1^{(1)}\left(\beta_0^{(2)}\gamma_0^{(1)}-\beta_{-1}^{(2)}\gamma_1^{(1)}\right)-\alpha_0^{(2)}\left(-\beta_0^{(1)}\gamma_1^{(1)}+\beta_1^{(1)}\gamma_0^{(1)}\right)}{\beta_1^{(1)}\xi_1^{(1)}-\alpha_1^{(1)}\gamma_1^{(1)}}, \tag{91a}$$

$$B_6=\frac{\alpha_1^{(1)}}{\beta_1^{(1)}\xi_1^{(1)}-\alpha_1^{(1)}\gamma_1^{(1)}},\ B_4=\frac{\alpha_0^{(2)}\beta_1^{(1)}-\alpha_1^{(1)}\beta_0^{(2)}}{\beta_1^{(1)}\xi_1^{(1)}-\alpha_1^{(1)}\gamma_1^{(1)}},\ B_2=\frac{\alpha_0^{(1)}\xi_1^{(1)}-\alpha_1^{(1)}\xi_0^{(1)}}{\beta_1^{(1)}\xi_1^{(1)}-\alpha_1^{(1)}\gamma_1^{(1)}},$$
$$B_0=\frac{\xi_1^{(1)}\left(-\alpha_0^{(1)}\beta_0^{(2)}+\alpha_{-1}^{(2)}\beta_1^{(1)}\right)+\alpha_1^{(1)}\left(-\alpha_{-1}^{(2)}\gamma_1^{(1)}+\beta_0^{(2)}\xi_0^{(1)}\right)-\alpha_0^{(2)}\left(-\alpha_0^{(1)}\gamma_1^{(1)}+\beta_1^{(1)}\xi_0^{(1)}\right)}{\beta_1^{(1)}\xi_1^{(1)}-\alpha_1^{(1)}\gamma_1^{(1)}}, \tag{91b}$$

$$C_6=-\frac{\gamma_1^{(1)}}{\alpha_1^{(1)}\gamma_1^{(1)}-\beta_1^{(1)}\xi_1^{(1)}},\ C_4=\frac{\beta_0^{(1)}\gamma_1^{(1)}-\beta_1^{(1)}\gamma_0^{(1)}}{\alpha_1^{(1)}\gamma_1^{(1)}-\beta_1^{(1)}\xi_1^{(1)}},\ C_2=\frac{-\gamma_0^{(2)}\xi_1^{(1)}+\gamma_1^{(1)}\xi_0^{(2)}}{\alpha_1^{(1)}\gamma_1^{(1)}-\beta_1^{(1)}\xi_1^{(1)}},$$
$$C_0=\frac{\gamma_1^{(1)}\left(\alpha_1^{(1)}\gamma_{-1}^{(2)}-\beta_0^{(1)}\xi_0^{(2)}\right)+\beta_1^{(1)}\left(\gamma_0^{(1)}\xi_0^{(2)}-\gamma_{-1}^{(2)}\xi_1^{(1)}\right)+\gamma_0^{(2)}\left(-\alpha_1^{(1)}\gamma_0^{(1)}+\beta_0^{(1)}\xi_1^{(1)}\right)}{\alpha_1^{(1)}\gamma_1^{(1)}-\beta_1^{(1)}\xi_1^{(1)}}, \tag{91c}$$

$$D_8=\frac{\beta_1^{(1)}}{\alpha_1^{(1)}\gamma_1^{(1)}-\beta_1^{(1)}\xi_1^{(1)}},\ D_6=0,\ D_4=\frac{\alpha_0^{(1)}\gamma_1^{(1)}+\alpha_1^{(1)}\gamma_0^{(2)}-\beta_1^{(1)}\left(\xi_0^{(1)}+\xi_0^{(2)}\right)}{\alpha_1^{(1)}\gamma_1^{(1)}-\beta_1^{(1)}\xi_1^{(1)}},\ D_2=0,$$
$$D_0=\frac{\gamma_1^{(1)}\left(-\alpha_0^{(1)}\xi_0^{(2)}+\alpha_1^{(1)}\xi_{-1}^{(2)}\right)+\beta_1^{(1)}\left(\xi_0^{(1)}\xi_0^{(2)}-\xi_{-1}^{(2)}\xi_1^{(1)}\right)-\gamma_0^{(2)}\left(-\alpha_0^{(1)}\xi_1^{(1)}+\alpha_1^{(1)}\xi_0^{(1)}\right)}{\alpha_1^{(1)}\gamma_1^{(1)}-\beta_1^{(1)}\xi_1^{(1)}}, \tag{91d}$$

$$P_1=\frac{1}{\alpha_1^{(1)}\gamma_1^{(1)}-\beta_1^{(1)}\xi_1^{(1)}}\Bigg\{\left(\alpha_{-1}^{(1)}\xi_1^{(1)}-\alpha_1^{(1)}\xi_{-1}^{(1)}\right)\frac{\mathrm{d}^2\tau_{zz}^{(0)}}{\mathrm{d}\hat{x}^2}+\left(-\alpha_1^{(1)}\gamma_{-1}^{(1)}+\beta_{-1}^{(1)}\xi_1^{(1)}\right)\frac{\mathrm{d}^2\tau_{\hat{x}z,\hat{x}}^{(0)}}{\mathrm{d}\hat{x}^2}$$
$$-\alpha_1^{(1)}\frac{\mathrm{d}^2\chi_z^{(1)}}{\mathrm{d}\hat{x}^2}+\xi_1^{(1)}\frac{\mathrm{d}^2\eta_{\hat{x}}^{(1)}}{\mathrm{d}\hat{x}^2}+\xi_1^{(1)}\frac{\mathrm{d}^2\eta_z^{(1)}}{\mathrm{d}\hat{x}^2}+\Big[-\alpha_{-1}^{(1)}\beta_0^{(2)}\xi_1^{(1)}+\alpha_1^{(1)}\beta_0^{(2)}\xi_{-1}^{(1)}$$
$$-\alpha_0^{(2)}\left(-\alpha_{-1}^{(1)}\gamma_1^{(1)}+\beta_1^{(1)}\xi_{-1}^{(1)}\right)\Big]\tau_{zz}^{(0)}+\Big[-\beta_0^{(2)}\beta_{-1}^{(1)}\xi_1^{(1)}+\alpha_1^{(1)}\beta_0^{(2)}\gamma_{-1}^{(1)}$$

$$+\alpha_0^{(2)}\left(\beta_{-1}^{(1)}\gamma_1^{(1)}-\beta_1^{(1)}\gamma_{-1}^{(1)}\right)\Big]\tau_{\hat{x}z,\hat{x}}^{(0)}+\left(-\alpha_0^{(2)}\beta_1^{(1)}+\alpha_1^{(1)}\beta_0^{(2)}\right)\chi_z^{(1)}+\left(\alpha_0^{(2)}\gamma_1^{(1)}-\beta_0^{(2)}\xi_1^{(1)}\right)\left(\eta_{\hat{x}}^{(1)}+\eta_z^{(1)}\right)$$
$$+\left(-\alpha_1^{(1)}\gamma_1^{(1)}+\beta_1^{(1)}\xi_1^{(1)}\right)\left(\alpha_1^{(2)}\tau_{zz}^{(3)}+\beta_1^{(2)}\tau_{\hat{x}z,\hat{x}}^{(3)}+\eta_{\hat{x}}^{(2)}+\eta_z^{(2)}\right)\Bigg\}, \tag{91e}$$

$$P_2=\frac{-1}{\alpha_1^{(1)}\gamma_1^{(1)}-\beta_1^{(1)}\xi_1^{(1)}}\Bigg\{\left(\alpha_{-1}^{(1)}\gamma_1^{(1)}-\beta_1^{(1)}\xi_{-1}^{(1)}\right)\frac{\mathrm{d}^4\tau_{zz}^{(0)}}{\mathrm{d}\hat{x}^4}+\left(\beta_{-1}^{(1)}\gamma_1^{(1)}-\beta_1^{(1)}\gamma_{-1}^{(1)}\right)\frac{\mathrm{d}^4\tau_{\hat{x}z,\hat{x}}^{(0)}}{\mathrm{d}\hat{x}^4}$$
$$-\beta_1^{(1)}\frac{\mathrm{d}^4\chi_z^{(1)}}{\mathrm{d}\hat{x}^4}+\gamma_1^{(1)}\frac{\mathrm{d}^4\eta_{\hat{x}}^{(1)}}{\mathrm{d}\hat{x}^4}+\gamma_1^{(1)}\frac{\mathrm{d}^4\eta_z^{(1)}}{\mathrm{d}\hat{x}^4}+\Big[-\alpha_{-1}^{(1)}\gamma_1^{(1)}\xi_0^{(2)}+\beta_1^{(1)}\xi_0^{(2)}\xi_{-1}^{(1)}-\gamma_0^{(2)}\left(-\alpha_{-1}^{(1)}\xi_1^{(1)}+\alpha_1^{(1)}\xi_{-1}^{(1)}\right)\Big]\tau_{zz}^{(0)}$$
$$+\Big[-\beta_{-1}^{(1)}\gamma_1^{(1)}\xi_0^{(2)}+\beta_1^{(1)}\gamma_{-1}^{(1)}\xi_0^{(2)}-\gamma_0^{(2)}\left(\alpha_1^{(1)}\gamma_{-1}^{(1)}-\beta_{-1}^{(1)}\xi_1^{(1)}\right)\Big]\tau_{\hat{x}z,\hat{x}}^{(0)}+\left(-\alpha_1^{(1)}\gamma_0^{(2)}+\beta_1^{(1)}\xi_0^{(2)}\right)\chi_z^{(1)}$$
$$+\left(\gamma_0^{(2)}\xi_1^{(1)}-\gamma_1^{(1)}\xi_0^{(2)}\right)\left(\eta_{\hat{x}}^{(1)}+\eta_z^{(1)}\right)+\left(\alpha_1^{(1)}\gamma_1^{(1)}-\beta_1^{(1)}\xi_1^{(1)}\right)\left(\gamma_1^{(2)}\tau_{\hat{x}z,\hat{x}}^{(3)}+\xi_1^{(2)}\tau_{zz}^{(3)}+\chi_z^{(2)}\right)\Bigg\}. \tag{91f}$$

The two coupled ODEs in Eqs. (90a) and (90b) can be solved simultaneously by using a software package for symbolic mathematical operations.

When P_1 and P_2 are constants, the general solution of Eqs. (90a) and (90b) can be obtained as (see Eqs. (61a) and (61b))

$$\tau_{\hat{x}z,\hat{x}}^{(1)}=\sum_{n=1}^{12}\overline{C}_n\Lambda_n\exp\left(\lambda_n\hat{x}\right)-\frac{B_0P_2-D_0P_1}{A_0D_0-B_0C_0}, \tag{92a}$$
$$\tau_{zz}^{(1)}=\sum_{n=1}^{12}\overline{C}_n\exp\left(\lambda_n\hat{x}\right)+\frac{A_0P_2-C_0P_1}{A_0D_0-B_0C_0}, \tag{92b}$$

where $\hat{x}=x$ or y, and λ_n (with $n\in\{1,2,\ldots,12\}$) are the roots of the following 12th-degree polynomial equation (see Eq. (62)):

$$\begin{aligned}&(A_4D_8-B_6C_6)\lambda^{12}+(A_2D_8+A_4D_6-B_4C_6-B_6C_4)\lambda^{10}\\&+(A_0D_8+A_2D_6+A_4D_4-B_2C_6-B_4C_4-B_6C_2)\lambda^8\\&+(A_0D_6+A_2D_4+A_4D_2-B_0C_6-B_2C_4-B_4C_2-B_6C_0)\lambda^6\\&+(A_0D_4+A_2D_2+A_4D_0-B_0C_4-B_2C_2-B_4C_0)\lambda^4\\&+(A_0D_2+A_2D_0-B_0C_2-B_2C_0)\lambda^2+A_0D_0-B_0C_0=0.\end{aligned} \tag{93a}$$

In terms of $Z=\lambda^2$, Eq. (93a) becomes

$$\begin{aligned}&(A_4D_8-B_6C_6)Z^6+(A_2D_8+A_4D_6-B_4C_6-B_6C_4)Z^5\\&+(A_0D_8+A_2D_6+A_4D_4-B_2C_6-B_4C_4-B_6C_2)Z^4\\&+(A_0D_6+A_2D_4+A_4D_2-B_0C_6-B_2C_4-B_4C_2-B_6C_0)Z^3\\&+(A_0D_4+A_2D_2+A_4D_0-B_0C_4-B_2C_2-B_4C_0)Z^2\\&+(A_0D_2+A_2D_0-B_0C_2-B_2C_0)Z+A_0D_0-B_0C_0=0.\end{aligned} \tag{93b}$$

In addition, Λ_n (with $n\in\{1,2,\ldots,12\}$) in Eqs. (92a) and (92b) are given by (see Eq. (63))

$$\Lambda_n=-\frac{Q_{10}\lambda_n^{10}+Q_8\lambda_n^8+Q_6\lambda_n^6+Q_4\lambda_n^4+Q_2\lambda_n^2+Q_0}{Q_d}, \tag{94}$$

where

$$Q_{10}=-(A_4D_8-B_6C_6)\left[C_2A_4^2+A_4(-A_0C_6-A_2C_4)+C_6A_2^2\right], \tag{95a}$$

$$Q_8=A_4^3\left(C_0D_8-C_2D_6\right)+A_4^2\Big[A_0\left(-C_4D_8+C_6D_6\right)-C_6B_6C_0+C_2B_4C_6+A_2\left(-C_2D_8+C_4D_6\right)$$
$$+C_2C_4B_6\Big]+A_4\Big[A_0\left(2A_2C_6D_8-B_4C_6^2\right)+C_6\left(-A_2^2D_6-A_2B_4C_4\right)-C_4^2A_2B_6+C_4D_8A_2^2\Big]$$

$$+ C_6 A_2\Big[-C_6 B_6 A_0 + A_2\Big(-D_8 A_2 + B_4 C_6 + B_6 C_4\Big)\Big], \tag{95b}$$

$$\begin{aligned} Q_6 = {} & A_4^3(C_0 D_6 - C_2 D_4) + A_4^2\big[A_0(-C_4 D_6 + C_6 D_4) + C_0(-B_4 C_6 - B_6 C_4) \\ & + C_2^2 B_6 + C_2 C_4 B_4 + C_2 C_6 B_2 - C_2 D_6 A_2 + C_4 D_4 A_2\big] \\ & + A_4\{A_0\big[-C_6^2 B_2 + (2A_2 D_6 - 2B_6 C_2)C_6 + C_4^2 B_6\big] \\ & - A_2\big[-C_6 B_6 C_0 + C_6(A_2 D_4 + B_2 C_4) + C_4(-A_2 D_6 + B_4 C_4 + B_6 C_2)\big]\} \\ & + C_6\big[C_6 B_6 A_0^2 - A_2 A_0(B_4 C_6 + B_6 C_4) + A_2^2(-A_2 D_6 + C_6 B_2 + B_4 C_4 + B_6 C_2)\big], \end{aligned} \tag{95c}$$

$$\begin{aligned} Q_4 = {} & A_4^3(C_0 D_4 - C_2 D_2) + A_4^2\big[A_0(-C_4 D_4 + C_6 D_2) + C_2 C_6 B_0 \\ & + C_0(-C_6 B_2 - B_4 C_4) + C_2^2 B_4 + C_2 C_4 B_2 - C_2 D_4 A_2 + C_4 D_2 A_2\big] \\ & + A_4\{A_0\big[-C_6^2 B_0 + C_6(2A_2 D_4 - 2B_4 C_2) + C_4^2 B_4\big] \\ & - A_2\big[C_4 C_6 B_0 - C_6 B_4 C_0 + C_6 D_2 A_2 + C_4(-A_2 D_4 + B_2 C_4 + B_4 C_2)\big]\} \\ & + C_6\big[C_6 B_4 A_0^2 - A_2 A_0(B_2 C_6 + B_4 C_4) + A_2^2(-A_2 D_4 + B_0 C_6 + B_2 C_4 + B_4 C_2)\big], \end{aligned} \tag{95d}$$

$$\begin{aligned} Q_2 = {} & A_4^3(C_0 D_2 - C_2 D_0) + A_4^2\big[A_0(-C_4 D_2 + C_6 D_0) + B_0(-C_0 C_6 + C_2 C_4) \\ & - C_4 B_2 C_0 + A_2(-C_2 D_2 + C_4 D_0) + C_2^2 B_2\big] + A_4\Big\{A_0\big[C_6(2A_2 D_2 - 2B_2 C_2) + C_4^2 B_2\big] \\ & - A_2\big[C_4^2 B_0 - B_2 C_6 C_0 + D_0 A_2 C_6 + C_4(-A_2 D_2 + B_2 C_2)\big]\Big\} \\ & + C_6\big[B_2 C_6 A_0^2 - A_2 A_0(B_0 C_6 + B_2 C_4) + A_2^2(-A_2 D_2 + B_0 C_4 + B_2 C_2)\big], \end{aligned} \tag{95e}$$

$$\begin{aligned} Q_0 = {} & A_4^3 D_0 C_0 + A_4^2\big[-C_4 D_0 A_0 + B_0(-C_0 C_4 + C_2^2) - C_2 D_0 A_2\big] \\ & + A_4\{A_0\big[B_0(-2C_2 C_6 + C_4^2) + 2D_0 A_2 C_6\big] - A_2\big[B_0(-C_0 C_6 + C_2 C_4) - C_4 D_0 A_2\big]\} \\ & + C_6\big[C_6 B_0 A_0^2 - C_4 A_2 B_0 A_0 + A_2^2(-A_2 D_0 + B_0 C_2)\big], \end{aligned} \tag{95f}$$

$$\begin{aligned} Q_d = {} & A_4^3 C_0^2 + A_4^2\big[A_0\big(-2C_0 C_4 + C_2^2\big) - C_0 C_2 A_2\big] \\ & + A_4\big[A_0^2\big(-2C_2 C_6 + C_4^2\big) - A_2 A_0(-3C_0 C_6 + C_2 C_4) + C_0 C_4 A_2^2\big] \\ & + C_6\big(A_0^3 C_6 - A_0^2 A_2 C_4 + A_0 A_2^2 C_2 - A_2^3 C_0\big). \end{aligned} \tag{95g}$$

For a three-layer plate, the following eight boundary conditions for the interfacial stresses can be applied (see Eqs. (66a) and (66b)):

$$\tau^{(1)}_{\hat{x}z,\hat{x}}\,|_{\hat{x}=\pm L/2} = K_s^{(1)}\left[\frac{\overline{N}^{(2)}}{c_{11}^{(2)} t_2} - \frac{\overline{N}^{(1)}}{c_{11}^{(1)} t_1} + \frac{d_{11}^{(2)}}{c_{11}^{(2)}}\Delta T^{(2)} - \frac{d_{11}^{(1)}}{c_{11}^{(1)}}\Delta T^{(1)} + 6\left(\frac{\overline{M}^{(2)}}{c_{11}^{(2)} t_2^2} + \frac{\overline{M}^{(1)}}{c_{11}^{(1)} t_1^2}\right)\right]\Bigg|_{\hat{x}=\pm\frac{L}{2}}, \tag{96a}$$

$$\tau^{(2)}_{\hat{x}z,\hat{x}}\,|_{\hat{x}=\pm L/2} = K_s^{(2)}\left[\frac{\overline{N}^{(3)}}{c_{11}^{(3)} t_3} - \frac{\overline{N}^{(2)}}{c_{11}^{(2)} t_2} + \frac{d_{11}^{(3)}}{c_{11}^{(3)}}\Delta T^{(3)} - \frac{d_{11}^{(2)}}{c_{11}^{(2)}}\Delta T^{(2)} + 6\left(\frac{\overline{M}^{(3)}}{c_{11}^{(3)} t_3^2} + \frac{\overline{M}^{(2)}}{c_{11}^{(2)} t_2^2}\right)\right]\Bigg|_{\hat{x}=\pm\frac{L}{2}}, \tag{96b}$$

$$\tau^{(1)}_{zz,\hat{x}\hat{x}}\,|_{\hat{x}=\pm L/2} = 12K_n^{(1)}\left(\frac{\overline{M}^{(2)}}{c_{11}^{(2)} t_2^3} - \frac{\overline{M}^{(1)}}{c_{11}^{(1)} t_1^3}\right)\Bigg|_{\hat{x}=\pm\frac{L}{2}}, \tag{96c}$$

$$\tau^{(2)}_{zz,\hat{x}\hat{x}}\,|_{\hat{x}=\pm L/2} = 12K_n^{(2)}\left(\frac{\overline{M}^{(3)}}{c_{11}^{(3)} t_3^3} - \frac{\overline{M}^{(2)}}{c_{11}^{(2)} t_2^3}\right)\Bigg|_{\hat{x}=\pm\frac{L}{2}}. \tag{96d}$$

For a three-layer plate represented by a well-posed BVP, the polynomial equation in Eq. (93b) should have two real roots (i.e., $R_r = 2$) and two pairs of conjugated complex roots (i.e., $R_{cc} = 2$) for $Z = \lambda^2$. As demonstrated in Appendix A, each pair of conjugated complex roots gives two relations for the constants $\overline{C}_n$. Therefore, the two pairs of the conjugated complex roots lead to four additional relations, which can be used along with the eight boundary conditions in Eqs. (96a)–(96d) to determine the 12 constants $\overline{C}_n$ (with $n =$

{1,2, ..., 12}) involved in Eqs. (92a) and (92b). This is similar to what is done for the two-layer plate case in Sect. 4.1.

For the case of a symmetrically loaded composite square plate, the interfacial stresses can be obtained from Eqs. (68a) and (68b) as, with $R_r = 2$ and $R_{cc} = 2$,

$$\tau^{(1)}_{\hat{x}z,\hat{x}} = \mathcal{S}_1\Omega_1\cosh\left(w_1\hat{x}\right) + \mathcal{S}_2\Omega_2\cosh\left(w_2\hat{x}\right) + \overline{S}_1\left[\overline{\Lambda}_1\cosh\left(\omega_1\hat{x}\right)\cos\left(\omega_1^*\hat{x}\right) - \overline{\Lambda}_1^*\sinh\left(\omega_1\hat{x}\right)\sin\left(\omega_1^*\hat{x}\right)\right] + \overline{S}_2\left[\overline{\Lambda}_2\cosh\left(\omega_2\hat{x}\right)\cos\left(\omega_2^*\hat{x}\right) - \overline{\Lambda}_2^*\sinh\left(\omega_2\hat{x}\right)\sin\left(\omega_2^*\hat{x}\right)\right] - \frac{B_0P_2 - D_0P_1}{A_0D_0 - B_0C_0}, \tag{97a}$$

$$\tau^{(1)}_{zz}\left(\hat{x}\right) = \mathcal{S}_1\cosh\left(w_1\hat{x}\right) + \mathcal{S}_2\cosh\left(w_2\hat{x}\right) + \overline{S}_1\cosh\left(\omega_1\hat{x}\right)\cos\left(\omega_1^*\hat{x}\right) + \overline{S}_2\cosh\left(\omega_2\hat{x}\right)\cos\left(\omega_2^*\hat{x}\right) + \frac{A_0P_2 - C_0P_1}{A_0D_0 - B_0C_0}, \tag{97b}$$

where $\mathcal{S}_1$, $\mathcal{S}_2$, $\overline{S}_1$ and $\overline{S}_2$ are four constants to be determined from the boundary conditions, w_1 and w_2 are two absolute values of the real roots of Eq. (93a), and ω_1 and ω_2 and ω_1^* and ω_2^* are, respectively, the absolute values of the real and imaginary parts of the complex roots $\pm\omega_1 \pm \mathrm{i}\omega_1^*$ and $\pm\omega_2 \pm \mathrm{i}\omega_2^*$ of Eq. (93a). The parameters Ω_1, Ω_2, $\overline{\Lambda}_1$, $\overline{\Lambda}_2$, $\overline{\Lambda}_1^*$ and $\overline{\Lambda}_2^*$ in Eq. (97a) can be obtained from Eq. (94) as

$$\Omega_1 = -\frac{Q_{10}w_1^{10} + Q_8w_1^8 + Q_6w_1^6 + Q_4w_1^4 + Q_2w_1^2 + Q_0}{Q_d}, \quad \Omega_2 = -\frac{Q_{10}w_2^{10} + Q_8w_2^8 + Q_6w_2^6 + Q_4w_2^4 + Q_2w_2^2 + Q_0}{Q_d}, \tag{98a,b}$$

$$\left[\overline{\Lambda}_1, \overline{\Lambda}_2\right] = \left[\mathrm{Re}(\Lambda_1), \mathrm{Re}(\Lambda_2)\right], \left[\overline{\Lambda}_1^*, \overline{\Lambda}_2^*\right] = \left[\left|\mathrm{Im}(\Lambda_1)\right|, \left|\mathrm{Im}(\Lambda_2)\right|\right], \tag{98c,d}$$

with

$$\Lambda_1 = -\frac{1}{Q_d}\left\{Q_{10}\left(\omega_1^2 - \omega_1^{*2} - \mathrm{i}2\omega_1\omega_1^*\right)^5 + Q_8\left(\omega_1^2 - \omega_1^{*2} - \mathrm{i}2\omega_1\omega_1^*\right)^4 + Q_6\left(\omega_1^2 - \omega_1^{*2} - \mathrm{i}2\omega_1\omega_1^*\right)^3 + Q_4\left(\omega_1^2 - \omega_1^{*2} - \mathrm{i}2\omega_1\omega_1^*\right)^2 + Q_2\left(\omega_1^2 - \omega_1^{*2} - \mathrm{i}2\omega_1\omega_1^*\right) + Q_0\right\}, \tag{98e}$$

$$\Lambda_2 = -\frac{1}{Q_d}\left\{Q_{10}\left(\omega_2^2 - \omega_2^{*2} - \mathrm{i}2\omega_2\omega_2^*\right)^5 + Q_8\left(\omega_2^2 - \omega_2^{*2} - \mathrm{i}2\omega_2\omega_2^*\right)^4 + Q_6\left(\omega_2^2 - \omega_2^{*2} - \mathrm{i}2\omega_2\omega_2^*\right)^3 + Q_4\left(\omega_2^2 - \omega_2^{*2} - \mathrm{i}2\omega_2\omega_2^*\right)^2 + Q_2\left(\omega_2^2 - \omega_2^{*2} - \mathrm{i}2\omega_2\omega_2^*\right) + Q_0\right\}, \tag{98f}$$

where Q_0, Q_2, Q_4, Q_6, Q_8, Q_{10} and Q_d can be obtained from Eqs. (95a)–(95g).

To determine the constants $\mathcal{S}_1$, $\mathcal{S}_2$, $\overline{S}_1$ and $\overline{S}_2$, $\tau^{(2)}_{\hat{x}z,\hat{x}}$ and $\tau^{(2)}_{zz}$ are first derived from Eqs. (57a) and (57b) as (see Appendix B):

$$\tau^{(2)}_{\hat{x}z,\hat{x}} = \left(\frac{1}{\beta_1^{(1)}\xi_1^{(1)} - \alpha_1^{(1)}\gamma_1^{(1)}}\right)\left\{\xi_1^{(1)}\tau^{(1)}_{\hat{x}z,\hat{x}\hat{x}\hat{x}} + \left(\gamma_0^{(1)}\alpha_1^{(1)} - \beta_0^{(1)}\xi_1^{(1)}\right)\tau^{(1)}_{\hat{x}z,\hat{x}} + \left(\gamma_{-1}^{(1)}\alpha_1^{(1)} - \beta_{-1}^{(1)}\xi_1^{(1)}\right)\tau^{(0)}_{\hat{x}z,\hat{x}} - \alpha_1^{(1)}\tau^{(1)}_{zz,\hat{x}\hat{x}\hat{x}\hat{x}} + \left(\xi_0^{(1)}\alpha_1^{(1)} - \alpha_0^{(1)}\xi_1^{(1)}\right)\tau^{(1)}_{zz} + \left(\xi_{-1}^{(1)}\alpha_1^{(1)} - \alpha_{-1}^{(1)}\xi_1^{(1)}\right)\tau^{(0)}_{zz} - \xi_1^{(1)}\left(\eta_{\hat{x}}^{(1)} + \eta_z^{(1)}\right) + \alpha_1^{(1)}\chi_z^{(1)}\right\}, \tag{99a}$$

$$\tau^{(2)}_{zz} = \frac{\beta_1^{(1)}}{\beta_1^{(1)}\xi_1^{(1)} - \alpha_1^{(1)}\gamma_1^{(1)}}\left\{\tau^{(1)}_{zz,\hat{x}\hat{x}\hat{x}\hat{x}} - \frac{\gamma_1^{(1)}}{\beta_1^{(1)}}\tau^{(1)}_{\hat{x}z,\hat{x}\hat{x}\hat{x}} - \left(\gamma_0^{(1)} - \frac{\gamma_1^{(1)}\beta_0^{(1)}}{\beta_1^{(1)}}\right)\tau^{(1)}_{\hat{x}z,\hat{x}} - \left(\gamma_{-1}^{(1)} - \frac{\gamma_1^{(1)}\beta_{-1}^{(1)}}{\beta_1^{(1)}}\right)\tau^{(0)}_{\hat{x}z,\hat{x}} - \left(\xi_0^{(1)} - \frac{\gamma_1^{(1)}\alpha_0^{(1)}}{\beta_1^{(1)}}\right)\tau^{(1)}_{zz} - \left(\xi_{-1}^{(1)} - \frac{\gamma_1^{(1)}\alpha_{-1}^{(1)}}{\beta_1^{(1)}}\right)\tau^{(0)}_{zz} + \frac{\gamma_1^{(1)}}{\beta_1^{(1)}}\eta_{\hat{x}}^{(1)} + \frac{\gamma_1^{(1)}}{\beta_1^{(1)}}\eta_z^{(1)} - \chi_z^{(1)}\right\}, \tag{99b}$$

where Eq. (99a) is obtained from substituting Eq. (B4) into Eq. (B2) (see Appendix B). Using Eqs. (97a) and (97b) in Eqs. (99a) and (99b) then yields

$$\tau^{(2)}_{\hat{x}z,\hat{x}} = \frac{1}{\beta_1^{(1)}\xi_1^{(1)} - \alpha_1^{(1)}\gamma_1^{(1)}}\left\{\bar{S}_1\left[\left(\Lambda_1\omega_1^2 - \Lambda_1\omega_1^{*2} - 2\omega_1\Lambda_1^*\omega_1^*\right)\xi_1^{(1)} - \omega_1^4\alpha_1^{(1)} + 6\omega_1^2\alpha_1^{(1)}\omega_1^{*2}\right.\right.$$

$$-\alpha_1^{(1)}\omega_1^{*4}+\Lambda_1\Big(\gamma_0^{(1)}\alpha_1^{(1)}-\beta_0^{(1)}\xi_1^{(1)}\Big)+\xi_0^{(1)}\alpha_1^{(1)}-\alpha_0^{(1)}\xi_1^{(1)}\Big]\cosh(\omega_1\hat{x})\cos(\omega_1^*\hat{x})$$
$$+\bar{S}_2\Big[\Big(\Lambda_2\omega_2^2-\Lambda_2\omega_2^{*2}-2\omega_2\Lambda_2^*\omega_2^*\Big)\xi_1^{(1)}+\Lambda_2\Big(\gamma_0^{(1)}\alpha_1^{(1)}-\beta_0^{(1)}\xi_1^{(1)}\Big)$$
$$-\Big(\omega_2^4-6\omega_2^2\omega_2^{*2}+\omega_2^{*4}\Big)\alpha_1^{(1)}+\xi_0^{(1)}\alpha_1^{(1)}-\alpha_0^{(1)}\xi_1^{(1)}\Big]\cosh(\omega_2\hat{x})\cos(\omega_2^*\hat{x})-\bar{S}_1\Big[\Big(\omega_1^2\Lambda_1^*$$
$$+2\omega_1\Lambda_1\omega_1^*-\omega_1^{*2}\Lambda_1^*\Big)\xi_1^{(1)}-4\omega_1^3\omega_1^*\alpha_1^{(1)}+4\omega_1\omega_1^{*3}\alpha_1^{(1)}+\Lambda_1^*\Big(\gamma_0^{(1)}\alpha_1^{(1)}-\beta_0^{(1)}\xi_1^{(1)}\Big)\Big]\sinh(\omega_1\hat{x})\sin(\omega_1^*\hat{x})$$
$$-\bar{S}_2\Big[\Big(2\Lambda_2\omega_2\omega_2^*+\omega_2^2\Lambda_2^*-\Lambda_2^*\omega_2^{*2}\Big)\xi_1^{(1)}+\Lambda_2^*\Big(\gamma_0^{(1)}\alpha_1^{(1)}-\beta_0^{(1)}\xi_1^{(1)}\Big)$$
$$-4\bar{S}_2\omega_2\omega_2^*\alpha_1^{(1)}(\omega_2-\omega_2^*)(\omega_2+\omega_2^*)\Big]\sinh(\omega_2\hat{x})\sin(\omega_2^*\hat{x})$$
$$+\mathcal{S}_1\Big[-\alpha_1^{(1)}w_1^4+\xi_1^{(1)}\Omega_1w_1^2+\Big(\gamma_0^{(1)}\alpha_1^{(1)}-\beta_0^{(1)}\xi_1^{(1)}\Big)\Omega_1+\xi_0^{(1)}\alpha_1^{(1)}-\alpha_0^{(1)}\xi_1^{(1)}\Big]\cosh(w_1\hat{x})$$
$$+\mathcal{S}_2\Big[-\alpha_1^{(1)}w_2^4+\xi_1^{(1)}\Omega_2w_2^2+\Big(\gamma_0^{(1)}\alpha_1^{(1)}-\beta_0^{(1)}\xi_1^{(1)}\Big)\Omega_2+\xi_0^{(1)}\alpha_1^{(1)}-\alpha_0^{(1)}\xi_1^{(1)}\Big]\cosh(w_2\hat{x})$$
$$-\Big(\gamma_0^{(1)}\alpha_1^{(1)}-\beta_0^{(1)}\xi_1^{(1)}\Big)\Big(\frac{B_0P_2-D_0P_1}{A_0D_0-B_0C_0}\Big)+\Big(\xi_0^{(1)}\alpha_1^{(1)}-\alpha_0^{(1)}\xi_1^{(1)}\Big)\Big(\frac{A_0P_2-C_0P_1}{A_0D_0-B_0C_0}\Big)$$
$$+\Big(\gamma_{-1}^{(1)}\alpha_1^{(1)}-\beta_{-1}^{(1)}\xi_1^{(1)}\Big)\tau_{\hat{x}z,\hat{x}}^{(0)}+\Big(\xi_{-1}^{(1)}\alpha_1^{(1)}-\alpha_{-1}^{(1)}\xi_1^{(1)}\Big)\tau_{zz}^{(0)}-\xi_1^{(1)}\Big(\eta_{\hat{x}}^{(1)}+\eta_z^{(1)}\Big)+\alpha_1^{(1)}\chi_z^{(1)}\Big\}, \tag{100a}$$

$$\tau_{zz}^{(2)}=\frac{1}{\beta_1^{(1)}\xi_1^{(1)}-\alpha_1^{(1)}\gamma_1^{(1)}}\Big\{\bar{S}_1\Big[-\gamma_1^{(1)}(\Lambda_1\omega_1^2-\Lambda_1\omega_1^{*2}-2\omega_1\Lambda_1^*\omega_1^*)+\omega_1^4\beta_1^{(1)}-6\omega_1^2\omega_1^{*2}\beta_1^{(1)}$$
$$+\omega_1^{*4}\beta_1^{(1)}-\Lambda_1\Big(\gamma_0^{(1)}\beta_1^{(1)}-\gamma_1^{(1)}\beta_0^{(1)}\Big)+\gamma_1^{(1)}\alpha_0^{(1)}-\xi_0^{(1)}\beta_1^{(1)}\Big]\cosh(\omega_1\hat{x})\cos(\omega_1^*\hat{x})$$
$$+\bar{S}_2\Big[-\gamma_1^{(1)}(\Lambda_2\omega_2^2-\Lambda_2\omega_2^{*2}-2\omega_2\Lambda_2^*\omega_2^*)-\Lambda_2\Big(\gamma_0^{(1)}\beta_1^{(1)}-\gamma_1^{(1)}\beta_0^{(1)}\Big)$$
$$+(\omega_2^4-6\omega_2^2\omega_2^{*2}+\omega_2^{*4})\beta_1^{(1)}+\gamma_1^{(1)}\alpha_0^{(1)}-\xi_0^{(1)}\beta_1^{(1)}\Big]\cosh(\omega_2\hat{x})\cos(\omega_2^*\hat{x})$$
$$-\bar{S}_1\Big[-\gamma_1^{(1)}(\omega_1^2\Lambda_1^*+2\omega_1\Lambda_1\omega_1^*-\omega_1^{*2}\Lambda_1^*)+4\omega_1^3\omega_1^*\beta_1^{(1)}-4\omega_1\omega_1^{*3}\beta_1^{(1)}$$
$$-\Lambda_1^*\Big(\gamma_0^{(1)}\beta_1^{(1)}-\gamma_1^{(1)}\beta_0^{(1)}\Big)\Big]\sinh(\omega_1\hat{x})\sin(\omega_1^*\hat{x})-\bar{S}_2\Big[-\gamma_1^{(1)}(2\Lambda_2\omega_2\omega_2^*+\omega_2^2\Lambda_2^*-\Lambda_2^*\omega_2^{*2})$$
$$-\Lambda_2^*\Big(\gamma_0^{(1)}\beta_1^{(1)}-\gamma_1^{(1)}\beta_0^{(1)}\Big)+4\omega_2\omega_2^*\beta_1^{(1)}(\omega_2-\omega_2^*)(\omega_2+\omega_2^*)\Big]\sinh(\omega_2\hat{x})\sin(\omega_2^*\hat{x})$$
$$+\mathcal{S}_1\Big[w_1^4\beta_1^{(1)}-\gamma_1^{(1)}\Omega_1w_1^2-\Omega_1\Big(\gamma_0^{(1)}\beta_1^{(1)}-\gamma_1^{(1)}\beta_0^{(1)}\Big)+\gamma_1^{(1)}\alpha_0^{(1)}-\xi_0^{(1)}\beta_1^{(1)}\Big]\cosh(w_1\hat{x})$$
$$+\mathcal{S}_2\Big[w_2^4\beta_1^{(1)}-\gamma_1^{(1)}\Omega_2w_2^2-\Omega_2\Big(\gamma_0^{(1)}\beta_1^{(1)}-\gamma_1^{(1)}\beta_0^{(1)}\Big)+\gamma_1^{(1)}\alpha_0^{(1)}-\xi_0^{(1)}\beta_1^{(1)}\Big]\cosh(w_2\hat{x})$$
$$+\Big(\gamma_0^{(1)}\beta_1^{(1)}-\gamma_1^{(1)}\beta_0^{(1)}\Big)\Big(\frac{B_0P_2-D_0P_1}{A_0D_0-B_0C_0}\Big)+\Big(\gamma_1^{(1)}\alpha_0^{(1)}-\xi_0^{(1)}\beta_1^{(1)}\Big)\Big(\frac{A_0P_2-C_0P_1}{A_0D_0-B_0C_0}\Big)$$
$$+\Big(-\beta_1^{(1)}\gamma_{-1}^{(1)}+\gamma_1^{(1)}\beta_{-1}^{(1)}\Big)\tau_{\hat{x}z,\hat{x}}^{(0)}+\Big(-\beta_1^{(1)}\xi_{-1}^{(1)}+\gamma_1^{(1)}\alpha_{-1}^{(1)}\Big)\tau_{zz}^{(0)}+\gamma_1^{(1)}\eta_{\hat{x}}^{(1)}+\gamma_1^{(1)}\eta_z^{(1)}-\beta_1^{(1)}\chi_z^{(1)}\Big\}, \tag{100b}$$

where A_0, B_0, C_0, D_0, P_1 and P_2 are defined in Eqs. (91a)–(91f).

Substituting Eqs. (97a), (97b), (100a) and (100b) into Eqs. (96a)–(96d) leads to

$$\mathcal{S}_1\Omega_1\cosh\Big(\frac{w_1L}{2}\Big)+\mathcal{S}_2\Omega_2\cosh\Big(\frac{w_2L}{2}\Big)+\bar{S}_1\Big[\bar{\Lambda}_1\cosh\Big(\frac{\omega_1L}{2}\Big)\cos\Big(\frac{\omega_1^*L}{2}\Big)-\bar{\Lambda}_1^*\sinh\Big(\frac{\omega_1L}{2}\Big)\sin\Big(\frac{\omega_1^*L}{2}\Big)\Big]$$
$$+\bar{S}_2\Big[\bar{\Lambda}_2\cosh\Big(\frac{\omega_2L}{2}\Big)\cos\Big(\frac{\omega_2^*L}{2}\Big)-\bar{\Lambda}_2^*\sinh\Big(\frac{\omega_2L}{2}\Big)\sin\Big(\frac{\omega_2^*L}{2}\Big)\Big]-\frac{B_0P_2-D_0P_1}{A_0D_0-B_0C_0}$$
$$-K_s^{(1)}\Bigg[\frac{\overline{N}^{(2)}}{c_{11}^{(2)}t_2}-\frac{\overline{N}^{(1)}}{c_{11}^{(1)}t_1}+\frac{d_{11}^{(2)}}{c_{11}^{(2)}}\Delta T^{(2)}-\frac{d_{11}^{(1)}}{c_{11}^{(1)}}\Delta T^{(1)}+6\Bigg(\frac{\overline{M}^{(2)}}{c_{11}^{(2)}t_2^2}+\frac{\overline{M}^{(1)}}{c_{11}^{(1)}t_1^2}\Bigg)\Bigg]\Bigg|_{\hat{x}=\frac{L}{2}}=0, \tag{101a}$$

$$\frac{1}{\beta_1^{(1)}\xi_1^{(1)}-\alpha_1^{(1)}\gamma_1^{(1)}}\Big\{\bar{S}_1\Big[(\Lambda_1\omega_1^2-\Lambda_1\omega_1^{*2}-2\omega_1\Lambda_1^*\omega_1^*)\xi_1^{(1)}-\omega_1^4\alpha_1^{(1)}+6\omega_1^2\alpha_1^{(1)}\omega_1^{*2}$$

$$-\alpha_1^{(1)}\omega_1^{*4}+\Lambda_1\left(\gamma_0^{(1)}\alpha_1^{(1)}-\beta_0^{(1)}\xi_1^{(1)}\right)+\xi_0^{(1)}\alpha_1^{(1)}-\alpha_0^{(1)}\xi_1^{(1)}\Big]\cosh\left(\frac{\omega_1 L}{2}\right)\cos\left(\frac{\omega_1^* L}{2}\right)$$
$$+\bar{S}_2\Big[\left(\Lambda_2\omega_2^2-\Lambda_2\omega_2^{*2}-2\omega_2\Lambda_2^*\omega_2^*\right)\xi_1^{(1)}+\Lambda_2\left(\gamma_0^{(1)}\alpha_1^{(1)}-\beta_0^{(1)}\xi_1^{(1)}\right)-\left(\omega_2^4-6\omega_2^2\omega_2^{*2}\right.$$
$$\left.+\omega_2^{*4}\right)\alpha_1^{(1)}+\xi_0^{(1)}\alpha_1^{(1)}-\alpha_0^{(1)}\xi_1^{(1)}\Big]\cosh\left(\frac{\omega_2 L}{2}\right)\cos\left(\frac{\omega_2^* L}{2}\right)-\bar{S}_1\Big[\left(\omega_1^2\Lambda_1^*+2\omega_1\Lambda_1\omega_1^*\right.$$
$$\left.-\omega_1^{*2}\Lambda_1^*\right)\xi_1^{(1)}-4\omega_1^3\omega_1^*\alpha_1^{(1)}+4\omega_1\omega_1^{*3}\alpha_1^{(1)}+\Lambda_1^*\left(\gamma_0^{(1)}\alpha_1^{(1)}-\beta_0^{(1)}\xi_1^{(1)}\right)\Big]\sinh\left(\frac{\omega_1 L}{2}\right)\sin\left(\frac{\omega_1^* L}{2}\right)$$
$$-\bar{S}_2\Big[\left(2\Lambda_2\omega_2\omega_2^*+\omega_2^2\Lambda_2^*-\Lambda_2^*\omega_2^{*2}\right)\xi_1^{(1)}+\Lambda_2^*\left(\gamma_0^{(1)}\alpha_1^{(1)}-\beta_0^{(1)}\xi_1^{(1)}\right)$$
$$-4\bar{S}_2\omega_2\omega_2^*\alpha_1^{(1)}\left(\omega_2-\omega_2^*\right)\left(\omega_2+\omega_2^*\right)\Big]\sinh\left(\frac{\omega_2 L}{2}\right)\sin\left(\frac{\omega_2^* L}{2}\right)$$
$$+\mathcal{S}_1\Big[-\alpha_1^{(1)}w_1^4+\xi_1^{(1)}\Omega_1 w_1^2+\left(\gamma_0^{(1)}\alpha_1^{(1)}-\beta_0^{(1)}\xi_1^{(1)}\right)\Omega_1+\xi_0^{(1)}\alpha_1^{(1)}-\alpha_0^{(1)}\xi_1^{(1)}\Big]\cosh\left(\frac{w_1 L}{2}\right)$$
$$+\mathcal{S}_2\Big[-\alpha_1^{(1)}w_2^4+\xi_1^{(1)}\Omega_2 w_2^2+\left(\gamma_0^{(1)}\alpha_1^{(1)}-\beta_0^{(1)}\xi_1^{(1)}\right)\Omega_2+\xi_0^{(1)}\alpha_1^{(1)}-\alpha_0^{(1)}\xi_1^{(1)}\Big]\cosh\left(\frac{w_2 L}{2}\right)$$
$$-\left(\gamma_0^{(1)}\alpha_1^{(1)}-\beta_0^{(1)}\xi_1^{(1)}\right)\left(\frac{B_0P_2-D_0P_1}{A_0D_0-B_0C_0}\right)+\left(\xi_0^{(1)}\alpha_1^{(1)}-\alpha_0^{(1)}\xi_1^{(1)}\right)\left(\frac{A_0P_2-C_0P_1}{A_0D_0-B_0C_0}\right)$$
$$+\left(\gamma_{-1}^{(1)}\alpha_1^{(1)}-\beta_{-1}^{(1)}\xi_1^{(1)}\right)\tau_{\hat{x}z,\hat{x}}^{(0)}\Big|_{\hat{x}=\frac{L}{2}}+\left(\xi_{-1}^{(1)}\alpha_1^{(1)}-\alpha_{-1}^{(1)}\xi_1^{(1)}\right)\tau_{zz}^{(0)}\Big|_{\hat{x}=\frac{L}{2}}-\xi_1^{(1)}\left(\eta_{\hat{x}}^{(1)}\Big|_{\hat{x}=\frac{L}{2}}+\eta_z^{(1)}\Big|_{\hat{x}=\frac{L}{2}}\right)$$
$$+\alpha_1^{(1)}\chi_z^{(1)}\Big\}-K_s^{(2)}\left[\frac{\overline{N}^{(3)}}{c_{11}^{(3)}t_3}-\frac{\overline{N}^{(2)}}{c_{11}^{(2)}t_2}+\frac{d_{11}^{(3)}}{c_{11}^{(3)}}\Delta T^{(3)}-\frac{d_{11}^{(2)}}{c_{11}^{(2)}}\Delta T^{(2)}+6\left(\frac{\overline{M}^{(3)}}{c_{11}^{(3)}t_3^2}+\frac{\overline{M}^{(2)}}{c_{11}^{(2)}t_2^2}\right)\right]\Bigg|_{\hat{x}=\frac{L}{2}}=0, \tag{101b}$$

$$\mathcal{S}_1 w_1^2\cosh\left(\frac{w_1 L}{2}\right)+\mathcal{S}_2 w_2^2\cosh\left(\frac{w_2 L}{2}\right)+\bar{S}_1\omega_1^2\cosh\left(\frac{\omega_1 L}{2}\right)\cos\left(\frac{\omega_1^* L}{2}\right)$$
$$-2\bar{S}_1\omega_1\omega_1^*\sinh\left(\frac{\omega_1 L}{2}\right)\sin\left(\frac{\omega_1^* L}{2}\right)-\bar{S}_1\omega_1^{*2}\cosh\left(\frac{\omega_1 L}{2}\right)\cos\left(\frac{\omega_1^* L}{2}\right)$$
$$+\bar{S}_2\omega_2^2\cosh\left(\frac{\omega_2 L}{2}\right)\cos\left(\frac{\omega_2^* L}{2}\right)-2\bar{S}_2\omega_2\omega_2^*\sinh\left(\frac{\omega_2 L}{2}\right)\sin\left(\frac{\omega_2^* L}{2}\right)$$
$$-\bar{S}_2\omega_2^{*2}\cosh\left(\frac{\omega_2 L}{2}\right)\cos\left(\frac{\omega_2^* L}{2}\right)-12K_n^{(1)}\left(\frac{\overline{M}^{(2)}}{c_{11}^{(2)}t_2^3}-\frac{\overline{M}^{(1)}}{c_{11}^{(1)}t_1^3}\right)\Bigg|_{\hat{x}=\frac{L}{2}}=0, \tag{101c}$$

$$\bar{S}_1\Big[-\gamma_1^{(1)}\left(\Lambda_1\omega_1^2-\Lambda_1\omega_1^{*2}-2\omega_1\Lambda_1^*\omega_1^*\right)+\omega_1^4\beta_1^{(1)}-6\omega_1^2\omega_1^{*2}\beta_1^{(1)}+\omega_1^{*4}\beta_1^{(1)}-\Lambda_1\left(\gamma_0^{(1)}\beta_1^{(1)}\right.$$
$$\left.-\gamma_1^{(1)}\beta_0^{(1)}\right)+\gamma_1^{(1)}\alpha_0^{(1)}-\xi_0^{(1)}\beta_1^{(1)}\Big]\Big[\omega_1^2\cosh\left(\frac{\omega_1 L}{2}\right)\cos\left(\frac{\omega_1^* L}{2}\right)-2\omega_1\omega_1^*\sinh\left(\frac{\omega_1 L}{2}\right)\sin\left(\frac{\omega_1^* L}{2}\right)$$
$$-\omega_1^{*2}\cosh\left(\frac{\omega_1 L}{2}\right)\cos\left(\frac{\omega_1^* L}{2}\right)\Big]+\bar{S}_2\Big[-\gamma_1^{(1)}\left(\Lambda_2\omega_2^2-\Lambda_2\omega_2^{*2}-2\omega_2\Lambda_2^*\omega_2^*\right)-\Lambda_2\Big[\left(\gamma_0^{(1)}\beta_1^{(1)}-\gamma_1^{(1)}\beta_0^{(1)}\right)$$
$$+\left(\omega_2^4-6\omega_2^2\omega_2^{*2}+\omega_2^{*4}\right)\beta_1^{(1)}+\gamma_1^{(1)}\alpha_0^{(1)}-\xi_0^{(1)}\beta_1^{(1)}\Big]\Big[\omega_2^2\cosh\left(\frac{\omega_2 L}{2}\right)\cos\left(\frac{\omega_2^* L}{2}\right)$$
$$-2\omega_2\omega_2^*\sinh\left(\frac{\omega_2 L}{2}\right)\sin\left(\frac{\omega_2^* L}{2}\right)-\omega_2^{*2}\cosh\left(\frac{\omega_2 L}{2}\right)\cos\left(\frac{\omega_2^* L}{2}\right)\Big]$$
$$-\bar{S}_1\Big[-\gamma_1^{(1)}\left(\omega_1^2\Lambda_1^*+2\omega_1\Lambda_1\omega_1^*-\omega_1^{*2}\Lambda_1^*\right)+4\omega_1^3\omega_1^*\beta_1^{(1)}-4\omega_1\omega_1^{*3}\beta_1^{(1)}$$
$$-\Lambda_1^*\left(\gamma_0^{(1)}\beta_1^{(1)}-\gamma_1^{(1)}\beta_0^{(1)}\right)\Big]\Big[\omega_1^2\sinh\left(\frac{\omega_1 L}{2}\right)\sin\left(\frac{\omega_1^* L}{2}\right)+2\omega_1\omega_1^*\cosh\left(\frac{\omega_1 L}{2}\right)\cos\left(\frac{\omega_1^* L}{2}\right)$$
$$-\omega_1^{*2}\sinh\left(\frac{\omega_1 L}{2}\right)\sin\left(\frac{\omega_1^* L}{2}\right)\Big]-\bar{S}_2\Big[-\gamma_1^{(1)}\left(2\Lambda_2\omega_2\omega_2^*+\omega_2^2\Lambda_2^*-\Lambda_2^*\omega_2^{*2}\right)-\Lambda_2^*\left(\gamma_0^{(1)}\beta_1^{(1)}-\gamma_1^{(1)}\beta_0^{(1)}\right)$$
$$+4\omega_2\omega_2^*\beta_1^{(1)}\left(\omega_2-\omega_2^*\right)\left(\omega_2+\omega_2^*\right)\Big]\Big[\omega_2^2\sinh\left(\frac{\omega_2 L}{2}\right)\sin\left(\frac{\omega_2^* L}{2}\right)+2\omega_2\omega_2^*\cosh\left(\frac{\omega_2 L}{2}\right)\cos\left(\frac{\omega_2^* L}{2}\right)$$

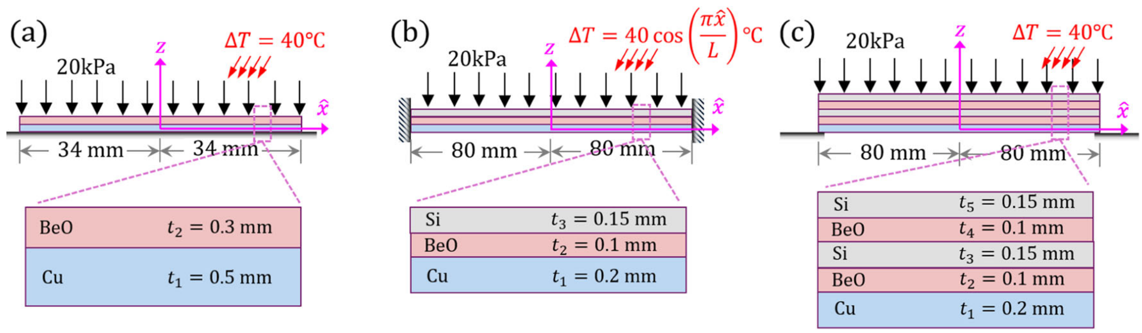

Fig. 2 Geometrical parameters and loading conditions for the multi-layered composite plates: **a** two-layer plate; **b** three-layer plate; **c** five-layer plate

$$-\omega_2^{*2}\sinh\left(\frac{\omega_2 L}{2}\right)\sin\left(\frac{\omega_2^* L}{2}\right)\Big] + \mathcal{S}_1 w_1^2\Big[w_1^4\beta_1^{(1)} - \gamma_1^{(1)}\Omega_1 w_1^2 - \Omega_1\left(\gamma_0^{(1)}\beta_1^{(1)} - \gamma_1^{(1)}\beta_0^{(1)}\right) + \gamma_1^{(1)}\alpha_0^{(1)} - \xi_0^{(1)}\beta_1^{(1)}\Big]\cosh\left(\frac{w_1 L}{2}\right)$$
$$+ \mathcal{S}_2 w_2^2\Big[w_2^4\beta_1^{(1)} - \gamma_1^{(1)}\Omega_2 w_2^2 - \Omega_2\left(\gamma_0^{(1)}\beta_1^{(1)} - \gamma_1^{(1)}\beta_0^{(1)}\right) + \gamma_1^{(1)}\alpha_0^{(1)} - \xi_0^{(1)}\beta_1^{(1)}\Big]\cosh\left(\frac{w_2 L}{2}\right)$$
$$+ \left(-\beta_1^{(1)}\gamma_{-1}^{(1)} + \gamma_1^{(1)}\beta_{-1}^{(1)}\right)\tau_{\hat{x}z,\hat{x}\hat{x}\hat{x}}^{(0)}\Big|_{\hat{x}=\frac{L}{2}} + \left(-\beta_1^{(1)}\xi_{-1}^{(1)} + \gamma_1^{(1)}\alpha_{-1}^{(1)}\right)\tau_{zz,\hat{x}\hat{x}}^{(0)}\Big|_{\hat{x}=\frac{L}{2}} + \gamma_1^{(1)}\eta_{\hat{x},\hat{x}\hat{x}}^{(1)}\Big|_{\hat{x}=\frac{L}{2}}$$
$$+\gamma_1^{(1)}\eta_{z,\hat{x}\hat{x}}^{(1)}\Big|_{\hat{x}=\frac{L}{2}} - \beta_1^{(1)}\chi_{z,\hat{x}\hat{x}}^{(1)}\Big|_{\hat{x}=\frac{L}{2}} - 12K_n^{(2)}\left(\frac{\overline{M}^{(3)}}{c_{11}^{(3)}t_3^3} - \frac{\overline{M}^{(2)}}{c_{11}^{(2)}t_2^3}\right)\Bigg|_{\hat{x}=\frac{L}{2}} = 0. \tag{101d}$$

Solving Eqs. (101a)–(101d), which form a system of four linear algebraic equations, will lead to the determination of the four constants $\mathcal{S}_1$, $\mathcal{S}_2$, $\overline{S}_1$ and $\overline{S}_2$. Substituting these constants into Eqs. (97a), (97b), (100a) and (100b) will give the final expressions for $\tau_{\hat{x}z,\hat{x}}^{(1)}$, $\tau_{\hat{x}z,\hat{x}}^{(2)}$, $\tau_{zz}^{(1)}$ and $\tau_{zz}^{(2)}$. Other quantities for the three-layer plate, including $N^{(m)}$, $M^{(m)}$, $\epsilon_0^{(m)}$ and $\kappa^{(m)}$ (with $m \in \{1, 2, 3\}$), can be determined by following the procedure outlined in Sect. 3.2.1.

5 Numerical results

In this section, the analytical model and closed-form solutions developed in Sects. 3 and 4 are utilized to study the effects of imperfect interfaces on thermomechanical responses of multi-layered composite plates. Three numerical examples of two-, three- and five-layer composite plates under different loading and boundary conditions are respectively analyzed here (see Fig. 2).

In the first example, a two-layer composite plate consisting of a copper (Cu) layer (bottom) and a beryllium oxide (BeO) layer (top) and resting on a rigid substrate, as shown in Fig. 2a, is examined. The composite plate is subjected to a uniform pressure of 20kPa on its top surface (i.e., $\tau_{zz}^{(0)} = \tau_{zz}^{(2)} = -20$kPa, $\tau_{\hat{x}z}^{(0)} = \tau_{\hat{x}z}^{(2)} = 0$, $f_{\hat{x}}^{(1)} = f_z^{(1)} = f_{\hat{x}}^{(2)} = f_z^{(2)} = 0$) and a uniform temperature change of $\Delta T^{(1)} = \Delta T^{(2)} = \Delta T = 40$°C. These lead to $q_{\hat{x}}^{(1)} = q_z^{(1)} = q_{\hat{x}}^{(2)} = q_z^{(2)} = m_{\hat{x}}^{(1)} = m_{\hat{x}}^{(2)} = 0$ (see Eqs. (22a-c)), $\eta_{\hat{x}}^{(1)} = \eta_z^{(1)} = \chi_z^{(1)} = 0$ (see Eq. (71)), and thus $P_1 = 0$ and $\left(\tau_{\hat{x}z,\hat{x}}^{(1)}\right)_p = 0$ (see Eqs. (73) and (74)). In view of the general boundary conditions (BCs) given in Eqs. (43a)–(43c), the following BCs can be identified for this case:

$$N^{(1)} = N^{(2)} = 0 \text{ at } \hat{x} = \pm\frac{L}{2}, \tag{102a}$$

$$M_{,\hat{x}}^{(1)} - \frac{t_1}{2}\tau_{\hat{x}z}^{(1)} = 0, M_{,\hat{x}}^{(2)} - \frac{t_2}{2}\tau_{\hat{x}z}^{(1)} = 0 \text{ at } \hat{x} = \pm\frac{L}{2}, \tag{102b}$$

$$M^{(1)} = M^{(2)} = 0 \text{ at } \hat{x} = \pm\frac{L}{2}, \tag{102c}$$

$$\tau_{\hat{x}z,\hat{x}}^{(1)} = K_s^{(1)}\left[\frac{d_{11}^{(2)}}{c_{11}^{(2)}} - \frac{d_{11}^{(1)}}{c_{11}^{(1)}}\right]\Delta T \text{ at } \hat{x} = \pm\frac{L}{2}, \tag{102d}$$

$$\tau_{zz,\hat{x}\hat{x}}^{(1)} = 0 \text{ at } \hat{x} = \pm\frac{L}{2}. \tag{102e}$$

Note that the BCs in Eqs. (102d) and (102e) are directly obtained from Eqs. (83a), (83b), (102a) and (102c).

In the second example, a three-layer composite plate made from a Cu layer (bottom), a BeO layer (middle) and a silicon (Si) layer (top), as shown in Fig. 2b, is considered, which is clamped on all four edges and subjected to a uniform pressure of 20kPa on its top surface (i.e., $\tau_{zz}^{(0)} = 0$, $\tau_{zz}^{(3)} = -20\text{kPa}$, $\tau_{\hat{x}z}^{(0)} = \tau_{\hat{x}z}^{(3)} = 0$, $f_{\hat{x}}^{(1)} = f_z^{(1)} = f_{\hat{x}}^{(2)} = f_z^{(2)} = f_{\hat{x}}^{(3)} = f_z^{(3)} = 0$) and a temperature distribution of $\Delta T^{(1)} = \Delta T^{(2)} = \Delta T^{(3)} = \Delta T = 40\cos(\pi\hat{x}/L)^{\circ}\text{C}$. These lead to $q_{\hat{x}}^{(1)} = q_z^{(1)} = q_{\hat{x}}^{(2)} = q_z^{(2)} = q_{\hat{x}}^{(3)} = q_z^{(3)} = m_{\hat{x}}^{(1)} = m_{\hat{x}}^{(2)} = m_{\hat{x}}^{(3)} = 0$ (see Eqs. (22a-c)), and $\eta_z^{(1)} = \eta_z^{(2)} = \chi_z^{(1)} = \chi_z^{(2)} = 0$ (see Eqs. (51) and (56)). In view of the general BCs given in Eqs. (43a)–(43c), the following BCs can be identified for the current three-layer plate:

$$u_{0\hat{x}}^{(1)} = u_{0\hat{x}}^{(2)} = u_{0\hat{x}}^{(3)} = 0 \text{ at } \hat{x} = \pm\frac{L}{2}, \tag{103a}$$

$$w^{(1)} = w^{(2)} = w^{(3)} = 0 \text{ at } \hat{x} = \pm\frac{L}{2}, \tag{103b}$$

$$w_{,\hat{x}}^{(1)} = w_{,\hat{x}}^{(2)} = w_{,\hat{x}}^{(3)} = 0 \text{ at } \hat{x} = \pm\frac{L}{2}, \tag{103c}$$

$$\tau_{\hat{x}z}^{(1)} = \tau_{\hat{x}z}^{(2)} = 0 \text{ at } \hat{x} = \pm\frac{L}{2}, \tag{103d}$$

$$\tau_{zz}^{(1)} = \tau_{zz}^{(2)} = 0 \text{ at } \hat{x} = \pm\frac{L}{2}, \tag{103e}$$

Note that the BCs in Eqs. (103d) and (103e) follow directly from Eqs. (11a), (11b) and (103a)–(103c).

In the third example, a five-layer plate composed of a Cu layer (bottom), two BeO layers (second and fourth from the bottom) and two Si layers (top and middle), as shown Fig. 2c, is analyzed, which is supported by a rigid substrate at its free edges and subjected to a uniform pressure of 20kPa on its top surface (i.e., $\tau_{zz}^{(0)} = 0$, $\tau_{zz}^{(5)} = -20\text{kPa}$, $\tau_{\hat{x}z}^{(0)} = \tau_{\hat{x}z}^{(5)} = 0$, $f_{\hat{x}}^{(1)} = f_z^{(1)} = f_{\hat{x}}^{(2)} = f_z^{(2)} = f_{\hat{x}}^{(3)} = f_z^{(3)} = f_{\hat{x}}^{(4)} = f_z^{(4)} = f_{\hat{x}}^{(5)} = f_z^{(5)} = 0$) and a uniform temperature of $\Delta T^{(1)} = \Delta T^{(2)} = \Delta T^{(3)} = \Delta T^{(4)} = \Delta T^{(5)} = \Delta T = 40^{\circ}\text{C}$. These lead to $q_{\hat{x}}^{(1)} = q_z^{(1)} = q_{\hat{x}}^{(2)} = q_z^{(2)} = q_{\hat{x}}^{(3)} = q_z^{(3)} = q_{\hat{x}}^{(4)} = q_z^{(4)} = q_{\hat{x}}^{(5)} = q_z^{(5)} = 0$, $m_{\hat{x}}^{(1)} = m_{\hat{x}}^{(2)} = m_{\hat{x}}^{(3)} = m_{\hat{x}}^{(4)} = m_{\hat{x}}^{(5)} = 0$ (see Eqs. (22a-c)), and $\eta_{\hat{x}}^{(1)} = \eta_z^{(1)} = \eta_{\hat{x}}^{(2)} = \eta_z^{(2)} = \eta_{\hat{x}}^{(3)} = \eta_z^{(3)} = \eta_{\hat{x}}^{(4)} = \eta_z^{(4)} = \eta_{\hat{x}}^{(5)} = \eta_z^{(5)} = \chi_z^{(1)} = \chi_z^{(2)} = \chi_z^{(3)} = \chi_z^{(4)} = \chi_z^{(5)} = 0$ (see Eqs. (51) and (56)). In view of the general BCs given in Eqs. (43a)–(43c), the following BCs can be identified for this case:

$$N^{(1)} = N^{(2)} = N^{(3)} = N^{(4)} = N^{(5)} = 0 \text{ at } \hat{x} = \pm\frac{L}{2}, \tag{104a}$$

$$w^{(1)} = w^{(2)} = w^{(3)} = w^{(4)} = w^{(5)} = 0 \text{ at } \hat{x} = \pm\frac{L}{2}, \tag{104b}$$

$$M^{(1)} = M^{(2)} = M^{(3)} = M^{(4)} = M^{(5)} = 0 \text{ at } \hat{x} = \pm\frac{L}{2}, \tag{104c}$$

$$\tau_{\hat{x}z,\hat{x}}^{(1)} = K_s^{(1)}\left[\frac{d_{11}^{(2)}}{c_{11}^{(2)}} - \frac{d_{11}^{(1)}}{c_{11}^{(1)}}\right]\Delta T,\ \tau_{\hat{x}z,\hat{x}}^{(2)} = K_s^{(2)}\left[\frac{d_{11}^{(3)}}{c_{11}^{(3)}} - \frac{d_{11}^{(2)}}{c_{11}^{(2)}}\right]\Delta T,\ \tau_{\hat{x}z,\hat{x}}^{(3)} = K_s^{(3)}\left[\frac{d_{11}^{(4)}}{c_{11}^{(4)}} - \frac{d_{11}^{(3)}}{c_{11}^{(3)}}\right]\Delta T,$$
$$\tau_{\hat{x}z,\hat{x}}^{(4)} = K_s^{(4)}\left[\frac{d_{11}^{(5)}}{c_{11}^{(5)}} - \frac{d_{11}^{(4)}}{c_{11}^{(4)}}\right]\Delta T \text{ at } \hat{x} = \pm\frac{L}{2}, \tag{104}$$

$$\tau_{zz,\hat{x}\hat{x}}^{(1)} = \tau_{zz,\hat{x}\hat{x}}^{(2)} = \tau_{zz,\hat{x}\hat{x}}^{(3)} = \tau_{zz,\hat{x}\hat{x}}^{(4)} = 0 \text{ at } \hat{x} = \pm\frac{L}{2}, \tag{104e}$$

where Eqs. (104d) and (104e) are directly obtained from Eqs. (66a), (66b), (104a) and (104c).

The material properties, including Young's modulus E, Poisson's ratio ν and the coefficient of thermal expansion (CTE) α, for Cu, BeO and Si are listed in Table 1, which are the same as those employed in [64]. These properties are used to compute the material constants $C_{11}^{(m)}$ and $d_{11}^{(m)}$ from Eqs. (16) and (45a,b) for each

Table 1 Materials properties of layers of the composite plates

Materials	Young's modulus $E^{(m)}$ (GPa)	Poisson's ratio $\nu^{(m)}$	CTE $\alpha^{(m)}$ (10^{-6}/°C)
Copper (Cu)	126	0.34	16.5
Beryllium Oxide (BeO)	345	0.3	6.3
Silicon (Si)	120	0.42	2.6

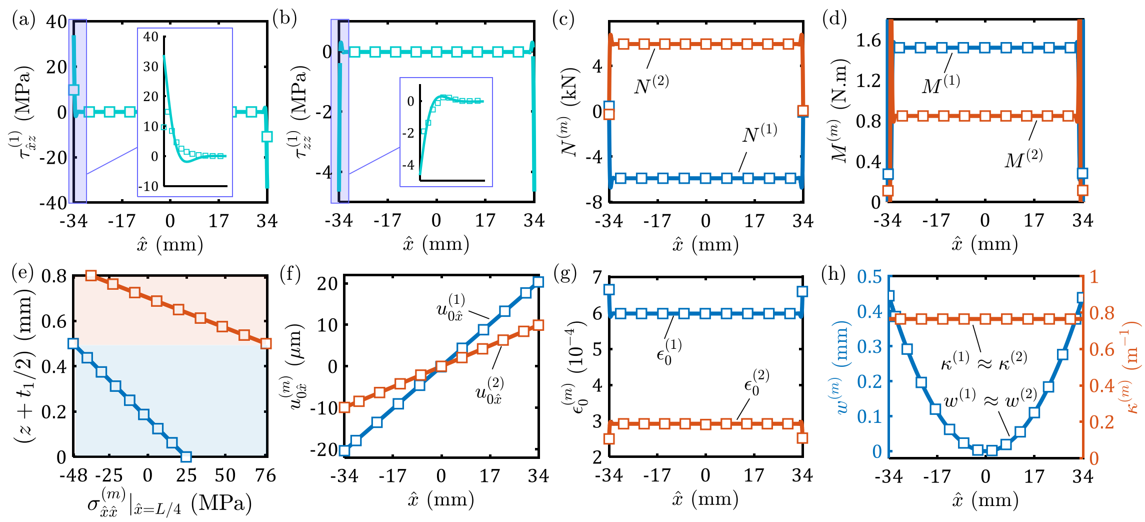

Fig. 3 Thermomechanical responses of the two-layer composite plate: **a** interfacial shear stress $\tau_{\hat{x}z}^{(1)}$, **b** interfacial normal stress $\tau_{zz}^{(1)}$; **c** normal forces $N^{(m)}$, **d** bending moments $M^{(m)}$, **e** distribution of the axial normal stresses $\sigma_{\hat{x}\hat{x}}^{(m)}$ (on $\hat{x} = L/4$) through the plate thickness, **f** axial displacements $u_{0\hat{x}}^{(m)}$, **g** axial normal strains $\epsilon_0^{(m)}$, and **h** deflections $w^{(m)}$ and curvatures $\kappa^{(m)}$, with $m \in \{1,2\}$. The solid curves depict the predictions by the current analytical model, and the markers represent the FE simulation results using COMSOL. Here $\ell_m \tilde{t}_m = 1$ µm

plane-stress layer considered here. In addition, the interfacial stiffness constants $K_s^{(m)}$ and $K_n^{(m)}$ are determined from Eq. (11c), with the Lamé constants of the mth interface, $\tilde{\lambda}_m$ and $\tilde{\mu}_m$ (with $m \in \{1,2, .., N_l\}$), given by

$$\tilde{\lambda}_m = \frac{\ell_m \tilde{t}_m}{t_m + t_{m+1}}[2(\lambda_m + \lambda_{m+1}) + (\mu_m + \mu_{m+1})], \;\; \tilde{\mu}_m = \frac{\ell_m \tilde{t}_m}{2(t_m + t_{m+1})}(\mu_m + \mu_{m+1}), \tag{105a,b}$$

where λ_m, μ_m and λ_{m+1}, μ_{m+1} are, respectively, the Lamé constants of the mth and $(m+1)$th layers, and ℓ_m is a non-dimensional parameter introduced as a measure of the interfacial stiffness. The range for ℓ_m is $0 < \ell_m < \infty$, with $\ell_m \to \infty$ representing an interface between two perfectly bonding layers and $\ell_m \to 0$ standing for an interface between two separated layers. For illustration purposes, the range of 4×10^{-5} µm $< \ell_m \tilde{t}_m < 1$ µm is used in the examples presented here.

To validate the analytical model and closed-form solutions developed in Sects. 3 and 4 and applied to the example problems herein, the numerical results predicted by the current model are compared to those obtained from finite element (FE) simulations using COMSOL [12], as shown in Figs. 3, 4 and 5. In the FE analyses, each layer of the composite plate is modeled as a 2D linear elastic solid with a Young's modulus of $C_{11}^{(m)}$, a Poisson's ratio of zero, and a coefficient of thermal expansion of α_m. In addition, each imperfect interface between two adjacent layers is regarded as a thin layer with the tangential stiffness $K_s^{(m)}$ and normal stiffness $K_n^{(m)}$.

Figure 3 displays the results for the two-layer composite plate, which shows how the CTE mismatch affects the mechanical response of the plate. Under the boundary and loading conditions indicated in Fig. 2a, $\tau_{\hat{x}z}^{(1)}$ and $\tau_{zz}^{(1)}$ are developed at the interface due to the mismatch in the CTE between the two materials (see Figs. 3a and 3b), resulting in the plate bending. The numerical values of $\tau_{\hat{x}z}^{(1)}$ and $\tau_{zz}^{(1)}$ plotted in Fig. 3a and 3b are obtained

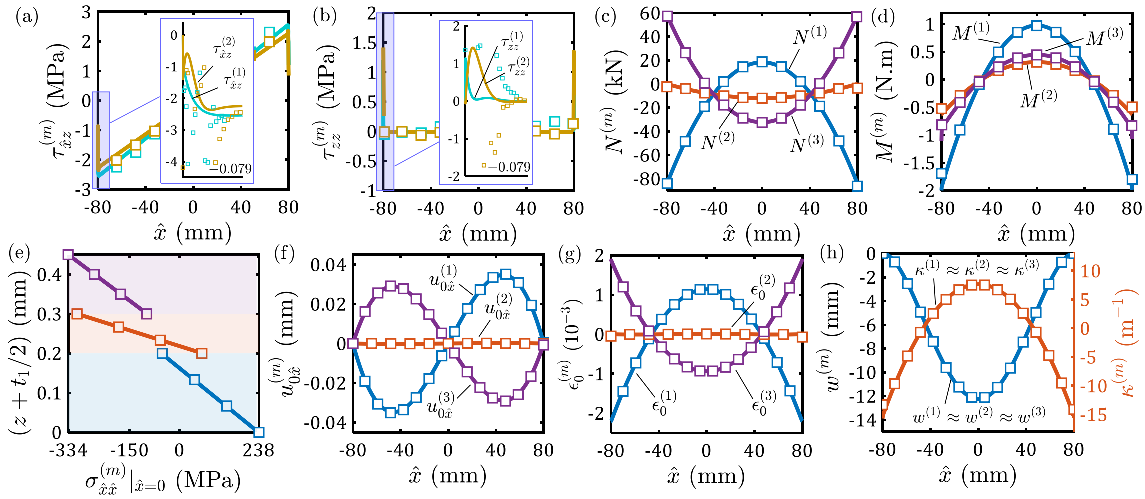

Fig. 4 Thermomechanical responses of the three-layer composite plate: **a** interfacial shear stresses $\tau_{\hat{x}z}^{(m)}$, **b** interfacial normal stresses $\tau_{zz}^{(m)}$, with $m \in \{1{,}2\}$; **c** normal forces $N^{(m)}$, **d** bending moments $M^{(m)}$, **e** distribution of the axial normal stresses $\sigma_{\hat{x}\hat{x}}^{(m)}$ $\left(\text{on } \hat{x} = 0\right)$ through the plate thickness, **f** axial displacements $u_{0\hat{x}}^{(m)}$, **g** axial normal strains $\epsilon_0^{(m)}$, and **h** deflections $w^{(m)}$ and curvatures $\kappa^{(m)}$, with $m \in \{1{,}2, 3\}$. The solid curves depict the predictions by the current analytical model, and the markers represent the FE simulation results using COMSOL. Here $\ell_m \tilde{t}_m = 1$ µm

from Eqs. (79), (80) and (87a)–(87c), with $\tau_{zz}^{(0)} = \tau_{zz}^{(2)} = -20\text{kPa}$, $\tau_{\hat{x}z}^{(0)} = \tau_{\hat{x}z}^{(2)} = 0$, $\Delta T^{(1)} = \Delta T^{(2)} = 40°\text{C}$, $\overline{N}^{(1)} = \overline{N}^{(2)} = 0$, $\overline{M}^{(1)} = \overline{M}^{(2)} = 0$, $\eta_{\hat{x}}^{(1)} = \eta_z^{(1)} = 0$, and $\left(\tau_{\hat{x}z,\hat{x}}^{(1)}\right)_p = 0$.

When the two-layer plate under the loading and boundary conditions shown in Fig. 2a expands (see Figs. 3f and 3g), the CTE mismatch (i.e., 16.5 μ/°C for Cu versus 6.3 μ/°C for BeO) results in a tensile axial force (i.e., $N^{(1)} > 0$) in the BeO layer and a compressive axial force of the same magnitude (i.e., $N^{(2)} = -N^{(1)} < 0$) in the Cu layer (see Fig. 3c). As a result, bending moments develop in the two layers (i.e., $M^{(1)} \neq 0$ and $M^{(2)} \neq 0$) (see Fig. 3d), leading to non-zero values of the deflection and curvature in each layer of the plate (i.e., $w^{(1)} \neq 0$, $w^{(2)} \neq 0$, $\kappa^{(1)} \neq 0$ and $\kappa^{(2)} \neq 0$) (see Fig. 3h). Note that $w^{(1)} \approx w^{(2)}$ and $\kappa^{(1)} \approx \kappa^{(2)}$ in the current problem with the specified geometrical parameters and material constants. In addition, the presence of the bending moments $M^{(1)}$ and $M^{(2)}$ makes the axial normal stress $\sigma_{\hat{x}\hat{x}}^{(m)}(m \in \{1,\ 2\})$ discontinuous at the interface between the two layers, as shown in Fig. 3e.

Figure 4 illustrates the numerical results for the three-layer composite plate with the support and loading shown in Fig. 3b. The numerical values of $\tau_{\hat{x}z}^{(1)}$ and $\tau_{zz}^{(1)}$ plotted in Figs. 4a and 4b are obtained using Eqs. (97a), (97b), (95a)–(95g), (98a)–(98f) and (103a)–(103e), with $\tau_{zz}^{(0)} = 0$, $\tau_{zz}^{(3)} = -20\text{kPa}$, $\tau_{\hat{x}z}^{(0)} = \tau_{\hat{x}z}^{(3)} = 0$, and $\Delta T^{(1)} = \Delta T^{(2)} = \Delta T^{(3)} = \Delta T = 40\cos\left(\pi\hat{x}/L\right)°\text{C}$. Note that $w^{(1)} \approx w^{(2)} \approx w^{(3)}$ and $\kappa^{(1)} \approx \kappa^{(2)} \approx \kappa^{(3)}$ in this three-layer plate example problem with the specified geometrical parameters and material constants.

Figure 5 shows the results for the five-layer composite plate with the support and loading illustrated in Fig. 3c. The numerical values of $\tau_{\hat{x}z}^{(m)}$, $\tau_{zz}^{(m)}$, $N^{(m)}$, $M^{(m)}$, $\sigma_{\hat{x}\hat{x}}^{(m)}$, $u_{0\hat{x}}^{(m)}$, $\epsilon_0^{(m)}$, $w^{(m)}$ and $\kappa^{(m)}$ displayed in Fig. 5a–5h are, respectively, obtained using the formulas for the general case given in Eqs. (64), (61b), (65a), (65b), (18a), (2a), (44a), (3c) and (44b), with $\tau_{zz}^{(0)} = 0$, $\tau_{zz}^{(5)} = -20\text{kPa}$, $\tau_{\hat{x}z}^{(0)} = \tau_{\hat{x}z}^{(5)} = 0$, $\Delta T^{(1)} = \Delta T^{(2)} = \Delta T^{(3)} = \Delta T^{(4)} = \Delta T^{(5)} = \Delta T = 40°\text{C}$, $q_{\hat{x}}^{(1)} = q_z^{(1)} = q_{\hat{x}}^{(2)} = q_z^{(2)} = q_{\hat{x}}^{(3)} = q_z^{(3)} = q_{\hat{x}}^{(4)} = q_z^{(4)} = q_{\hat{x}}^{(5)} = q_z^{(5)} = m_{\hat{x}}^{(1)} = m_{\hat{x}}^{(2)} = m_{\hat{x}}^{(3)} = m_{\hat{x}}^{(4)} = m_{\hat{x}}^{(5)} = 0$, $\eta_{\hat{x}}^{(1)} = \eta_z^{(1)} = \eta_{\hat{x}}^{(2)} = \eta_z^{(2)} = \eta_{\hat{x}}^{(3)} = \eta_z^{(3)} = \eta_{\hat{x}}^{(4)} = \eta_z^{(4)} = \eta_{\hat{x}}^{(5)} = \eta_z^{(5)} = \chi_z^{(1)} = \chi_z^{(2)} = \chi_z^{(3)} = \chi_z^{(4)} = \chi_z^{(5)} = 0$, $N^{(1)} = N^{(2)} = N^{(3)} = N^{(4)} = N^{(5)} = 0$ at $\hat{x} = \pm\frac{L}{2}$, and $M^{(1)} = M^{(2)} = M^{(3)} = M^{(4)} = M^{(5)} = 0$ at $\hat{x} = \pm\frac{L}{2}$. Note that $w^{(1)} \approx w^{(2)} \approx w^{(3)} \approx w^{(4)} \approx w^{(5)}$ and $\kappa^{(1)} \approx \kappa^{(2)} \approx \kappa^{(3)} \approx \kappa^{(4)} \approx \kappa^{(5)}$ in the example problem here with the specified geometrical parameters and material constants.

A comparison of Figs. 4 and 5 with Fig. 3 reveals that trends similar to those for the two-layer composite plate are observed for the three- and five-layer composite plates, where the mismatch in the CTE and elastic

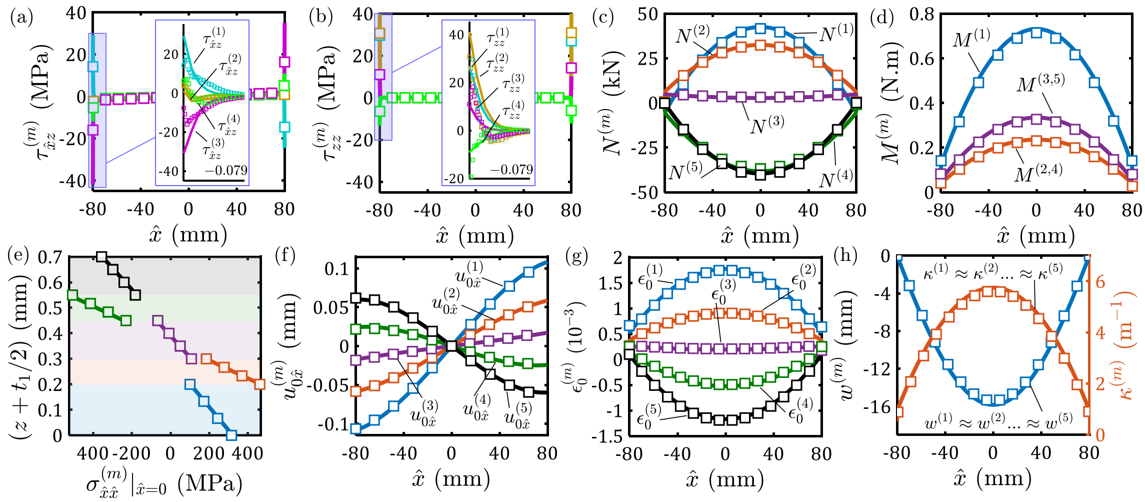

Fig. 5 Thermomechanical responses of the five-layer composite plate: **a** interfacial shear stresses $\tau_{\hat{x}z}^{(m)}$, **b** interfacial normal stresses $\tau_{zz}^{(m)}$, with $m \in \{1,2,3,4\}$; **c** normal forces $N^{(m)}$, **d** bending moments $M^{(m)}$, **e** distribution of the axial normal stresses $\sigma_{\hat{x}\hat{x}}^{(m)}$ (on $\hat{x}=0$) through the plate thickness, **f** axial displacements $u_{0\hat{x}}^{(m)}$, **g** axial normal strains $\epsilon_0^{(m)}$, and **h** deflections $w^{(m)}$ and curvatures $\kappa^{(m)}$, with $m \in \{1,2,3,4,5\}$. The solid curves depict the predictions by the current analytical model, and the markers represent the FE simulation results using COMSOL. Here $\ell_m \tilde{t}_m = 1$ µm

properties leads to the interfacial stresses $\tau_{\hat{x}z}^{(m)}$ and $\tau_{zz}^{(m)}$ at the interfaces (see Figs. 4a, 4b, 5a and 5b), resulting in the discontinuities in the axial normal stresses $\sigma_{\hat{x}\hat{x}}^{(m)}$ at these interfaces (see Figs. 4e and 5e). The mismatch also brings about the layer-to-layer variations of the axial displacements $u_{0\hat{x}}^{(m)}$ (see Figs. 4f and 5f), axial normal strains $\epsilon_0^{(m)}$ (see Figs. 4g and 5g), and axial normal forces $N^{(m)}$ (see Figs. 4c and 5c). In addition, the bending moments $M^{(m)}$ are developed in the layers (see Figs. 4d and 5d), leading to the deflections $w^{(m)}$ and curvatures $\kappa^{(m)}$ in the plates (see Figs. 4h and 5h).

Figures 3, 4 and 5 illustrate that the interfacial shear stress $\tau_{\hat{x}z}^{(m)}$ and normal stress $\tau_{zz}^{(m)}$ both change sharply near the plate edges, indicating a pronounced edge (or boundary) effect. When the plate has free edges (i.e., without normal forces and moments there), as in the cases of the two-layer (see Fig. 2a) and five-layer (see Fig. 2c) plates, $\tau_{\hat{x}z}^{(m)}$ and $\tau_{zz}^{(m)}$ remain non-zero at the edges $\hat{x} = \pm L/2$, depending on the applied thermal load, as shown in Eqs. (102d) and (104d). However, in the case of the three-layer composite plate shown in Fig. 2b, where the edges are clamped, $\tau_{\hat{x}z}^{(m)}$ and $\tau_{zz}^{(m)}$ are both zero at $\hat{x} = \pm L/2$, as given in Eqs. (103d) and (103e). Nonetheless, $\tau_{\hat{x}z}^{(m)}$ and $\tau_{zz}^{(m)}$ remain varying sharply near the edges, indicating the presence of an edge effect.

In addition, it is observed from Figs. 3, 4 and 5 that the predictions by the current analytical model agree very well with the FE simulation results obtained using COMSOL in all three examples considered here.

Finally, it should be mentioned that in the newly developed analytical model, each layer of the composite plate is regarded as an elastic thin plate interacting with adjacent layers through adhesive bonding that depend on the stiffness of the interface (see Eqs. (11a) and (11b)). In layer-wise plate theories (e.g., [5, 6, 51, 62]), continuities in both the displacement and stress fields across each interface are assumed a priori. As a result, such theories cannot capture discontinuities arising from imperfect interfaces. Unlike the layer-wise plate models, the current new model predicts the interfacial shear and normal stresses $\tau_{\hat{x}z}^{(m)}$ and $\tau_{zz}^{(m)}$ between adjacent layers in terms of the stiffness constants $K_s^{(m)}$ and $K_n^{(m)}$ of the interface and can account for discontinuities in the displacement and stress fields at imperfect interfaces in multi-layered composite plates. This is further illustrated in Figs. 6 and 7. It is seen from Fig. 6 that reducing the interface stiffness, through decreasing the parameter ℓ_m (see Eqs. (105a,b)), leads to increased differences in the displacement and stress fields across each interface for the three-layer composite plate depicted in Fig. 2b. Moreover, it is observed from Fig. 7 that the difference in the deflection between two adjacent layers increases as the plate length L $(= a = b)$ decreases for the three-layer plate with the given value of ℓ_m.

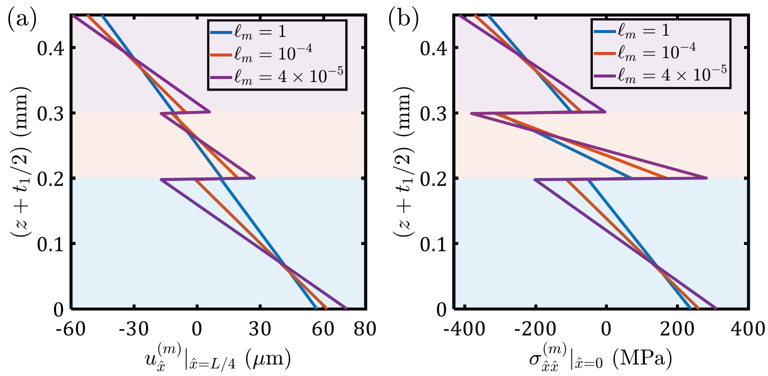

Fig. 6 Discontinuities in the **a** displacement field and **b** stress field due to imperfect (weakened) interfaces in the three-layer composite plate. Here $\tilde{t}_m = 1$ µm

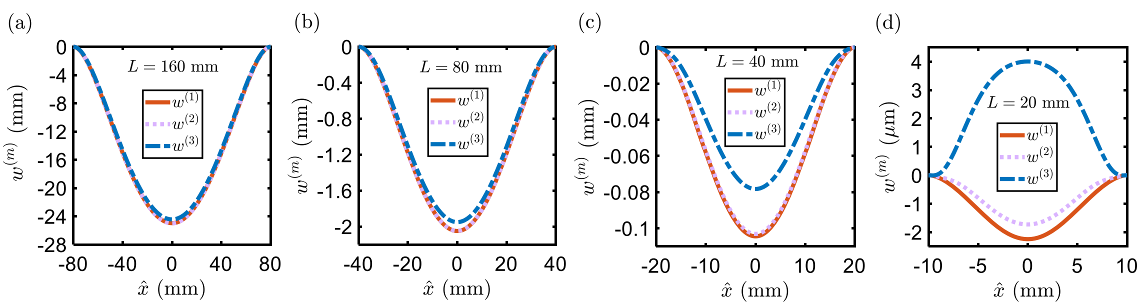

Fig. 7 Deflections varying with the plate length L in the three-layer composite plate: **a** $L = 160$ mm, **b** $L = 80$ mm, **c** $L = 40$ mm, and **d** $L = 20$ mm. Here $\ell_m \tilde{t}_m = 4 \times 10^{-5}$ µm

6 Conclusions

A new analytical model is provided for characterizing the thermoelastic behavior of a multi-layered composite plate with an arbitrary number of imperfectly bonded layers, which is under general thermal and mechanical loading. A variational method based on the first and second laws of thermodynamics is applied to obtain the governing equations and boundary conditions simultaneously, unlike in existing studies. The Kirchhoff plate theory and a spring-layer imperfect interface model are employed in the formulation. The former is used to describe deformations of each layer of the composite plate, while the latter is adopted to represent every imperfect interface between two adjacent layers, which is regarded as a thin spring layer having an infinitesimal thickness and two stiffness constants. This interface model accounts for discontinuities in the displacement and stress fields across the interface.

A general analytical solution for a symmetrically loaded composite square plate with an arbitrary number of layers and imperfect interfaces is derived by using a newly proposed approach, which reduces the governing equations for a multi-layered plate to a system of two coupled ordinary differential equations to solve for the interfacial normal and shear stress components on one interface.

By directly applying the general analytical solution, closed-form solutions are obtained as examples for two- and three-layer composite square plates under specified thermomechanical loading.

Numerical results are presented for two-, three-, and five-layer composite square plates under different loading and boundary conditions by using the general analytical model and two closed-form solutions. These results predicted by the current new model are compared against those from finite element simulations using COMSOL. The two sets of results for each of the three composite plates agree very well, which validates and supports the newly developed analytical model.

Being capable of describing multi-layered plates with imperfect interfaces, containing an arbitrary number of layers of dissimilar materials and subjected to general thermomechanical loading, the current analytical model offers a new approach for interface design and structural optimization of stacked composite plates.

Finally, it should be mentioned that the newly developed analytical model is based on the Kirchhoff plate theory, which is the simplest among all plate theories. The use of a higher-order plate model such as Mindlin's (linear) or von Karman's (nonlinear) would make the analytical formulations even more challenging. Such formulations based on higher-order or nonlinear plate theories can be explored in the future.

Acknowledgements The authors would like to gratefully acknowledge the support by the Moody School of Graduate and Advanced Studies at SMU through a post-doctoral fellowship to MS. The authors also wish to thank Prof. Shaofan Li of UC-Berkeley and two anonymous reviewers for their encouragement and helpful comments on an earlier version of the paper.

Funding Open access funding provided by SCELC, Statewide California Electronic Library Consortium.

Declarations

Conflict of interest The authors have no relevant financial or non-financial interests to disclose.

Appendix A

Consider a pair of conjugated complex roots of the polynomial equation in Eq. (67):

$$Z_{2n-1}, Z_{2n} = \omega_n^2 - \omega_n^{*2} \pm \mathrm{i}2\omega_n\omega_n^*, \tag{A1}$$

where Z_{2n-1} and Z_{2n} are two conjugated roots of Eq. (67), ω_n and ω_n^* are real numbers, and i $(=\sqrt{-1})$ is the imaginary unit. The four roots of the polynomial equation in Eq. (62) that correspond to the two conjugated complex roots Z_{2n-1} and Z_{2n} can be written as

$$\lambda_{4n-3}, \lambda_{4n-2} = \omega_n \pm \mathrm{i}\omega_n^*, \quad \lambda_{4n-1}, \lambda_{4n} = -\omega_n \pm \mathrm{i}\omega_n^*. \tag{A2}$$

From Eq. (A2), the exponential functions $\overline{C}_n \Lambda_n \exp(\lambda_n \hat{x})$ and $\overline{C}_n \exp(\lambda_n \hat{x})$ involved in Eqs. (61a) and (61b) that are associated with the pair of conjugated complex roots shown in Eq. (A1) can be expressed as

$$\overline{C}_{4n-3}\Lambda_{4n-3}\exp(\lambda_{4n-3}\hat{x}) + \overline{C}_{4n-2}\Lambda_{4n-2}\exp(\lambda_{4n-2}\hat{x}) + \overline{C}_{4n-1}\Lambda_{4n-1}\exp(\lambda_{4n-1}\hat{x}) + \overline{C}_{4n}\Lambda_{4n}\exp(\lambda_{4n}\hat{x}), \tag{A3a}$$

$$\overline{C}_{4n-3}\exp(\lambda_{4n-3}\hat{x}) + \overline{C}_{4n-2}\exp(\lambda_{4n-2}\hat{x}) + \overline{C}_{4n-1}\exp(\lambda_{4n-1}\hat{x}) + \overline{C}_{4n}\exp(\lambda_{4n}\hat{x}). \tag{A3b}$$

In light of Eq. (63), the constants Λ_{4n-3}, Λ_{4n-2}, Λ_{4n-1} and Λ_{4n} that correspond to the conjugated complex roots listed in Eq. (A2) can be identified as

$$\Lambda_{4n-3}, \Lambda_{4n-2} = \bar{\Lambda}_n \pm \mathrm{i}\bar{\Lambda}_n^*, \quad \Lambda_{4n-1}, \Lambda_{4n} = \bar{\Lambda}_n \mp \mathrm{i}\bar{\Lambda}_n^*, \tag{A4}$$

where $\overline{\Lambda}_n$ and $\overline{\Lambda}_n^*$ are real numbers.

Substituting Eqs. (A2) and (A4) into Eq. (A3a) gives, with the help of Euler's formula,

$$\begin{aligned}
&\left[\overline{C}_{4n-3}\left(\overline{\Lambda}_n + \mathrm{i}\overline{\Lambda}_n^*\right) + \overline{C}_{4n-2}\left(\overline{\Lambda}_n - \mathrm{i}\overline{\Lambda}_n^*\right) + \overline{C}_{4n-1}\left(\overline{\Lambda}_n - \mathrm{i}\overline{\Lambda}_n^*\right) + \overline{C}_{4n}\left(\overline{\Lambda}_n + \mathrm{i}\overline{\Lambda}_n^*\right)\right]\cosh(\omega_n\hat{x})\cos(\omega_n^*\hat{x})\\
&+\left[\overline{C}_{4n-3}\left(\overline{\Lambda}_n + \mathrm{i}\overline{\Lambda}_n^*\right) + \overline{C}_{4n-2}\left(\overline{\Lambda}_n - \mathrm{i}\overline{\Lambda}_n^*\right) - \overline{C}_{4n-1}\left(\overline{\Lambda}_n - \mathrm{i}\overline{\Lambda}_n^*\right) - \overline{C}_{4n}\left(\overline{\Lambda}_n + \mathrm{i}\overline{\Lambda}_n^*\right)\right]\sinh(\omega_n\hat{x})\cos(\omega_n^*\hat{x})\\
&+\mathrm{i}\left[\overline{C}_{4n-3}\left(\overline{\Lambda}_n + \mathrm{i}\overline{\Lambda}_n^*\right) - \overline{C}_{4n-2}\left(\overline{\Lambda}_n - \mathrm{i}\overline{\Lambda}_n^*\right) + \overline{C}_{4n-1}\left(\overline{\Lambda}_n - \mathrm{i}\overline{\Lambda}_n^*\right) - \overline{C}_{4n}\left(\overline{\Lambda}_n + \mathrm{i}\overline{\Lambda}_n^*\right)\right]\cosh(\omega_n\hat{x})\sin(\omega_n^*\hat{x})\\
&+\mathrm{i}\left[\overline{C}_{4n-3}\left(\overline{\Lambda}_n + \mathrm{i}\overline{\Lambda}_n^*\right) - \overline{C}_{4n-2}\left(\overline{\Lambda}_n - \mathrm{i}\overline{\Lambda}_n^*\right) - \overline{C}_{4n-1}\left(\overline{\Lambda}_n - \mathrm{i}\overline{\Lambda}_n^*\right) + \overline{C}_{4n}\left(\overline{\Lambda}_n + \mathrm{i}\overline{\Lambda}_n^*\right)\right]\sinh(\omega_n\hat{x})\sin(\omega_n^*\hat{x}).
\end{aligned} \tag{A5}$$

Similarly, using Eqs. (A2) and (A4) in Eq. (A3b) yields

$$\left(\overline{C}_{4n-3} + \overline{C}_{4n-2} + \overline{C}_{4n-1} + \overline{C}_{4n}\right)\cosh(\omega_n\hat{x})\cos(\omega_n^*\hat{x})$$

$$+\left(\overline{C}_{4n-3}+\overline{C}_{4n-2}-\overline{C}_{4n-1}-\overline{C}_{4n}\right)\sinh(\omega_n\hat{x})\cos(\omega_n^*\hat{x})$$
$$+\,\mathrm{i}\left(\overline{C}_{4n-3}-\overline{C}_{4n-2}+\overline{C}_{4n-1}-\overline{C}_{4n}\right)\cosh(\omega_n\hat{x})\sin(\omega_n^*\hat{x})$$
$$+\,\mathrm{i}\left(\overline{C}_{4n-3}-\overline{C}_{4n-2}-\overline{C}_{4n-1}+\overline{C}_{4n}\right)\sinh(\omega_n\hat{x})\sin(\omega_n^*\hat{x}). \tag{A6}$$

It is seen that the relations (A5) and (A6) contain imaginary terms, which would render the interfacial stresses in Eqs. (68a) and (68b) complex. As the interfacial stresses are real at any position $\hat{x}$, when P_1 and P_2 are constants, the following relations can be obtained by eliminating the imaginary terms in Eq. (A6):

$$\overline{C}_{4n-3}=\overline{C}_{4n-2},\quad \overline{C}_{4n-1}=\overline{C}_{4n}. \tag{A7a,b}$$

Substituting Eqs. (A7a,b) into Eqs. (A5) and (A6) leads to

$$2\left(\overline{C}_{4n-2}+\overline{C}_{4n}\right)\overline{\Lambda}_n\cosh(\omega_n\hat{x})\cos(\omega_n^*\hat{x})+2\left(\overline{C}_{4n-2}-\overline{C}_{4n}\right)\overline{\Lambda}_n\sinh(\omega_n\hat{x})\cos(\omega_n^*\hat{x})$$
$$+\,2\left(-\overline{C}_{4n-2}+\overline{C}_{4n}\right)\overline{\Lambda}_n^*\cosh(\omega_n\hat{x})\sin(\omega_n^*\hat{x})+2\left(-\overline{C}_{4n-2}-\overline{C}_{4n}\right)\overline{\Lambda}_n^*\sinh(\omega_n\hat{x})\sin(\omega_n^*\hat{x}), \tag{A8a}$$

$$2\left(\overline{C}_{4n-2}+\overline{C}_{4n}\right)\cosh(\omega_n\hat{x})\cos(\omega_n^*\hat{x})+2\left(\overline{C}_{4n-2}-\overline{C}_{4n}\right)\sinh(\omega_n\hat{x})\cos(\omega_n^*\hat{x}). \tag{A8b}$$

It follows that the terms in Eqs. (A8a) and (A8b) are all real, thereby leading to real-valued interfacial stresses.

Under symmetric loading, Eqs. (A8a) and (A8b) reduce to, after eliminating the anti-symmetric terms by setting $\overline{C}_{4n-2}=\overline{C}_{4n}$,

$$\overline{S}_n\overline{\Lambda}_n\cosh(\omega_n\hat{x})\cos(\omega_n^*\hat{x})-\overline{S}_n\overline{\Lambda}_n^*\sinh(\omega_n\hat{x})\sin(\omega_n^*\hat{x}), \tag{A9a}$$

$$\overline{S}_n\cosh(\omega_n\hat{x})\cos(\omega_n^*\hat{x}), \tag{A9b}$$

where $\overline{S}_n=4\overline{C}_{4n}$.

The relations in Eqs. (A9a)and (A9b) define the stresses that correspond to the pair of conjugated complex roots Z_{2n-1} and Z_{2n} listed in Eq. (A1). For a real root Z_{2n-1} or Z_{2n} with $\omega_n^*=0$ and $\overline{\Lambda}_n^*=0$, Eqs. (A9a) and (A9b) become.

$$\mathcal{S}_n\Omega_n\cosh(\varpi_n\hat{x}), \tag{A10a}$$

$$\mathcal{S}_n\cosh(\varpi_n\hat{x}), \tag{A10b}$$

where ϖ_n is the nth real root of Eq. (62), $\mathcal{S}_n$ is a constant, and $\Omega_n=-\frac{\sum_{q=0}^{2(2N_l-3)-1}Q_{2q}\varpi_n^{2q}}{Q_d}$ is obtained from Eq. (63).

By introducing R_r and R_{cc} as, respectively, the number of real roots and the number of pairs of complex conjugate roots of Eq. (67) and by using Eqs. (A9a) and (A9b) for each pair of complex roots and Eqs. (A10a) and (A10b) for each real root, the interfacial stresses in Eqs. (61a) and (61b) can be expressed as

$$\tau_{\hat{x}z,\hat{x}}^{(1)}=\sum_{p=1}^{R_r}\mathcal{S}_p\Omega_p\cosh(\varpi_p\hat{x})+\sum_{n=1}^{R_{cc}}\left[\overline{S}_n\overline{\Lambda}_n\cosh(\omega_n\hat{x})\cos(\omega_n^*\hat{x})-\overline{S}_n\overline{\Lambda}_n^*\sinh(\omega_n\hat{x})\sin(\omega_n^*\hat{x})\right]$$
$$-\frac{B_0P_2-D_0P_1}{A_0D_0-B_0C_0}, \tag{A11a}$$

$$\tau_{zz}^{(1)}(\hat{x})=\sum_{p=1}^{R_r}\mathcal{S}_p\cosh(\varpi_p\hat{x})+\sum_{n=1}^{R_{cc}}\overline{S}_n\cosh(\omega_n\hat{x})\cos(\omega_n^*\hat{x})+\frac{A_0P_2-C_0P_1}{A_0D_0-B_0C_0}, \tag{A11b}$$

where $\hat{x}$ is either x or y.

Appendix B

The coefficients $A_0 - A_4$, $B_0 - B_6$, $C_0 - C_6$ and $D_0 - D_8$ and the inhomogeneous terms P_1 and P_2 in Eqs. (91a)–(91f) are determined for a three-layer plate by solving the following system of differential equations:

$$\tau^{(1)}_{\hat{x}z,\hat{x}\hat{x}\hat{x}} = \beta^{(1)}_1\tau^{(2)}_{\hat{x}z,\hat{x}} + \beta^{(1)}_0\tau^{(1)}_{\hat{x}z,\hat{x}} + \beta^{(1)}_{-1}\tau^{(0)}_{\hat{x}z,\hat{x}} + \alpha^{(1)}_1\tau^{(2)}_{zz} + \alpha^{(1)}_0\tau^{(1)}_{zz} + \alpha^{(1)}_{-1}\tau^{(0)}_{zz} + \eta^{(1)}_{\hat{x}} + \eta^{(1)}_z, \tag{B1a}$$

$$\tau^{(2)}_{\hat{x}z,\hat{x}\hat{x}\hat{x}} = \beta^{(2)}_1\tau^{(3)}_{\hat{x}z,\hat{x}} + \beta^{(2)}_0\tau^{(2)}_{\hat{x}z,\hat{x}} + \beta^{(2)}_{-1}\tau^{(1)}_{\hat{x}z,\hat{x}} + \alpha^{(2)}_1\tau^{(3)}_{zz} + \alpha^{(2)}_0\tau^{(2)}_{zz} + \alpha^{(2)}_{-1}\tau^{(1)}_{zz} + \eta^{(2)}_{\hat{x}} + \eta^{(2)}_z, \tag{B1b}$$

$$\tau^{(1)}_{zz,\hat{x}\hat{x}\hat{x}\hat{x}} = \gamma^{(1)}_1\tau^{(2)}_{\hat{x}z,\hat{x}} + \gamma^{(1)}_0\tau^{(1)}_{\hat{x}z,\hat{x}} + \gamma^{(1)}_{-1}\tau^{(0)}_{\hat{x}z,\hat{x}} + \xi^{(1)}_1\tau^{(2)}_{zz} + \xi^{(1)}_0\tau^{(1)}_{zz} + \xi^{(1)}_{-1}\tau^{(0)}_{zz} + \chi^{(1)}_z, \tag{B1c}$$

$$\tau^{(2)}_{zz,\hat{x}\hat{x}\hat{x}\hat{x}} = \gamma^{(2)}_1\tau^{(3)}_{\hat{x}z,\hat{x}} + \gamma^{(2)}_0\tau^{(2)}_{\hat{x}z,\hat{x}} + \gamma^{(2)}_{-1}\tau^{(1)}_{\hat{x}z,\hat{x}} + \xi^{(2)}_1\tau^{(3)}_{zz} + \xi^{(2)}_0\tau^{(2)}_{zz} + \xi^{(2)}_{-1}\tau^{(1)}_{zz} + \chi^{(2)}_z, \tag{B1d}$$

which can be readily obtained from Eqs. (57a) and (57b) by setting $N_l = 3$.

Solving Eqs. (B1a) for $\tau^{(2)}_{\hat{x}z,\hat{x}}$ gives

$$\tau^{(2)}_{\hat{x}z,\hat{x}} = \frac{1}{\beta^{(1)}_1}\left\{\tau^{(1)}_{\hat{x}z,\hat{x}\hat{x}\hat{x}} - \beta^{(1)}_0\tau^{(1)}_{\hat{x}z,\hat{x}} - \beta^{(1)}_{-1}\tau^{(0)}_{\hat{x}z,\hat{x}} - \alpha^{(1)}_1\tau^{(2)}_{zz} - \alpha^{(1)}_0\tau^{(1)}_{zz} - \alpha^{(1)}_{-1}\tau^{(0)}_{zz} - \eta^{(1)}_{\hat{x}} - \eta^{(1)}_z\right\}. \tag{B2}$$

Using Eq. (B2) in Eq. (B1c) yields

$$\begin{aligned}\tau^{(1)}_{zz,\hat{x}\hat{x}\hat{x}\hat{x}} = {}& \frac{\gamma^{(1)}_1}{\beta^{(1)}_1}\tau^{(1)}_{\hat{x}z,\hat{x}\hat{x}\hat{x}} + \left(\gamma^{(1)}_0 - \frac{\gamma^{(1)}_1\beta^{(1)}_0}{\beta^{(1)}_1}\right)\tau^{(1)}_{\hat{x}z,\hat{x}} + \left(\gamma^{(1)}_{-1} - \frac{\gamma^{(1)}_1\beta^{(1)}_{-1}}{\beta^{(1)}_1}\right)\tau^{(0)}_{\hat{x}z,\hat{x}} + \left(\xi^{(1)}_1 - \frac{\gamma^{(1)}_1\alpha^{(1)}_1}{\beta^{(1)}_1}\right)\tau^{(2)}_{zz}\\ &+ \left(\xi^{(1)}_0 - \frac{\gamma^{(1)}_1\alpha^{(1)}_0}{\beta^{(1)}_1}\right)\tau^{(1)}_{zz} + \left(\xi^{(1)}_{-1} - \frac{\gamma^{(1)}_1\alpha^{(1)}_{-1}}{\beta^{(1)}_1}\right)\tau^{(0)}_{zz} - \frac{\gamma^{(1)}_1}{\beta^{(1)}_1}\eta^{(1)}_{\hat{x}} - \frac{\gamma^{(1)}_1}{\beta^{(1)}_1}\eta^{(1)}_z + \chi^{(1)}_z.\end{aligned} \tag{B3}$$

From Eq. (B3), $\tau^{(2)}_{zz}$ can be obtained as

$$\begin{aligned}\tau^{(2)}_{zz} = {}& \frac{\beta^{(1)}_1}{\beta^{(1)}_1\xi^{(1)}_1 - \alpha^{(1)}_1\gamma^{(1)}_1}\left\{\tau^{(1)}_{zz,\hat{x}\hat{x}\hat{x}\hat{x}} - \frac{\gamma^{(1)}_1}{\beta^{(1)}_1}\tau^{(1)}_{\hat{x}z,\hat{x}\hat{x}\hat{x}} - \left(\gamma^{(1)}_0 - \frac{\gamma^{(1)}_1\beta^{(1)}_0}{\beta^{(1)}_1}\right)\tau^{(1)}_{\hat{x}z,\hat{x}} - \left(\gamma^{(1)}_{-1} - \frac{\gamma^{(1)}_1\beta^{(1)}_{-1}}{\beta^{(1)}_1}\right)\tau^{(0)}_{\hat{x}z,\hat{x}}\right.\\ &\left.-\left(\xi^{(1)}_0 - \frac{\gamma^{(1)}_1\alpha^{(1)}_0}{\beta^{(1)}_1}\right)\tau^{(1)}_{zz} - \left(\xi^{(1)}_{-1} - \frac{\gamma^{(1)}_1\alpha^{(1)}_{-1}}{\beta^{(1)}_1}\right)\tau^{(0)}_{zz} + \frac{\gamma^{(1)}_1}{\beta^{(1)}_1}\eta^{(1)}_{\hat{x}} + \frac{\gamma^{(1)}_1}{\beta^{(1)}_1}\eta^{(1)}_z - \chi^{(1)}_z\right\}.\end{aligned} \tag{B4}$$

The substitution of Eqs. (B2) and (B4) into Eqs. (B1b) and (B1d) leads to

$$\begin{aligned}&\frac{1}{\beta^{(1)}_1\xi^{(1)}_1 - \alpha^{(1)}_1\gamma^{(1)}_1}\left\{-\xi^{(1)}_1\tau^{(1)}_{\hat{x}z,\hat{x}\hat{x}\hat{x}\hat{x}\hat{x}} + \left[\left(\beta^{(1)}_0 + \beta^{(2)}_0\right)\xi^{(1)}_1 - \alpha^{(2)}_0\gamma^{(1)}_1 - \alpha^{(1)}_1\gamma^{(1)}_0\right]\tau^{(1)}_{\hat{x}z,\hat{x}\hat{x}\hat{x}}\right.\\ &+\left[\left(\beta^{(2)}_{-1}\beta^{(1)}_1 - \beta^{(2)}_0\beta^{(1)}_0\right)\xi^{(1)}_1 + \alpha^{(1)}_1\left(\beta^{(2)}_0\gamma^{(1)}_0 - \beta^{(2)}_{-1}\gamma^{(1)}_1\right) + \alpha^{(2)}_0\left(\gamma^{(1)}_1\beta^{(1)}_0 - \gamma^{(1)}_0\beta^{(1)}_1\right)\right]\tau^{(1)}_{\hat{x}z,\hat{x}} + \alpha^{(1)}_1\tau^{(1)}_{zz,\hat{x}\hat{x}\hat{x}\hat{x}\hat{x}\hat{x}}\\ &+\left[\alpha^{(2)}_0\beta^{(1)}_1 - \beta^{(2)}_0\alpha^{(1)}_1\right]\tau^{(1)}_{zz,\hat{x}\hat{x}\hat{x}\hat{x}} + \left(\alpha^{(1)}_0\xi^{(1)}_1 - \alpha^{(1)}_1\xi^{(1)}_0\right)\tau^{(1)}_{zz,\hat{x}\hat{x}} + \left[(\alpha^{(2)}_{-1}\beta^{(1)}_1 - \beta^{(2)}_0\alpha^{(1)}_0)\xi^{(1)}_1\right.\\ &+\left.\left(\beta^{(2)}_0\xi^{(1)}_0 - \alpha^{(2)}_{-1}\gamma^{(1)}_1\right)\alpha^{(1)}_1 + \alpha^{(2)}_0\left(\gamma^{(1)}_1\alpha^{(1)}_0 - \beta^{(1)}_1\xi^{(1)}_0\right)\right]\tau^{(1)}_{zz} + \left(\beta^{(1)}_{-1}\xi^{(1)}_1 - \gamma^{(1)}_{-1}\alpha^{(1)}_1\right)\tau^{(0)}_{\hat{x}z,\hat{x}\hat{x}\hat{x}}\\ &+\left[\beta^{(2)}_0\gamma^{(1)}_{-1}\alpha^{(1)}_1 - \beta^{(2)}_0\beta^{(1)}_{-1}\xi^{(1)}_1 + \alpha^{(2)}_0\left(\gamma^{(1)}_1\beta^{(1)}_{-1} - \beta^{(1)}_1\gamma^{(1)}_{-1}\right)\right]\tau^{(0)}_{\hat{x}z,\hat{x}} + \left(\alpha^{(1)}_{-1}\xi^{(1)}_1 - \xi^{(1)}_{-1}\alpha^{(1)}_1\right)\tau^{(0)}_{zz,\hat{x}\hat{x}}\\ &+\left[\beta^{(2)}_0\xi^{(1)}_{-1}\alpha^{(1)}_1 - \beta^{(2)}_0\alpha^{(1)}_{-1}\xi^{(1)}_1 + \alpha^{(2)}_0\left(\gamma^{(1)}_1\alpha^{(1)}_{-1} - \beta^{(1)}_1\xi^{(1)}_{-1}\right)\right]\tau^{(0)}_{zz} + \left[\alpha^{(2)}_0\gamma^{(1)}_1 - \beta^{(2)}_0\xi^{(1)}_1\right]\left(\eta^{(1)}_{\hat{x}} + \eta^{(1)}_z\right)\\ &\left.+\left[\beta^{(2)}_0\alpha^{(1)}_1 - \alpha^{(2)}_0\beta^{(1)}_1\right]\chi^{(1)}_z + \xi^{(1)}_1\left(\eta^{(1)}_{\hat{x},\hat{x}\hat{x}} + \eta^{(1)}_{z,\hat{x}\hat{x}}\right) - \alpha^{(1)}_1\chi^{(1)}_{z,\hat{x}\hat{x}} + \left(\beta^{(1)}_1\xi^{(1)}_1 - \gamma^{(1)}_1\alpha^{(1)}_1\right)\left[\alpha^{(2)}_1\tau^{(3)}_{zz} + \eta^{(2)}_{\hat{x}} + \eta^{(2)}_z + \beta^{(2)}_1\tau^{(3)}_{\hat{x}z,\hat{x}}\right]\right\} = 0,\end{aligned} \tag{B5a}$$

$$\begin{aligned}&\frac{1}{\beta^{(1)}_1\xi^{(1)}_1 - \alpha^{(1)}_1\gamma^{(1)}_1}\left\{\gamma^{(1)}_1\tau^{(1)}_{\hat{x}z,\hat{x}\hat{x}\hat{x}\hat{x}\hat{x}\hat{x}\hat{x}} + \left(\gamma^{(1)}_0\beta^{(1)}_1 - \gamma^{(1)}_1\beta^{(1)}_0\right)\tau^{(1)}_{\hat{x}z,\hat{x}\hat{x}\hat{x}\hat{x}\hat{x}} + \left(\gamma^{(2)}_0\xi^{(1)}_1 - \gamma^{(1)}_1\xi^{(2)}_0\right)\tau^{(1)}_{\hat{x}z,\hat{x}\hat{x}\hat{x}}\right.\\ &+\left[\gamma^{(1)}_1\left(\xi^{(2)}_0\beta^{(1)}_0 - \gamma^{(2)}_{-1}\alpha^{(1)}_1\right) + \beta^{(1)}_1\left(\gamma^{(2)}_{-1}\xi^{(1)}_1 - \gamma^{(1)}_0\xi^{(2)}_0\right) + \gamma^{(2)}_0\left(\gamma^{(1)}_0\alpha^{(1)}_1 - \beta^{(1)}_0\xi^{(1)}_1\right)\right]\tau^{(1)}_{\hat{x}z,\hat{x}}\\ &-\beta^{(1)}_1\tau^{(1)}_{zz,\hat{x}\hat{x}\hat{x}\hat{x}\hat{x}\hat{x}\hat{x}\hat{x}}\left[\beta^{(1)}_1\left(\xi^{(2)}_0 + \xi^{(1)}_0\right) - \alpha^{(1)}_1\gamma^{(2)}_0 - \gamma^{(1)}_1\alpha^{(1)}_0\right]\tau^{(1)}_{zz,\hat{x}\hat{x}\hat{x}\hat{x}}\end{aligned}$$

$$
\begin{aligned}
&+\left[\gamma_1^{(1)}\left(\alpha_0^{(1)}\xi_0^{(2)}-\xi_{-1}^{(2)}\alpha_1^{(1)}\right)+\beta_1^{(1)}\left(\xi_{-1}^{(2)}\xi_1^{(1)}-\xi_0^{(1)}\xi_0^{(2)}\right)+\gamma_0^{(2)}\left(\xi_0^{(1)}\alpha_1^{(1)}-\alpha_0^{(1)}\xi_1^{(1)}\right)\right]\tau_{zz}^{(1)}\\
&+\left(\beta_1^{(1)}\xi_1^{(1)}-\gamma_1^{(1)}\alpha_1^{(1)}\right)\left(\xi_1^{(2)}\tau_{zz}^{(3)}+\chi_z^{(2)}+\gamma_1^{(2)}\tau_{\hat{x}z,\hat{x}}^{(3)}\right)+\left(\gamma_1^{(1)}\xi_0^{(2)}-\gamma_0^{(2)}\xi_1^{(1)}\right)\left(\eta_{\hat{x}}^{(1)}+\eta_z^{(1)}\right)\\
&+\left[\xi_{-1}^{(1)}\alpha_1^{(1)}\gamma_0^{(2)}-\gamma_0^{(2)}\alpha_{-1}^{(1)}\xi_1^{(1)}-\xi_{-1}^{(1)}\xi_0^{(2)}\beta_1^{(1)}+\gamma_1^{(1)}\alpha_{-1}^{(1)}\xi_0^{(2)}\right]\tau_{zz}^{(0)}+\left[\alpha_1^{(1)}\gamma_0^{(2)}-\xi_0^{(2)}\beta_1^{(1)}\right]\chi_z^{(1)}\\
&+\left[\gamma_{-1}^{(1)}\alpha_1^{(1)}\gamma_0^{(2)}-\beta_{-1}^{(1)}\gamma_0^{(2)}\xi_1^{(1)}-\gamma_{-1}^{(1)}\xi_0^{(2)}\beta_1^{(1)}+\gamma_1^{(1)}\beta_{-1}^{(1)}\xi_0^{(2)}\right]\tau_{\hat{x}z,\hat{x}}^{(0)}+\left(\gamma_{-1}^{(1)}\beta_1^{(1)}-\gamma_1^{(1)}\beta_{-1}^{(1)}\right)\tau_{\hat{x}z,\hat{x}\hat{x}\hat{x}\hat{x}\hat{x}}^{(0)}\\
&+\left(\xi_{-1}^{(1)}\beta_1^{(1)}-\gamma_1^{(1)}\alpha_{-1}^{(1)}\right)\tau_{zz,\hat{x}\hat{x}\hat{x}\hat{x}}^{(0)}-\gamma_1^{(1)}\eta_{\hat{x},\hat{x}\hat{x}\hat{x}\hat{x}}^{(1)}-\gamma_1^{(1)}\eta_{z,\hat{x}\hat{x}\hat{x}\hat{x}}^{(1)}+\beta_1^{(1)}\chi_{z,\hat{x}\hat{x}\hat{x}\hat{x}}^{(1)}\Big\}=0. \qquad \text{(B5b)}
\end{aligned}
$$

Equations (B5a) and (B5b) are the same as those given in Eqs. (90a) and (90b), with the coefficients listed in Eqs. (91a)–(91f).

References

1. Alieldin, S.S., Alshorbagy, A.E., Shaat, M.: A first-order shear deformation finite element model for elastostatic analysis of laminated composite plates and the equivalent functionally graded plates. Ain Shams Eng. J. **2**(1), 53–62 (2011)
2. Barbero, E.J., Reddy, J.N.: Modeling of delamination in composite laminates using a layer-wise plate theory. Int. J. Solids Struct. **28**(3), 373–388 (1991)
3. Batista, M.: Comparison of Reissner, Mindlin and Reddy plate models with exact three dimensional solution for simply supported isotropic and transverse inextensible rectangular plate. Meccanica **47**(1), 257–268 (2012)
4. Benveniste, Y.: A general interface model for a three-dimensional curved thin anisotropic interphase between two anisotropic media. J. Mech. Phys. Solids **54**, 708–734 (2006)
5. Carrera, E.: Mixed layer-wise models for multilayered plates analysis. Compos. Struct. **43**(1), 57–70 (1998)
6. Carrera, E.: Layer-wise mixed models for accurate vibrations analysis of multilayered plate. J. Appl. Mech. **65**(4), 820–828 (1998)
7. Chen, W.Q., Cai, J.B., Ye, G.R.: Exact solutions of cross-ply laminates with bonding imperfections. AIAA J. **41**(11), 2244–2250 (2003)
8. Chen, W.Q., Wang, Y.F., Cai, J.B., Ye, G.R.: Three-dimensional analysis of cross-ply laminated cylindrical panels with weak interfaces. Int. J. Solids Struct. **41**(9–10), 2429–2446 (2004)
9. Chen, W.T., Nelson, C.W.: Thermal stress in bonded joints. IBM J. Res. Dev. **23**, 179–188 (1979)
10. Cheng, Z.Q., Jemah, A.K., Williams, F.W.: Theory for multilayered anisotropic plates with weakened interfaces. J. Appl. Mech. **63**(4), 1019–1026 (1996)
11. Cho, M., Parmerter, R.R.: Efficient higher order composite plate theory for general lamination configurations. AIAA J. **31**(7), 1299–1306 (1993)
12. COMSOL: COMSOL Multiphysics®, v. 6.1. COMSOL Inc., Stockholm, Sweden (2022)
13. Demasi, L.: Three-dimensional closed form solutions and exact thin plate theories for isotropic plates. Compos. Struct. **80**(2), 183–195 (2007)
14. Desai, Y.M., Ramtekkar, G.S., Shah, A.H.: Dynamic analysis of laminated composite plates using a layer-wise mixed finite element model. Compos. Struct. **59**(2), 237–249 (2003)
15. Dillner, U.: Thermal modeling of multilayer membranes for sensor applications. Sens. Actuators A **41**(1–3), 260–267 (1994)
16. Dingler, C., Müller, H., Wieland, M., Fauser, D., Steeb, H., Ludwigs, S.: From understanding mechanical behavior to curvature prediction of humidity-triggered bilayer actuators. Adv. Mater. **33**(9), 2007982-1–2007982-9 (2021)
17. Evans, A.G., Hutchinson, J.W.: The thermomechanical integrity of thin films and multilayers. Acta Metall. Mater. **43**(7), 2507–2530 (1995)
18. Ewolo Ngak, F.P., Ntamack, G.E., Azrar, L.: Semi-analytical solution for static and free vibration of multilayered functionally graded elastic plates with imperfect interfaces. Int. J. Comput. Methods Eng. Sci. Mech. **23**(4), 285–306 (2022)
19. Feng, X., Zhang, L., Zhang, H., Gao, Y.: Semi-analytical solution for mixed supported and multilayered two-dimensional thermo-elastic quasicrystal plates with interfacial imperfections. J. Therm. Stresses **46**(2), 91–116 (2023)
20. Gao, X.-L.: Critical velocities of anisotropic tubes under a moving pressure incorporating transverse shear and rotary inertia effects. Acta Mech. **233**, 3511–3534 (2022)
21. Gao, X.-L.: Critical velocities of a two-layer composite tube under a moving internal pressure. Acta Mech. **234**, 2021–2043 (2023)
22. Gao, X.-L.: Critical velocities of a two-layer composite tube incorporating the effects of transverse shear, rotary inertia and material anisotropy. Z. Angew. Math. Phys. **74**, 166-1–166-29 (2023). https://doi.org/10.1007/s00033-023-02023-8
23. Gao, X.-L.: Critical velocities of a three-layer composite tube incorporating the rotary inertia and material anisotropy. Math. Mech. Solids (in press) (2024). https://doi.org/10.1177/10812865241250015
24. Gao, X.-L., Li, K.: A shear-lag model for carbon nanotube-reinforced polymer composites. Int. J. Solids Struct. **42**, 1649–1667 (2005)
25. Gao, X.-L., Zhang, G.Y.: A non-classical Kirchhoff plate model incorporating microstructure, surface energy and foundation effects. Continuum Mech. Thermodyn. **28**, 195–213 (2016)
26. Gay, D.: Composite Materials: Design and Applications, 3rd edn. CRC Press, Boca Raton, FL (2022)
27. Gigliotti, M., Minervino, M.: The deformed shape of isotropic and orthotropic plates subjected to bending moments distributed along the edges. Meccanica **49**, 1367–1384 (2014)
28. Goland, M., Reissner, E.: The stress in cemented joints. J. Appl. Mech. **11**, 17–27 (1944)

29. Green, A.E., Lindsay, K.A.: Thermoelasticity. J. Elast. **2**, 1–7 (1972)
30. Gu, S.T., He, Q.C.: Interfacial discontinuity relations for coupled multifield phenomena and their application to the modeling of thin interphases as imperfect interfaces. J. Mech. Phys. Solids **59**, 1413–1426 (2011)
31. Gurtin, M.E., Fried, E., Anand, L.: The Mechanics and Thermodynamics of Continua. Cambridge University Press, New York (2010)
32. Hsueh, C.H., Luttrell, C.R., Lee, S., Wu, T.C., Lin, H.Y.: Interfacial peeling moments and shear forces at free edges of multilayers subjected to thermal stresses. J. Am. Ceram. Soc. **89**(5), 1632–1638 (2006)
33. Hsueh, C.H., Lee, S., Lin, H.Y.: Analyses of mode I edge delamination by thermal stresses in multilayer systems. Compos. B Eng. **37**(1), 1–9 (2006)
34. Hu, Y., Li, W., Zhu, J., Hao, S.M., Qin, X., Fan, L.Z., Zhang, L., Zhou, W.: Multi-layered electrolytes for solid-state lithium batteries. Next Energy **1**(3), 100042 (2023)
35. Huang, K.H., Dasgupta, A.: A layer-wise analysis for free vibration of thick composite cylindrical shells. J. Sound Vib. **186**(2), 207–222 (1995)
36. Jiang, Z.Q., Huang, Y., Chandra, A.: Thermal stresses in layered electronic assemblies. ASME J. Electron. Pack. **119**, 127–132 (1997)
37. Kim, J., Kumar, R., Bandodkar, A.J., Wang, J.: Advanced materials for printed wearable electrochemical devices: a review. Adv. Electron. Mater. **3**(1), 1600260-1–1600260-15 (2017)
38. Kim, K.J., Balaish, M., Wadaguchi, M., Kong, L., Rupp, J.L.: Solid-state Li–metal batteries: challenges and horizons of oxide and sulfide solid electrolytes and their interfaces. Adv. Energy Mater. **11**(1), 2002689 (2021)
39. Kim, H., Pyun, K.R., Lee, M.T., Lee, H.B., Ko, S.H.: Recent advances in sustainable wearable energy devices with nanoscale materials and macroscale structures. Adv. Func. Mater. **32**(16), 2110535 (2022)
40. Lee, J., Gurdal, Z., Griffin, O.H., Jr.: Layer-wise approach for the bifurcation problem in laminated composites with delaminations. AIAA J. **31**(2), 331–338 (1993)
41. Lee, J., Kim, J.S., Cho, M.: An asymptotic method-based composite plate model considering imperfect interfaces. Int. J. Solids Struct. **190**, 258–270 (2020)
42. Levinson, M.: The simply supported rectangular plate: an exact, three dimensional, linear elasticity solution. J. Elast. **15**(3), 283–291 (1985)
43. Li, J., Shen, Z., Chen, X., Yang, S., Zhou, W., Wang, M., Wang, L., Kou, Q., Liu, Y., Li, Q., Xu, Z.: Grain-orientation-engineered multilayer ceramic capacitors for energy storage applications. Nat. Mater. **19**(9), 999–1005 (2020)
44. Li, W., Song, Z., Zhong, J., Qian, J., Tan, Z., Wu, X., Chu, H., Nie, W., Ran, X.: Multilayer-structured transparent MXene/PVDF film with excellent dielectric and energy storage performance. J. Mater. Chem. C **7**(33), 10371–10378 (2019)
45. Liu, D., Xu, L., Lu, X.: Stress analysis of imperfect composite laminates with an interlaminar bonding theory. Int. J. Numer. Meth. Eng. **37**(16), 2819–2839 (1994)
46. Liu, D.Y., Chen, W.Q.: Thermal stresses in bilayer systems with weak interface. Mech. Res. Commun. **37**, 520–524 (2010)
47. Liu, D.Y., Chen, W.Q.: Thermal stress analysis of a trilayer film/substrate system with weak interfaces. Compos. B Eng. **43**(8), 3445–3452 (2012)
48. Lo, K.H., Christensen, R.M., Wu, E.M.: A high-order theory of plate deformation: part 1: homogeneous plates. J. Appl. Mech. **44**(4), 663–668 (1977)
49. Lubarda, V.: On thermodynamic potentials in linear thermoelasticity. Int. J. Solids Struct. **41**(26), 7377–7398 (2004)
50. Massabò, R., Campi, F.: An efficient approach for multilayered beams and wide plates with imperfect interfaces and delaminations. Compos. Struct. **116**, 311–324 (2014)
51. Milazzo, A.: Layer-wise and equivalent single layer models for smart multilayered plates. Compos. B Eng. **67**, 62–75 (2014)
52. Murray, C.E., Noyan, I.C.: Finite-size effects in thin-film composites. Philos. Mag. A **82**, 3087–3117 (2002)
53. Nairn, J.A.: On the use of shear-lag methods for analysis of stress transfer in unidirectional composites. Mech. Mater. **26**, 63–80 (1997)
54. Nguyen, V.C., Oliva-Torres, V., Bernadet, S., Rival, G., Richard, C., Capsal, J.F., Cottinet, P.J., Le, M.Q.: Haptic feedback device using 3D-printed flexible, multilayered piezoelectric coating for in-car touchscreen interface. Micromachines **14**(8), 1553 (2023)
55. Pagano, N.J.: Exact solutions for composite laminates in cylindrical bending. J. Compos. Mater. **3**(3), 398–411 (1969)
56. Pagano, N.J.: Exact solutions for rectangular bidirectional composites and sandwich plates. J. Compos. Mater. **4**(1), 20–34 (1970)
57. Pao, Y.-H., Eisele, E.: Interfacial shear and peel stresses in multilayered thin stacks subjected to uniform thermal loading. ASME J. Electron. Pack. **113**, 164–172 (1991)
58. Peeketi, A.R., Swaminathan, N., Annabattula, R.K.: Design of partially covered bilayer thin film actuators. Mech. Mater. **187**, 104816-1–104816-16 (2023)
59. Piltner, R.: Three-dimensional stress and displacement representations for plate problems. Mech. Res. Commun. **18**(1), 41–49 (1991)
60. Reddy, J.N.: A simple higher-order theory for laminated composite plates. J. Appl. Mech. **51**(4), 745–752 (1984)
61. Reddy, J.N.: Energy Principles and Variational Methods in Applied Mechanics, 2nd edn. Wiley, Hoboken, NJ (2002)
62. Reddy, J.N.: Mechanics of Laminated Composite Plates and Shells: Theory and Analysis, 2nd edn. CRC Press, Boca Raton, FL (2003)
63. Ru, C.Q.: Interfacial thermal stresses in bimaterial elastic beams: modified beam models revisited. ASME J. Electron. Pack. **124**(3), 141–146 (2002)
64. Shaat, M., Gao, X.-L., Li, K., Littlefield, A.G.: New analytical model for thermomechanical responses of multi-layered structures with imperfect interfaces. Acta Mech. **234**(11), 5779–5818 (2023)
65. Shaat, M., Faroughi, S.: Influence of long-range interatomic and interlayer interactions on dispersion of acoustic waves by multilayer graphene. Physica E **108**, 74–82 (2019)
66. Srinivas, S., Rao, A.K.: Flexure of thick rectangular plates. J. Appl. Mech. **40**(1), 298–299 (1973)

67. Srinivas, S., Rao, A.K., Rao, C.V.J.: Flexure of simply supported thick homogeneous and laminated rectangular plates. Z. Angew. Math. Mech. **49**(8), 449–458 (1969)
68. Steigmann, D.J., Bîrsan, M., Shirani, M.: Lecture Notes on the Theory of Plates and Shells: Classical and Modern Developments. Springer, Cham, Switzerland (2023)
69. Su, Y.Y., Gao, X.-L.: Analytical model for adhesively bonded composite panel-flange joints based on the Timoshenko beam theory. Compos. Struct. **107**, 112–118 (2014)
70. Thomas, J.M.: Sturm's theorem for multiple roots. Natl. Math. Mag. **15**(8), 391–394 (1941)
71. Volkersen, O.: Die nietkraftverteilung in zugbeanspruchten nietverbindungen mit konstanten laschenquerschnitten. Luftfahrtforschung **15**, 41–47 (1938)
72. Wang, K., Huang, Y., Chandra, A., Hu, K.X.: Interfacial shear stress, peeling stress, and die cracking stress in trilayer electronic assemblies. IEEE Trans. Compon. Packag. Manuf. Technol. **23**, 309–316 (2000)
73. Wang, H.T., Guo, J.H., Jiang, X., Gao, M.Z.: Bending and vibration of one-dimensional hexagonal quasicrystal layered plates with imperfect interface. Acta Mech. **233**(10), 4029–4046 (2022)
74. Wang, J.Y., Gu, C.-S., Gu, S.-T., Gao, X.-L., Gu, H.: Shear-lag model for discontinuous fiber-reinforced composites with a membrane-type imperfect interface. Acta Mech. **231**, 4717–4734 (2020)
75. Wang, P., Qu, W., Song, W.L., Chen, H., Chen, R., Fang, D.: Electro–chemo–mechanical issues at the interfaces in solid-state lithium metal batteries. Adv. Funct. Mater. **29**(27), 1900950 (2019)
76. Wang, Q.H., Kalantar-Zadeh, K., Kis, A., Coleman, J.N., Strano, M.S.: Electronics and optoelectronics of two-dimensional transition metal dichalcogenides. Nat. Nanotechnol. **7**(11), 699–712 (2012)
77. Wen, Y., Basaran, C.: An analytical model for thermal stress analysis of multi-layered microelectronic packaging. Mech. Mater. **36**, 369–385 (2004)
78. Xiong, X., Venkataraman, M., Jašíková, D., Yang, T., Mishra, R., Militký, J., Petrů, M.: An experimental evaluation of convective heat transfer in multi-layered fibrous materials composed by different middle layer structures. J. Ind. Text. **51**(3), 362–379 (2021)
79. Yu, Y.Y.: A new theory of elastic sandwich plates—one-dimensional case. J. Appl. Mech. **26**(3), 415–421 (1959)
80. Zhang, N.H.: Thermoelastic stresses in multilayered beams. Thin Solid Films **515**(23), 8402–8406 (2007)
81. Zhang, X.C., Xu, B.S., Wang, H.D., Wu, Y.X.: An analytical model for predicting thermal residual stresses in multilayer coating systems. Thin Solid Films **488**(1–2), 274–282 (2005)
82. Zhang, Y.: Extended Stoney's formula for a film-substrate bilayer with the effect of interfacial slip. J. Appl. Mech. **75**(1), 011008-1–011008-9 (2008)